



**KTH Architecture and
the Built Environment**

Analysis of Tripod shaped high rise building using Tubed Mega Frame Structures

SUJAN KUMAR RIMAL
LEVI GRENNVALL

Master of Science Thesis
Stockholm, Sweden 2017

TRITA-BKN. Master Thesis 518, 2017

ISSN 1103-4297

ISRN KTH/BKN/EX--518--SE

KTH School of ABE

SE-100 44 Stockholm

SWEDEN

© Sujan Kumar Rimal & Levi Grennvall, 2017
Royal Institute of Technology (KTH)
Department of Civil and Architectural Engineering
Division of Concrete Structures

Abstract

Most of the tall buildings that are built today have a straight and vertical shape, because vertical buildings are more stable and easily built than slanted ones. In the case of vertical building, bending moments in the base only exists from horizontal loads such as wind and seismic loads, but in slanted buildings there will also be bending moments from dead and live loads. In addition, transportation inside the building is also a challenge when it comes to slanted buildings. However, a new elevator system that ThyssenKrupp has developed will solve that problem. This new elevator has an ability to move in all direction both vertically and horizontally.

The new structural system, Tube Mega Frame (TMF), has been studied and proved to have better efficiency than the central core with outriggers. Moving the bearing structure to the perimeter of the building, gives smaller overturning moment and better stability due to longer lever arm from the center. This thesis focuses on applying the Tube Mega Frame system to a slanted building which has a tripod structure. Different types of TMFs were used to compare the efficiency of the buildings performance. The TMF contains perimeter frame and mega columns with different binding systems such as belt walls and bracings.

A pre-study has been carried out in order to see the overall behavior of the tripod shape. Different heights and inclinations have been analyzed with stick models. The analysis has been performed in the finite element software SAP2000 and deflections due to dead load was compared. The buildings with least deflection considering maximum height and maximum inclination was chosen for further model analysis in finite element software ETABS. Furthermore, a short study of different bracings system has been performed for the lateral loads and it concluded that X-bracing have better performance.

The main study of this thesis focused on the two building models of 450 m with 7° inclination and 270 and 15° inclination. For each model, five different TMF systems were applied and analyzed. The TMF includes perimeter frame, perimeter frame with belt wall, mega columns, mega columns with belt wall and mega columns with bracings. Deformations due to wind load, seismic load and modal vibration has been compared.

It concluded that the least deformation is achieved by the TMF mega columns with bracings for both models with two different heights. The periods of the building are comparatively lower than other systems. The deflection from TMF mega columns with belt walls did not differ much from the TMF mega columns with bracings. For the 270 m high building, the top story displacement was remarkably small because of the three legs, making it stiffer and stable. Even with the p delta effect, there were only millimeters of difference in top story displacement. TMF perimeter frame had a lower deflection than with belt wall, which should have been exact opposite. The reason was while making the total volume of buildings equal, the addition of belt walls led to thinner columns in the perimeter and lower stiffness.

Keywords: high-rise building, inclined, slanted, tubed mega frame, tripod

Sammanfattning

De flesta av de höga byggnaderna som byggs idag har en rak och vertikal form, eftersom raka byggnader är stabilare än snedställda. Raka byggnader är utsatta för böj moment i basen från externa krafter, till exempel vind last. Lutande byggnader utsätts för böj moment från egenvikt och nyttig last med mera. Dessutom är transport inom byggnaden också ett stort problem när det gäller lutande byggnader. Med det nya hissystemet som ThyssenKrupp har utvecklat kommer detta problem att lösas. Det nya hissystemet har förmågan att röra sig i alla riktningar både vertikalt och horisontellt.

Det nya konstruktionssystemet, Tube Mega Frame (TMF), har studerats och visat sig ha bättre effektivitet än den centrala kärnan med utriggare. Genom att flytta det bärande systemet till utkanten av byggnaden, kommer resultera i mindre vältande moment och ge bättre stabilitet på grund av längre hävarm från mitten. Denna uppsats fokuserar på att applicera TMF till en lutande byggnad som har en trebensform. Olika typer av TMF användes för att jämföra effektiviteten hos byggnadens prestanda. TMF består av pelare i utkanten av byggnaden med olika typer av avstyvningar.

En förundersökning utfördes för att se det övergripande beteendet hos den trebenta formen. Olika höjder och lutningar analyserades som stickmodeller. Analysen utfördes i ett finit element programvara SAP2000 och utböjningar på grund av egenvikt jämfördes. Byggnaderna med minst utböjning med tanke på maximal höjd och maximal lutning valdes för ytterligare modellanalys i finit element programmet ETABS. Vidare genomfördes en kort studie av olika fackverk system för horisontala laster och slutsatsen var att X-fackverk har bättre prestanda.

Huvudstudien av denna uppsats fokuserade på två hus modeller, 450 m med 7° lutning och 270 m med 15° lutning. För varje modell applicerades och analyserades fem olika TMF-system. TMF inkluderade perimeterram, perimeterram med sjuvvägg, mega pelare, mega pelare med sjuvvägg och mega pelare med fackverk. Deformationer på grund av vind belastning, seismisk belastning och vibrationer jämfördes.

Slutligen, den minsta deformationen uppnåddes genom TMF mega pelarna med fackverk för båda modellerna med två olika höjder. Byggnadens perioder var relativt lägre än andra system. Avvikelsen från TMF mega pelare med sjuvväggar skiljde sig inte så mycket från TMF mega pelare med fackverk. För den 270 m höga byggnaden, var den hösta utböjning anmärkningsvärt liten på grund av de tre benen, vilket gör den styvare och stabil. Även med P-delta effekten var det bara millimeter av skillnad i utböjningen. TMF perimeterramen hade en lägre utböjning än perimeterramen med sjuvväggar, vilket borde ha varit exakt motsatt. Anledningen var att samtidigt som den totala volymen av byggnader var lika, har tillägget av sjuvväggar lett till tunnare kolumner och lägre styvhet.

Nyckelord: höghus, vinklad, lutande, tubed mega frame, trefot

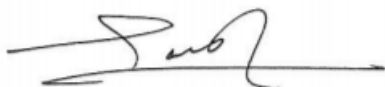
Preface

The projects aim is to develop new building forms and test new structural systems to accommodate new shared-shaft elevator technologies. The project is a part of a study group at Tyréns with collaboration with the Council on Tall Buildings and Urban Habitat (CTBUH) and ThyssenKrupp.

We would like to show our gratitude to Tyréns for providing this opportunity and platform for working on the thesis. A big thanks to our supervisor at Tyréns, Fritz King who guided us through this journey of learning about tall buildings. We are grateful to our examiner, Professor Mikael Hallgren for the guidance and knowledge he has provided.

Finally, we would like to thank our project group members for the discussions and shared ideas throughout the process.

Stockholm, June 2017



Sujan Kumar Rimal



Levi Grennvall

Notations

Latin capital letters

A	Cross-section area
A_b	Cross-sectional area of beams
A_{br}	Cross-sectional area of bracings
$A_{f,tot}$	Total floor area
A_{MF}	Cross-sectional area of moment frame
B	Width
C_p	External pressure coefficient
D	Diameter of the building
$\{D\}$	Displacement vector
E	Young's modulus
F	Force
F_a	Short period site coefficient
F_v	1 s period site coefficient
GC_{pi}	Internal pressure coefficient
G_f	Gust-effect factor for flexible buildings
H	Height
I	Second area moment of inertia
$[K]$	Global stiffness matrix
L	Length
$L_{b,tot}$	Total beam length
$L_{br,tot}$	Total bracing length
$L_{c,tot}$	Total column length
$L_{MF,tot}$	Total moment frame length (beams excluded)
M	Bending moment
N_{cr}	Critical normal load
$\{R\}$	Global load vector
S_1	Mapped MCE_R spectral response acceleration parameter at 1 s periods
S_a	Design spectral response acceleration
S_{D1}	Design earthquake spectral response acceleration parameter at 1 s period
S_{DS}	Design earthquake spectral response acceleration parameter at short period
S_{M1}	MCE_R spectral response acceleration parameter at 1 s periods adjusted for site class effects
S_{MS}	MCE_R spectral response acceleration parameter at short periods adjusted for site class effects
S_S	Mapped MCE_R spectral response acceleration parameter at short periods
St	Dimensionless parameter called Strouhal number for the shape
T	Period of the structure
V	Mean wind velocity at the top of the building
$V_{br,tot}$	Total bracing volume
$V_{bw,tot}$	Total belt wall volume
$V_{f,tot}$	Total floor volume
$V_{MC,tot}$	Total mega column volume
$V_{MF,tot}$	Total moment frame volume
V_{tot}	Total volume

Latin lower case letters

c_{pe}	Pressure coefficient for external pressures
c_{pi}	Pressure coefficient for internal pressures
g	Gravitational acceleration
f_v	Frequency of vortex shedding
h	Floor height
h_q	Quadratic cross-sectional height
$h_{q,b}$	Quadratic cross-sectional height for beams
$h_{q,MF}$	Quadratic cross-sectional height for moment frame
l	Lever arm
p	Design wind pressures for the main wind-force resisting system of flexible enclosed buildings
$q = q_h$	For leeward walls, side walls and roofs evaluated at height h
$q = q_z$	For windward walls evaluated at height z above the ground
$q_i = q_h$	For windward walls, side walls, leeward walls, and roofs of enclosed buildings and for negative internal pressure evaluation in partially enclosed buildings
$q_p(z_e)$	External peak velocity pressure
$q_p(z_i)$	Internal peak velocity pressure
t	Flange thickness
w	Net pressure acting on the surface
w_e	External pressure acting on the surface
w_i	Internal pressure acting on the surface
x	Length of the cross section
z_e	Reference height for external pressure
z_i	Reference height for internal pressure

Greek letters

α	Angle
βl	Critical buckling length
γ_c	Weight concrete
γ_{tot}	Total weight
δ	Displacement
ε	Strain
θ	Rotation
ρ	Density
ρ_c	Density concrete
σ	Stress
σ_c	Compressive stress
σ_{cr}	Critical mean stress

Contents

Abstract	iii
Sammanfattning	v
Preface	vii
Notations	ix
Contents	xi
1 Introduction	1
1.1 Background and problem description.....	1
1.2 Aim and scope	1
1.3 Limitations.....	2
2 Literature study of tall buildings	3
2.1 Structural mechanics	3
2.1.1 Wind loads.....	3
2.1.2 Seismic load	6
2.1.3 Stiffness theory.....	9
2.1.4 P-delta effects	10
2.1.5 Buckling	11
2.2 Structural systems.....	12
2.2.1 Central core and outrigger system.....	12
2.2.2 Tubed Mega Frame Structures	12
2.2.3 Shear wall	13
2.2.4 Bracings.....	13
2.3 Inclined buildings	14
2.3.1 The structural system of leaning tower	14
2.3.2 Structural approaches for leaning towers	14
2.3.3 The conceptual design of tripod structure	15
3 Finite Element Method	17
3.1 What is FEM	17
3.2 SAP2000.....	18
3.3 ETABS	18

4	Pre-study of the Tripod shaped building.....	19
4.1	SAP2000 analysis.....	19
4.1.1	Shape performance.....	19
4.1.2	Bracing performance.....	26
4.2	Structural systems.....	27
5	ETABS analysis.....	29
5.1	Loads acting on the building.....	29
5.1.1	Dead load.....	29
5.1.2	Live load.....	29
5.1.3	Wind load.....	29
5.1.4	Seismic load.....	32
5.2	Structural systems.....	32
5.2.1	Properties.....	33
5.2.2	Mega columns with belt wall.....	33
5.2.3	Six mega columns with belt wall.....	35
5.2.4	Mega columns with bracings.....	36
5.2.5	Perimeter frame with belt wall.....	36
5.2.6	Perimeter frame.....	37
5.3	Comparison.....	38
5.3.1	Deformations and periods for the 450 m high building.....	39
5.3.2	Deformations and periods for the 270 m high building.....	44
5.4	Verification.....	48
6	Discussion and conclusion.....	49
7	Further research.....	51
	Bibliography.....	53
	Appendix A – Deformations.....	55
	270 m high building.....	55
	Three mega columns with belt walls.....	55
	Six mega columns with belt walls.....	56
	Mega columns with bracings.....	57
	Moment frame with belt walls.....	58
	Moment frame.....	59
	450 m high building.....	60
	Three mega columns with belt walls.....	60

Six mega columns with belt walls	61
Mega columns with bracings	62
Moment frame with belt walls	63
Moment frame without belt walls	64
Appendix B – Displacements	65
270 m high building	65
Displacement due to wind load, P-delta included	65
Displacement due to wind load, P-delta excluded	66
Displacement due to seismic load, P-delta included	68
Displacement due to seismic load, P-delta excluded	69
450 m high building	71
Displacement due to wind load, P-delta included	71
Displacement due to wind load, P-delta excluded	72
Displacement due to seismic load, P-delta included	74
Displacement due to seismic load, P-delta excluded	75
Appendix C – Hand calculations.....	77
Cross-section calculation, 270 m	77
Three mega columns with belt wall	77
Six mega columns with belt walls	77
Three mega columns with bracings	78
Moment frame with belt walls.....	78
Moment frame without belt walls	79
Base reaction calculation, 270 m	79
Three mega columns with belt walls	79
Six mega columns with belt walls	79
Three mega columns with bracings	80
Moment frame with belt walls.....	80
Moment frame without belt walls	80
Cross-section calculations, 450 m	81
Three mega columns with belt wall	81
Six mega columns with belt walls	81
Three mega columns with bracings	81
Moment frame with belt walls.....	82
Moment frame without belt walls	82
Base reaction calculations, 450 m	83

Three mega columns with belt walls 83
Six mega columns with belt walls 83
Three mega columns with bracings 84
Moment frame with belt walls 84
Moment frame without belt walls 84

1 Introduction

1.1 Background and problem description

A big problem today on existing high-rise buildings is that the elevator shafts take a lot of space. The elevator shafts make the structural core of the building, which is called a “central core”. Because of new technologies on shared-shaft elevators, it is now possible to ignore the massive central core and start building slenderer high-rise buildings. The new elevator technologies make it possible to develop new and radical building forms and shapes. This is possible because the structural core can be put on the perimeter of the building instead of a central core.

By moving the bearing structure to the perimeter of the building, it is possible to make it thinner, because the lever arm at the base of the building will increase and therefore the bending moment at the foundation decrease.

The Council on Tall Buildings and Urban Habitat is the “world’s leading resource for professionals focused on the inception, design, construction and operation of tall buildings and future cities” (CTBUH, 2016).

ThyssensKrupp is a big company that has developed “MULTI”, the world’s first rope-free elevator (ThyssensKrupp, 2016). In addition, with this new revolutionary elevator technology they have “opened the door to new possibilities – in all directions”.

1.2 Aim and scope

This thesis aim was to test the performance of the Tripod shaped high-rise by analyzing different types of Tubed Mega Frame structures.

A literature study was carried out containing structural mechanics, structural systems and inclined buildings. The structural mechanics part contained some basics about wind and seismic loads, stiffness theory that the software had used, P-delta effects that will have a big impact on inclined and tall buildings and a brief explanation of buckling of columns. For the structural systems, only the central core with the outrigger system and the TMF were explained. Inclined buildings, and what is meant by that, will be explained and how structural systems can be approached for inclined buildings.

Thereafter, a pre-study was performed in SAP2000. Firstly, a shape performance where different heights and angles were tested to see how the building acts under dead load only. Secondly, a bracing performance study was carried out in SAP2000 to find the best performing bracing systems that would be applied to the building.

At last, a study was performed where different shapes and different structural systems were modeled in ETABS. Wind, seismic, live and dead load were taken into account. A comparison of the models was performed to highlight the best performing system.

1.3 Limitations

The analysis did not include loads from façade, installations and other rare imposed loads such as explosion. The main purpose of the thesis was to compare different structural systems under the same conditions.

The maximum deflection due to wind and seismic loads were chosen and compared to each other. There were twelve cases of wind loads and six cases of seismic loads that were imposed around the building laterally. And only one case of each load was chosen and compared for different structural systems for the ultimate limit state. The transverse wind effect was not included in the wind load case.

The buildings were modeled with concrete of same strength class to achieve constancy. Concrete and reinforcement bars had highest strength class and amount reinforcement was design by ETABS itself. Material nonlinearity such as cracking of concrete was not included in the analysis.

This study did not include any structural design of buildings as well as construction sequence because of lack of time that was given.

2 Literature study of tall buildings

How high does a building have to be to be called a “tall building”? How is a “tall building” defined? There is no clear definition of “tall building”. According to CTBUH a building can be called a tall building if it exhibits one or more of some specific categories (CTBUH, 2017).

For instance, the height relative to the environment can be considered when determining if a building can be called a tall building. For example, a 20-story building wouldn't be considered to be a tall building in New York, but if it would be placed in Stockholm it would be considered as a tall building. Another reason is the buildings technologies. If the building is constructed in a way that it uses technologies such as vertical transports or wind bracings etc. because of its height it could be considered as a tall building. The final category considers the proportion of the building. A building with a height/width ratio of 1 wouldn't be considered as a tall building even though it might be 100 m high. If a building with the same height would be very slender it would give the appearance to be a tall building (CTBUH, 2017).

2.1 Structural mechanics

2.1.1 Wind loads

Wind blows when there is pressure difference in the atmosphere. The air moves from areas with high pressure to areas with low pressure to balance the pressure difference (UCAR, 2017).

Wind load plays a big roll on designing tall and slender high rise building, since the stiffness of the building decreases with the increase of height and wind velocity increase with the increase of altitude as shown in Figure 2.1.

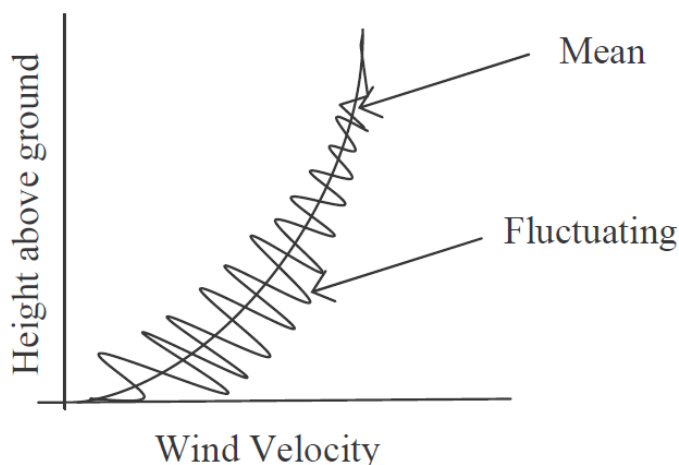


Figure 2.1: Variation of wind velocity with height (Dr. Bhandari, et al., u.d.)

The speed of wind is often unsteady. It changes its direction and intensity randomly which creates a gustiness in wind flow (Svärd & Partovi, 2016). The main reasons for the change in wind velocity is topography, terrain roughness and altitude. This kind of turbulent wind flow has both static and dynamic effect on the tall and slender structures. Since tall and slender buildings are more flexible, they have more dynamic response than static. The mean wind velocity is considered when it comes to the static wind load on the building because the period of a building is shorter than the time of a gust wind to reach its maximum speed. However, if the gust wind reaches its maximum velocity in a shorter time than the building's period, the maximum velocity of the fluctuated wind must be considered in the design of dynamic effect, because rapid change in velocity of wind is larger than the mean velocity (Svärd & Partovi, 2016).

The building shows two different responses when the wind is acted on it. The first is along wind response on the direction of the wind and the second is across wind response on the direction perpendicular to the wind flow as shown in Figure 2.2.

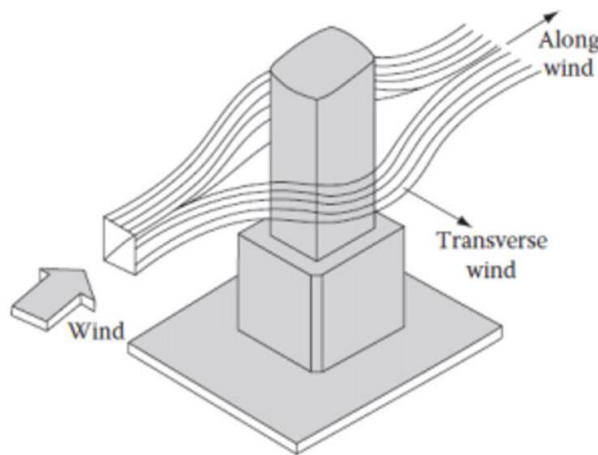


Figure 2.2: Simplified wind flow (Svärd & Partovi, 2016)

The main reason behind it is flow separation from the cross section of the building, which causes vortex shedding at the given frequency (Dr. Bhandari, et al., u.d.). The across wind response phenomenon is common on the tall and slender buildings. When the wind velocity is high, especially on the tall buildings, the wind will not separate evenly on the both side of the building. However, the wind will spread on the one side and will shift on the other side of the building causing transverse vibration which has half the frequency as the along wind response (Zhang, 2014).

Figure 2.3 shows that eddies and vortices are formed due to uneven wind flow separation causing low pressure on the one side of building and high on the other side and vice versa.

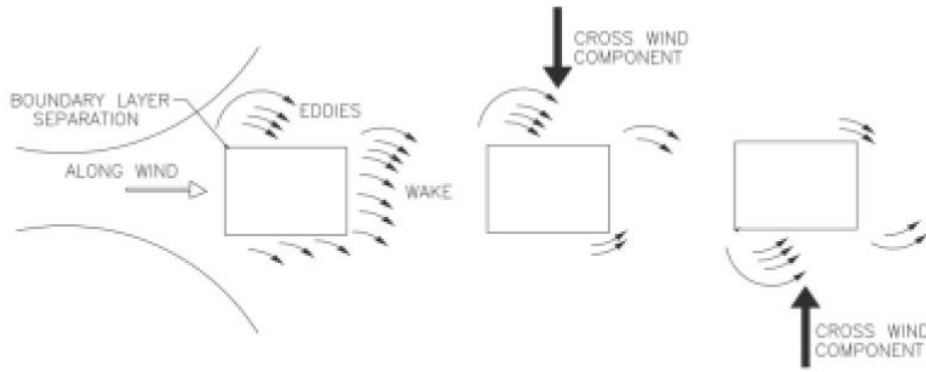


Figure 2.3: Vortex shedding (Svärd & Partovi, 2016)

The vibration caused by a cross wind response can be determined by equation (2-1) (Zhang, 2014).

$$f_v = \frac{V \times St}{D} \quad (2-1)$$

Where,

f_v is the frequency of vortex shedding [Hz]

V is the mean wind velocity at the top of the building, [m/s]

St is the dimensionless parameter called Strouhal number for the shape

D is the diameter of the building [m]

Wind velocity varies with the height of the building

Friction between wind flow and ground occurs because of the ground's roughness, which will result a certain drag on the wind velocity called frictional drag effect. The wind velocity at the ground is comparatively lower than at the top of the building because the frictional drag effect will decrease with increase of the height. As the altitude rises, the frictional drag effect will become negligible at some point and the wind velocity will be mainly influenced by seasonal and local wind variation. The height where the frictional drag effect starts disappearing is called gradient height and respective velocity is called gradient velocity (Zhang, 2014).

Wind load calculation with ASCE

The design wind pressures for the main wind-force resisting system of flexible enclosed buildings shall be calculated from the equation (2-2) according to ASCE 7-10 code:

$$p = qG_f C_p - q_i (G C_{pi}) \quad (N/m^2) \quad (2-2)$$

Where,

$q = q_z$ for windward walls evaluated at height z above the ground.

$q = q_h$ for leeward walls, side walls and roofs evaluated at height h.

$q_i = q_h$ for windward walls, side walls, leeward walls, and roofs of enclosed buildings and for negative internal pressure evaluation in partially enclosed buildings.

G_f = gust-effect factor for flexible buildings.

C_p = external pressure coefficient.

GC_{pi} = internal pressure coefficient.

Wind load calculation with Eurocode

The net pressures acting on the surfaces is obtained from the equation (2-3) according to Eurocode EN 1991-1-4:2005:

$$w = w_e - w_i = q_p(z_e) \cdot c_{pe} - q_p(z_i) \cdot c_{pi} \quad (N/m^2) \quad (2-3)$$

Where,

$q_p(z_e)$ and $q_p(z_i)$ are the external and internal peak velocity pressures, respectively.

z_e and z_i are the reference height for external and internal pressures, respectively.

c_{pe} and c_{pi} are the pressure coefficients for external and internal pressures, respectively.

2.1.2 Seismic load

The tectonic plates on the earth's outer layer called lithosphere is constantly in motion because of the convection on the mantle, which is the semi liquid part of the earth. The plates slides over, under and past on each other, which leads to exertion of stress on the boundaries. Sometimes the plates can lock each other and because of that, strain energy will be accumulated in the form of potential energy on the rocks. When this energy reaches the elastic limit of rocks, it will break free and releases energy by shaking the ground. This is called earthquakes (SMStsunamiwarning, 2017).

When the ground moves back and forth, the bottom part of the building or structures will follow the movement but the upper part of the buildings will not respond immediately. The delay of the building movement at the top is caused by the inertial stiffness and flexibility of the building itself. The inertial force created on the building is equal to the mass of the building times acceleration, which means the increasing the mass of the building leads to increased inertial force and increased inertial stiffness (Zhang, 2014).

Taller buildings are more flexible than the shorter ones. Which means that taller buildings have longer periods than shorter ones. And this is the reason why taller buildings can resist the vibration caused by earthquakes. The ground composed largely of rocks has ground shaking period of 0.5 to 2.5 seconds. If the periods of building fall in the same range of periods of ground shake, the result might be a collapse of the building. But tall buildings tend to have longer periods than that. The fundamental sway of a building can be estimated by the number of stories times 0.1 seconds. So, the building shorter than 25 stories tends to have more risk for collapse due to earthquakes (Klemencic, u.d.).

Different buildings and structures have different frequency and different response to seismic action. Therefore, while designing a building, a broad range of response periods must be considered. And those response spectrum is described by the equations (2-4), (2-5), (2-6), (2-7), (2-8), (2-9) and Figure 2.4 according to ASCE 7-10.

$$S_a = S_{DS} \left(0.4 + 0.6 \frac{T}{T_0} \right) \quad 0 \leq T \leq T_0 \quad (2-4)$$

$$S_a = S_{DS} \quad T_0 \leq T \leq T_S \quad (2-5)$$

$$S_a = \frac{S_{D1}}{T} \quad T_S \leq T \leq T_L \quad (2-6)$$

$$S_a = \frac{S_{D1} \cdot T_L}{T^2} \quad T_L < T \quad (2-7)$$

Where,

$$S_{DS} = \frac{2}{3} S_{MS} = \frac{2}{3} F_a S_S \quad (2-8)$$

$$S_{D1} = \frac{2}{3} S_{M1} = \frac{2}{3} F_v S_1 \quad (2-9)$$

T = the fundamental period of the structure, s

S_{DS} = is the design earthquake spectral response acceleration parameter at short period.

S_{D1} = is the design earthquake spectral response acceleration parameter at 1 s period.

S_a = design spectral response acceleration

S_S = mapped MCE_R spectral response acceleration parameter at short periods

S_1 = mapped MCE_R spectral response acceleration parameter at 1-s period

S_{MS} = MCE_R spectral response acceleration parameter at short periods adjusted for site class effects

S_{M1} = MCE_R spectral response acceleration parameter at 1-s period adjusted for site class effects

F_a = short period site coefficient

F_v = 1-s period site coefficient

The properties of the soil on the building site determines site class. According to ASCE 7-10, there are six different sit classes, namely A, B, C, D, E and F.

Figure 2.5 and Figure 2.6 gives the values for F_a and F_v . And the parameters S_S and S_1 can be taken from chapter 22 from ASCE 7-10, showing maps for Seismic Ground Motion Long-Period Transition and Risk Coefficient Maps.

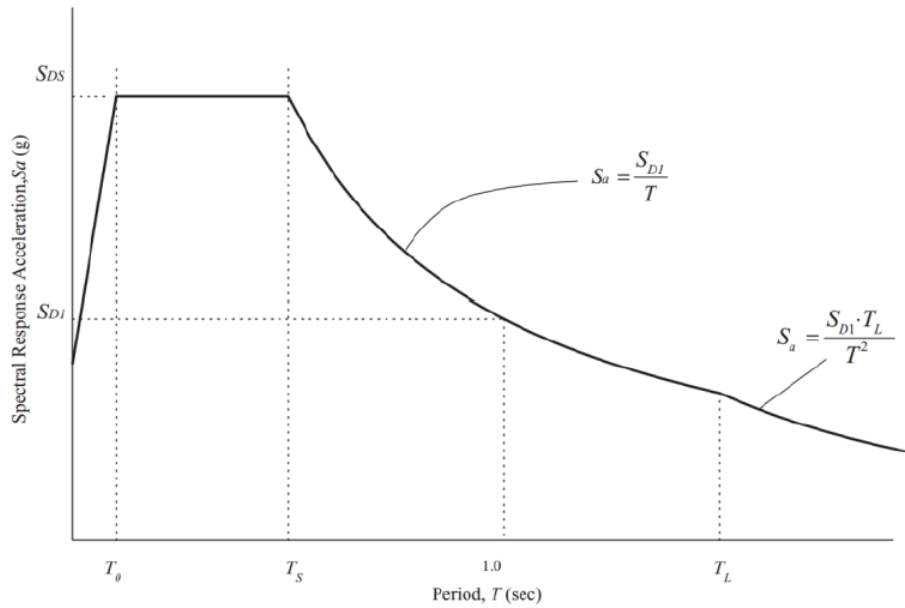


Figure 2.4: Design Response Spectrum (American Society of Civil Engineers, 2013)

Mapped Risk-Targeted Maximum Considered Earthquake (MCE _R) Spectral Response Acceleration Parameter at Short Period					
Site Class	$S_s \leq 0.25$	$S_s = 0.5$	$S_s = 0.75$	$S_s = 1.0$	$S_s \geq 1.25$
A	0.8	0.8	0.8	0.8	0.8
B	1.0	1.0	1.0	1.0	1.0
C	1.2	1.2	1.1	1.0	1.0
D	1.6	1.4	1.2	1.1	1.0
E	2.5	1.7	1.2	0.9	0.9
F	See Section 11.4.7				

Note: Use straight-line interpolation for intermediate values of S_s .

Figure 2.5: Site Coefficient, F_a (American Society of Civil Engineers, 2013)

Mapped Risk-Targeted Maximum Considered Earthquake (MCE _R) Spectral Response Acceleration Parameter at 1-s Period					
Site Class	$S_1 \leq 0.1$	$S_1 = 0.2$	$S_1 = 0.3$	$S_1 = 0.4$	$S_1 \geq 0.5$
A	0.8	0.8	0.8	0.8	0.8
B	1.0	1.0	1.0	1.0	1.0
C	1.7	1.6	1.5	1.4	1.3
D	2.4	2.0	1.8	1.6	1.5
E	3.5	3.2	2.8	2.4	2.4
F	See Section 11.4.7				

Note: Use straight-line interpolation for intermediate values of S_1 .

Figure 2.6: Site Coefficient, F_v (American Society of Civil Engineers, 2013)

2.1.3 Stiffness theory

A beam stiffness is depended on its length when considering a constant cross section along its length. The longer a beam is the less stiff it is on bending. When a bar is loaded with force F in its axial direction, then by Hookse' law, the axial stress is given by equation (2-10).

$$\sigma = E\varepsilon \quad (2-10)$$

Where, σ is the normal stress, E is elastic modulus or Young's modulus and ε is the strain. With the definition of stress and strain as shown in equation (2-11) and (2-12), the displacement δ can be deduced as shown in equation (2-13).

$$\sigma = \frac{F}{A} \quad (2-11)$$

$$\varepsilon = \frac{\delta}{L} \quad (2-12)$$

$$\delta = \frac{L}{EA}(-F) \quad (2-13)$$

Where δ is displacement, A is cross-section area and $\frac{L}{EA}$ is invers of the stiffness. From this equation, one can calculate displacement with the help of applied load and stiffness of the bar (Leander, 2015). When it comes to bending moment M , angular displacement or rotation θ is used as shown in equation (2-14).

$$\theta = \frac{L}{3EI}(-M) \quad (2-14)$$

Where I is second area moment of inertia. If the beams stiffness is unknown, then it can be calculated by the elementary case for end force and end displacement by using formulas in different elementary cases as shown in Figure 2.7.

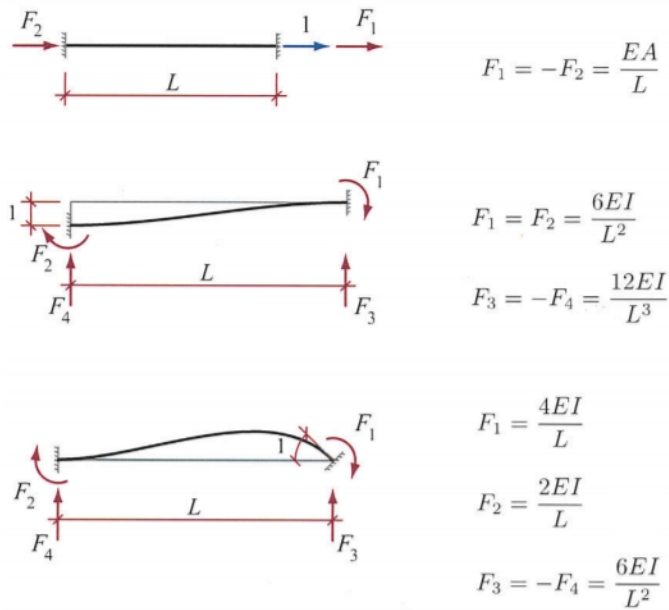


Figure 2.7: Elementary cases for end-forces caused by end- displacement (Leander, 2015)

2.1.4 P-delta effects

P-delta effect is a nonlinear effect and occur when lateral and axial loads affect a building (CSI knowledge base, 2013). This loads will give a second order moment on the building from the lateral deformation “delta” times the sum of the story weights “P” as shown in Figure 2.8.

When a building deflects from a lateral force, the weight of the building will give an additional bending moment due to the eccentricity of the axial force. This second order bending moment will contribute to a larger deflection and this is called the P-delta effect. The height of the building affects the magnitude of the effects since higher buildings deflections are larger than small buildings.

Figure 2.8 shows the P-delta effect and the contributing bending moment.

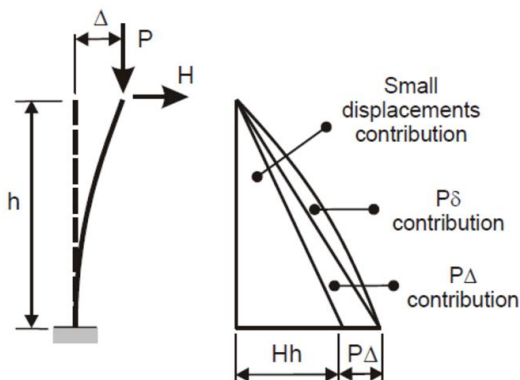


Figure 2.8: Second order bending moment from the P-delta effects of a column (CSI knowledge base, 2013)

2.1.5 Buckling

Buckling is an instability phenomenon that occurs when a beam is submitted to a large normal force (CSI knowledge base, 2014). The critical normal force can be derived from the linear elastic differential equation together with the normal force and the deflection. The general expression for the critical normal load (buckling load) is shown in equation (2-15).

$$N_{cr} = \frac{\pi^2 EI}{(\beta l)^2} \quad (2-15)$$

E = Elastic modulus

I = Second area moment of inertia

βl = Critical buckling length

This applies that the material is linear elastic, that the column is initially straight and has a constant cross section and that the force is applied centrally. If this is not true, second order theory for buckling is needed which is very complex.

Collapse of columns can originate from instability failure or from material failure. To determine which failure is the most critical, the mean stress can be calculated for the critical load as shown in equation (2-16).

$$\sigma_{cr} = \frac{N_{cr}}{A} = \frac{\pi^2 EI}{A(\beta l)^2} \quad (2-16)$$

Where A is the cross-section area. If the mean stress is equal to or smaller than the compressive strength σ_c as shown in equation (2-17).

$$\sigma_{cr} \leq \sigma_c \quad (2-17)$$

The instability stress will be the critical stress.

2.2 Structural systems

2.2.1 Central core and outrigger system

The outrigger system combines two structural systems to improve the performance of the building to be able to build higher. The system uses a central core combined with a perimeter system (Choi, et al., 2012). This reduces the bending moment on the core by adding tension and compression forces on the perimeter system, see figure 1.

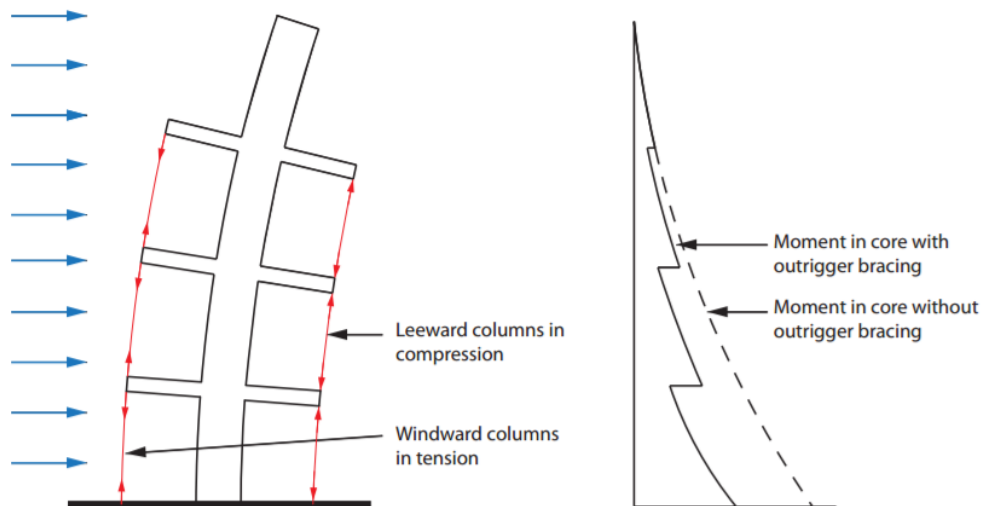


Figure 2.9: Interaction of core and outriggers (Choi, et al., 2012)

2.2.2 Tubed Mega Frame Structures

The Tubed Mega Frame (TMF) is a new structural system for high-rise buildings developed by Tyréns and is an alternative to the central core, see Figure 2.10. The systems have been developed and there are now four main systems: the mega hollow columns with belt or cross walls and the perimeter frame with belt or cross walls. The systems have one or two story belt or cross walls which gives eight different TMF structures. Each system consists of columns placed on the perimeter of the building. Since the bearing structures is moved to the perimeter of the building, the building can resist wind and seismic loads better (King, et al., 2016).



Perimeter frame with
one story belt walls

Perimeter frame with
two story cross walls

Mega Columns with
one story cross walls

Mega Columns with
two story belt walls

Figure 2.10: Tubed Mega Frame structural systems (Svärd & Partovi, 2016)

Jenny Svärd and Arezo Partovi did a global analysis of tall buildings using the TMF systems and compared them to a central core with outrigger perimeter frame. The analysis shows that the perimeter frame with one-story belt walls will give the smallest deflection for all tested heights due to wind load (Svärd & Partovi, 2016). Both including the P-delta effects and without. If the building is loaded with seismic load then the mega columns with one-story belt walls will give the smallest deflections for all heights. Regarding to their results this study will use the perimeter frame with one-story belt walls and the mega columns with one-story belt walls.

2.2.3 Shear wall

Shear walls are structural members designed to resist lateral forces, distribute the forces and connect the mega columns with each other. Shear walls are critical in high-rise buildings because of the increased lateral wind and seismic load (Civilsimplified, 2017).

2.2.4 Bracings

Bracings are structural members that stabilize the main structure by lowering the buckling length and distributing the forces through compression and tension.

2.3 Inclined buildings

The progress in developing high-rise buildings has been escalated in high rate since the first skyscraper has been built. However, the mainstream concept of building upwards in the vertical direction has been a hindrance to the innovation and development of new structural system of mega structure. The reason that lies behind this matter might be the transportation system in the buildings. The existing elevator system, which goes only on vertical direction, has been playing a key role on shape and design of high-rise buildings. Nevertheless, the new elevator system which is multi directional provides the possibilities to develop new design of mega structure in various shape rather than unidirectional.

2.3.1 The structural system of leaning tower

There are very few slanted tall buildings that have been built and because of the complexity of the structural system, and they are not that tall. The two towers in Madrid so called the gate of Europe are 114 meter high and 15° inclined. In order to counteract the overturning weight, the top of the building is anchored by cables to the ground with concrete piles. In addition, the main support system is steel diagrid at the perimeter and with a concrete core in the middle (Winstanley, 2011). The vertical concrete core will stick out of the perimeter of the building as the height increases with respect to inclination and this is the reason that the slanted buildings are not that tall. Further, the capital gate tower of Dubai is also constructed so that the concrete core fits the perimeter of the building from top to bottom. Moreover, 490 concrete piles have been driven down to the ground to support the whole structure and the overhanging of floors at the top (Schofield, 2012). It is difficult to build a building where the whole structural system is slanted because of the overturning dead load that disables the stability. However, with the new structural system like Tubed Mega Frame, it might be easier due to the reduced amount of material that is needed.

2.3.2 Structural approaches for leaning towers

There are different structural approaches that can be applied in order to achieve stability of leaning towers.

Center of gravity above the base

One way of preventing the building from tipping over is to adjust the center of mass right over the base of the building as shown in Figure 2.11. This leads to zero lever arm and zero moment on the base caused by overall building weight. This method might be difficult to accomplish because the building leans away from the base. However, by varying the effective density of different parts of the building from bottom to top and rotating the top of the building slightly to the base will move center of gravity close to the base (Scott, et al., 2007).

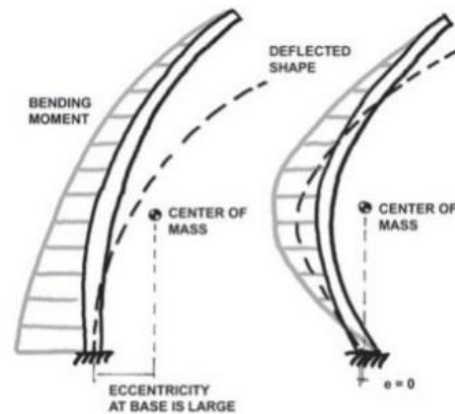


Figure 2.11: Reducing overall bending moment at the base by centering center of mass slightly over the base (Scott, et al., 2007)

Minimizing additional horizontal forces

In this case, the horizontal forces created by the inclination of the column have to be reduced. It can be done by allowing the loads to travel as vertically as possible. A possible approach for this is to minimize the use of inclined columns and use cantilevers instead or transferring out inclined columns to minimize loads on them. A diagrid system is a good example where it allows the loads to find a vertical path to ground (Scott, et al., 2007). The capital gate tower of Dubai was constructed with this system in order to carry loads from the overhang (Schofield, 2012).

Symmetrical Design

This method considers the fact that lateral forces created by opposite inclined column placed symmetrically balance the horizontal forces generated by inclined column. Here, the overall building system has to be symmetrical to ensure this concept (Scott, et al., 2007). However, the structure does not need to be perfectly symmetrical. In fact, the combination of above concepts can come in hand to solve the effect variation in shape.

2.3.3 The conceptual design of tripod structure

A tripod is a three-legged structure where all three legs are inclined to the center and joined at the top as shown in Figure 2.12. The concept of having symmetrical design and center of gravity close to the base is used in order to achieve a rather stable structure in general. The meeting point at the top assists in cancelling out all the horizontal forces that are generated from all three inclined legs due to dead load. However, the complexity arises from the prolonged part at the top, which gives a big bending moment at the joint. The triangular cross-section of the building presents a more distinctive feature compared to the conventional rectangular cross-section.

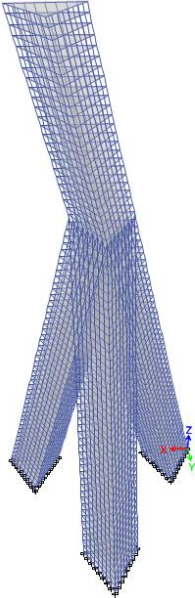


Figure 2.12: Tripod shaped building

3 Finite Element Method

3.1 What is FEM

A way of controlling if a structure, as a high-rise building, stands with no failure is to numerically simulate the boundary. Today, modern technology provides us with computers that are capable of handling complex data analysis and simulations.

Designing a high-rise building is a complex and costly project where every small part of it should be mathematically analyzed to describe its behavior in physical system. For a proper understanding, a mathematical model is needed in order to simulate the structural behavior in real case scenario where buildings are confronted with various loads and forces.

The finite element method is one of the most used methods for solving problems regarding steady or transient problems in linear and nonlinear region for one-, two- and three dimensional domains (Dhatt, et al., 2012). It can also be applied to the structures with complex geometrical form in heterogeneous environment. FEM can be described as a numerical solution method that consists of using simple approximation of unknown variables to transform partial differential equation to algebraic equations. The idea of this method is discretization, which consists of simplification of structure where a main domain is divided to simpler parts or finite elements and each element is formulated in the same manner and connected through nodes. All the elements are then assembled to form the complete structure.

FE method uses a system of algebraic equations to numerically solve differential equations. The general procedure is to find a local stiffness matrix $[k]$ for each element to transform and assemble the global stiffness matrix, $[K]$. Thereafter determine a global load vector, $[R]$ and reduce the system due to boundary conditions. The displacement at all nodes can now be determined by solving equation (3-1).

$$\{D\} = [K]^{-1}\{R\} \quad (3-1)$$

$\{D\}$ = Displacement vector

From the displacement, it is possible to calculate stresses and reaction forces.

There are plenty of different element types. There are bar, beam, shell, solid elements etc. Bar elements only consider axial stiffness and no bending stiffness. Therefore, it is important to have knowledge of them to be able to know that type of elements one should use. If shell elements are used there are two different theories that can be applied, Kirchoff or Mindlin theory. Kirchoff elements does now consider shear stress and are used for thin elements. Mindlin elements consider shear stress and are thicker.

There are two types of P-delta effects, P- δ (P-“small delta”) and P- Δ (P-“big delta”). The P- δ effects accounts for local deformations between two end nodes of an finite element while the P- Δ effects considers the displacement relative to member ends (CSI knowledge base, 2013).

The reasons for choosing the FE method is mainly about the various options it provides. In FEM, there are different types of element that can be applied to idealize different forms of physical system. The material properties can be defined by its parameter whether it is elastic, plastic, combination of elastic and plastic and homogenous or heterogeneous. The boundary conditions will define how the structure is supported and its rigidity. The various load types such as dead load, external load, wind and snow load, temperature load, creep load and more can be applied in the way where it resembles the real-world target. The possibility of having a control of variables and repeatability of the process makes it more reliable, flexible and robust.

3.2 SAP2000

SAP is a one of CSIs finite element methods software, which is used for both analysis, and design of structures in different fields, for instances; transportation, industries, buildings and other facilities. It can model from simple one-dimensional objects to 3D based advanced geometric objects. Apart from other finite element method programs, it allows engineers to work on different cases, namely, deformation analysis, Eigen and Ritz analyses based on stiffness of nonlinear shell cases, material nonlinear analysis with hinges, buckling analysis, catenary cable analysis, multi layered nonlinear shell element and lots of other features that involves finite nonlinear analyses (CSI SAP2000, 2017).

3.3 ETABS

CSI ETABS is an engineering software tool that uses finite element method for multi-story buildings analysis and design. Its refinement on the 3D based modeling, schematic drawings and visualization tools makes it easier for designer to understand and have more control on design and analysis (CSI ETABS, 2017). This automatically increases the internal validity of the outcome where the designer has full control of what he is doing. The complex building types has a complex geometry, which means more complexity on understanding structural behavior. Nevertheless, once this behavior is captured and visualized in details, the complications on understanding the results data can be decreased.

The additional features of ETABS is its interoperability with other related software. In this project, the model that architects have designed will be imported and analyzed. The compatibility it has with other design software makes it easier for engineer to detail, analyze and design the distinctive level of models (CSI ETABS, 2017).

4 Pre-study of the Tripod shaped building

4.1 SAP2000 analysis

4.1.1 Shape performance

A pre-study was performed to compare different heights and angles to find a “good” shape, by modeling simple stick models in SAP2000. The tested heights were: 270 m, 330 m, 390 m and 450 m. Different angles were tested. They were decided such that the distance between the “legs” base should not be less than 30 m. For the 270 m high tripod, the lowest angle is 11° to the vertical line. The highest angle is set to 15° , to be the same angle as Gate of Europe Towers in Spain. See Table 4-1 for all heights and angles.

Table 4-1: Heights and angles for stick model

HEIGHT [m]	ANGLE [$^{\circ}$]
270	11, 12, 13, 14, 15
330	9, 10, 11, 12, 13
390	8, 9, 10, 11
450	7, 8, 9, 10

In total, 18 different shapes were tested in SAP2000. The cross-section for the stick model was a concrete box with the dimension 10m x 10m and a thickness of 0.5 m. This box was the same for all heights and angles to be able to compare them. The only considered load in the pre-study analysis was dead load. The points at the base were fixed restraints.

The maximum deflections and bending moments were compared and shown in Table 4-2. Maximum deflections were found in the top part of the building (node 8), and the maximum bending moments are in node 7. See Figure 4.1 for the node numbering.

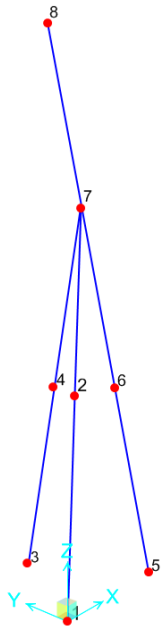


Figure 4.1: Node numbers of the stick model

Table 4-2: Bending moments and displacements for the stick models caused by dead load

Building		Bending moment (at node 7) [MNm]	Displacement U1 (at node 8) [m]	Displacement U2 (at node 8) [m]	Displacement U3 (at node 8) [m]
Height [m]	Inclination [°]				
270	11	-380.83	-0.1098	0.0634	-0.0380
	12	-417.92	-0.1181	0.0682	-0.0425
	13	-455.68	-0.1269	0.0733	-0.0475
	14	-494.18	-0.1366	0.0781	-0.0536
	15	-533.49	-0.1458	0.0842	-0.0592
330	9	-460.69	-0.1960	0.1132	-0.0553
	10	-514.41	-0.2138	0.1182	-0.0635
	11	-568.89	-0.2315	0.1337	-0.0718
	12	-624.30	-0.2506	0.1447	-0.0816
	13	-680.71	-0.2707	0.1563	-0.0925
390	8	-569.47	-0.3315	0.1914	-0.0807
	9	-643.45	-0.3646	0.2105	-0.0938
	10	-718.44	-0.3993	0.2306	-0.1087
	11	-794.56	-0.4358	0.2516	-0.1255
450	7	-660.86	-0.5084	0.2935	-0.1076
	8	-758.17	-0.5656	0.3265	-0.1275
	9	-856.66	-0.6258	0.3613	-0.1505
	10	-956.50	-0.6887	0.3976	-0.1766

Figure 4.2 to Figure 4.5 shows the bending moment for the stick models in each node and for all the angles caused by the dead load only. It is clear that the bending moment was linear when increasing the angles. The derivative of point 7 was the highest, which means that the bending moment would increase more in point 7 for every angle compared to the other points.

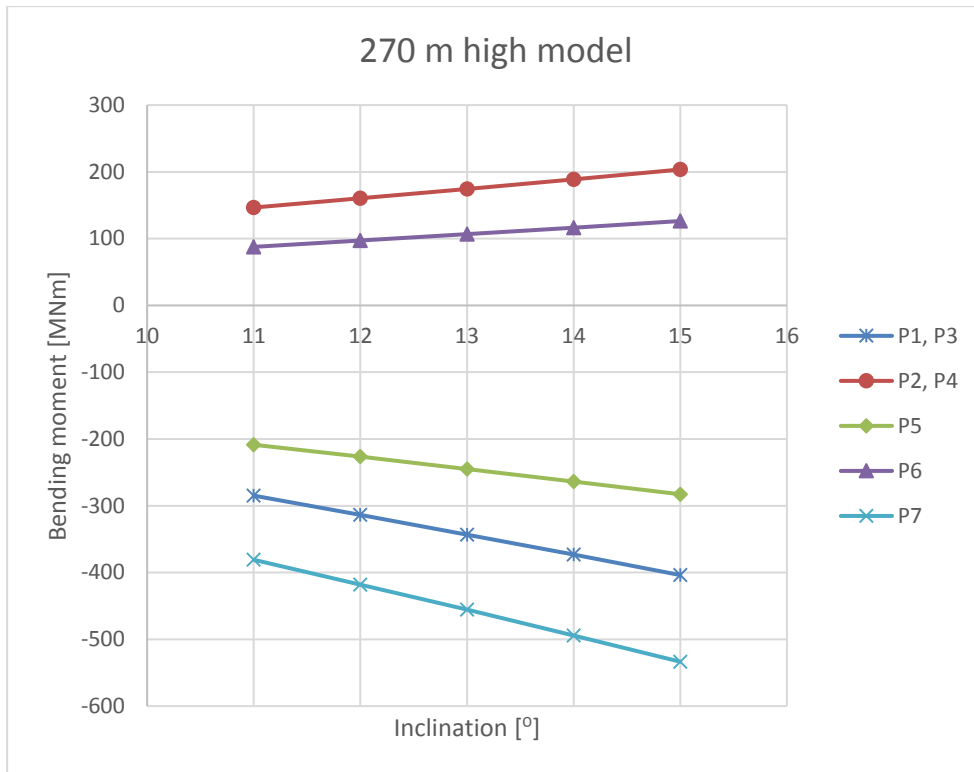


Figure 4.2: Bending moment at node P1-P7 for the 270 m high models caused by dead load



Figure 4.3: Bending moment at node P1-P7 for the 330 m high stick models caused by dead load

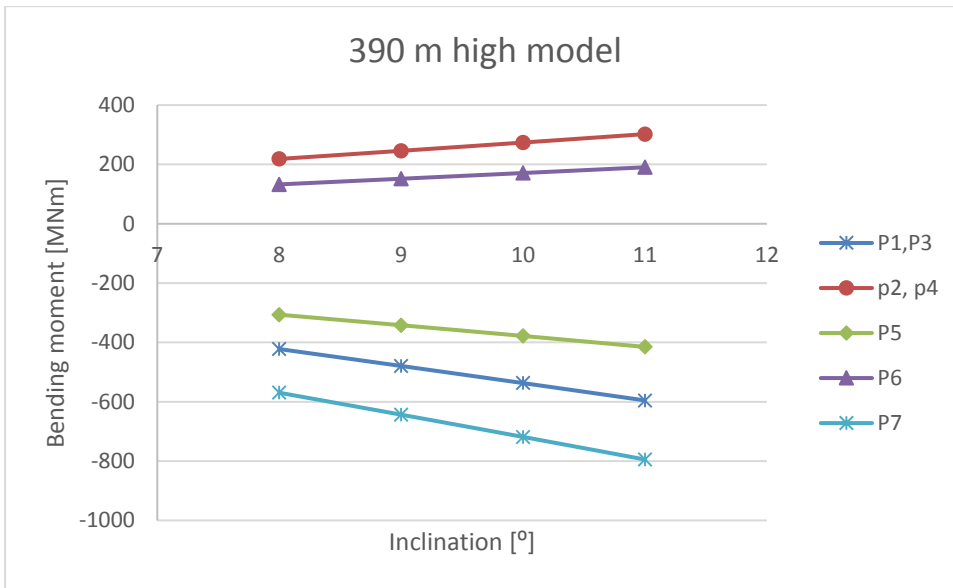


Figure 4.4: Bending moment at node P1-P7 for the 390 m high stick models caused by dead load

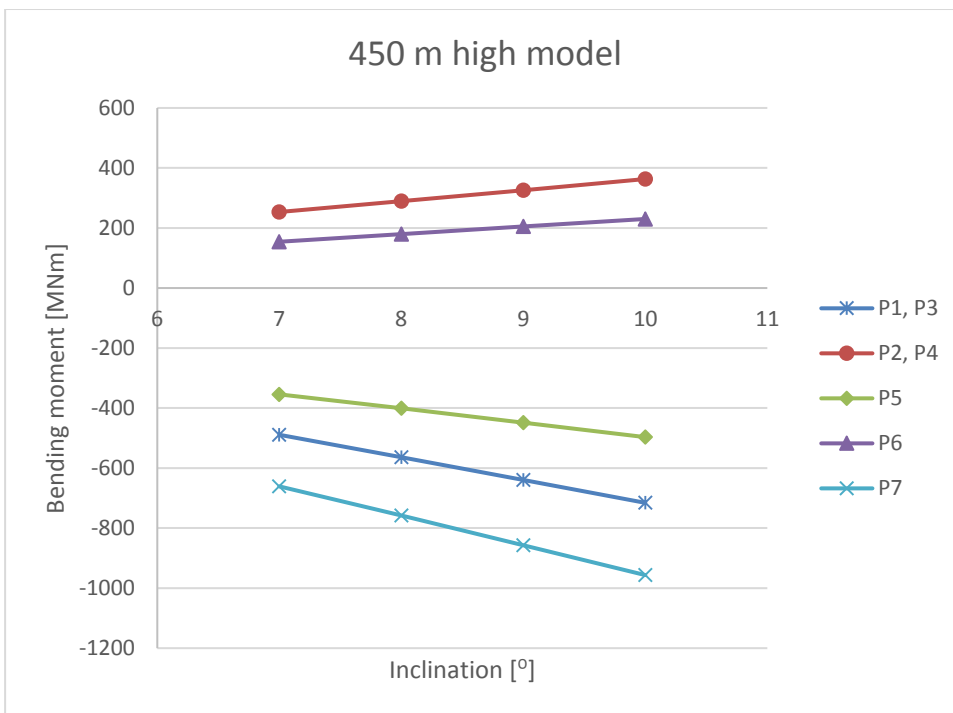


Figure 4.5: Bending moment at node P1-P7 for the 450 m high stick models caused by dead load

The higher the model, the higher became the bending moments. When the building had a fixed inclination and the bending moment was checked for different heights, Figure 4.6 and Figure 4.7 shows that the bending moment became nonlinear. This means that the height of the model had a bigger impact on the bending moment than the inclination. The bending moment at node 7 of the 270 m high, 14⁰-inclined model was compared to the 450 m high, 7⁰-inclined model. We can see the values from Table 4-2 to be -494.18 and -660.86 MNm. The inclination was

half but even though the height was not double, the bending moment was higher for the 450 m tall model. This made it more reasonable to continue with the 270 m high, 15° inclined model.

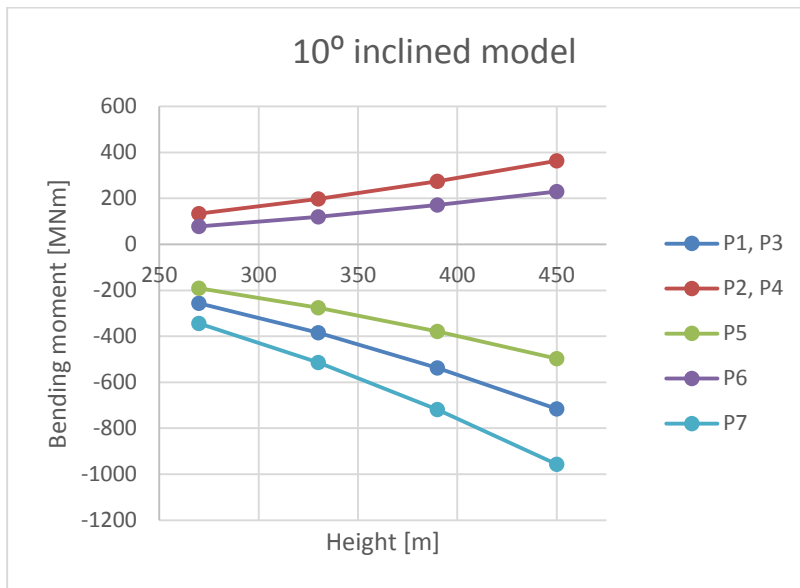


Figure 4.6, Bending moment at node P1-P7 for the 10° inclined models caused by dead load

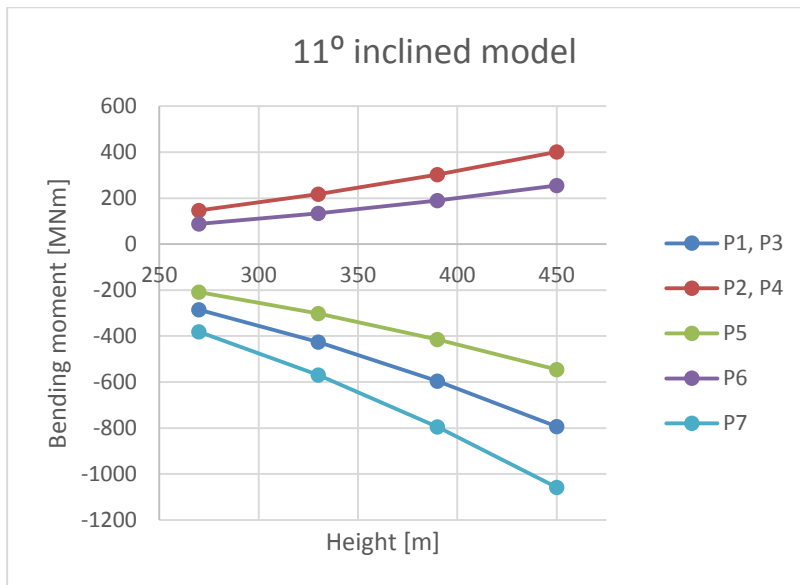


Figure 4.7, Bending moment at node P1-P7 for the 11° inclined models caused by dead load

This can also be clarified by expressing a formula for the bending moment for the model. The bending moment M is the force F times the lever arm l as shown in equation (4-1)

$$M = F \cdot l \tag{ 4-1 }$$

The force F is the dead load of the structure as shown in equation (4-2)

$$F = \rho g V = \rho g A x \tag{ 4-2 }$$

$\rho = \text{density of concrete}$
 $g = \text{gravitational acceleration}$
 $A = \text{cross sectional area}$
 $x = \text{the length of the cross section}$

Since the height H is the vertical height of the upper part of the building and the building is inclined the length of the upper part of the building x can be calculated by equation (4-3).

$$x = \frac{H}{\sin \alpha} \quad (4-3)$$

Where x is the member length from node 7-8 in Figure 4.1, where the angle α is the angle from the inclined member to a horizontal line, see Figure 4.8.

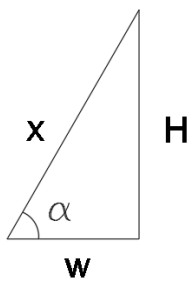


Figure 4.8: Angle for the top part of the building

The lever arm is half of w since the central of gravity will be in half of the length of x . In terms of H , the lever arm can be calculated by equation (4-4).

$$l = \frac{w}{2} = \frac{H}{2 \tan \alpha} \quad (4-4)$$

The total bending moment at point 7 will therefore be obtained from equation (4-5).

$$M = \rho g A \cdot \frac{H^2}{2 \sin(\alpha) \tan(\alpha)} \quad (4-5)$$

It is now clear that the bending moment is not linear to the height, however the bending moment is not linear to the angel either. When looking at the figures of the bending moment and inclinations (Figure 4.2 to Figure 4.5) it is hard to see that the bending moment is not increasing linear. Figure 4.9 and Figure 4.10 shows the non-linearity of the bending moment as the function of the height and the inclination angle respectively.

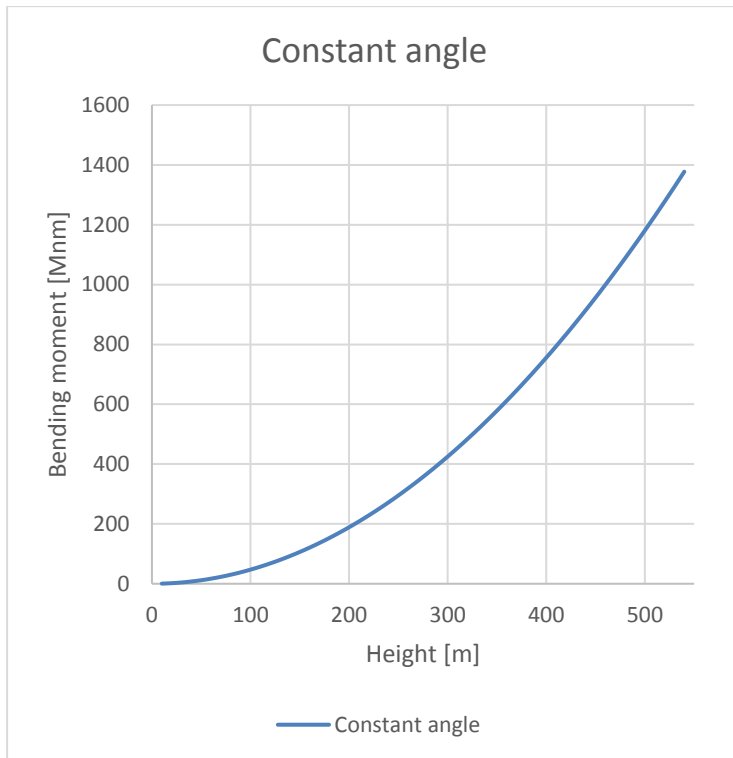


Figure 4.9: Constant angle

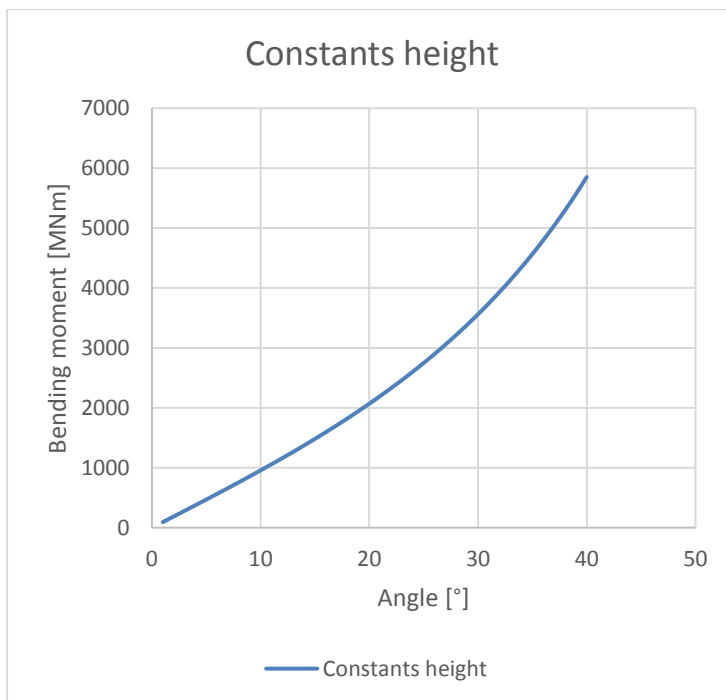


Figure 4.10: Constant height

Figure 4.10 shows that increasing of the angle seems close to linear until 20 degrees. This is why it was hard to notice non-linearity from the tables. With a constant angle (Figure 4.9), the bending moment is parabolic and will therefore increase with the height to the power of two.

4.1.2 Bracing performance

Different bracing-systems were analyzed in SAP2000 to check the performance regarding displacement, see Figure 4.11. The volume of the bracings was constant to be able to compare the different types. Both concrete and steel bracings were analyzed. Analysis of buckling and cracks were not performed in this study nor was the influence of dead or live loads.

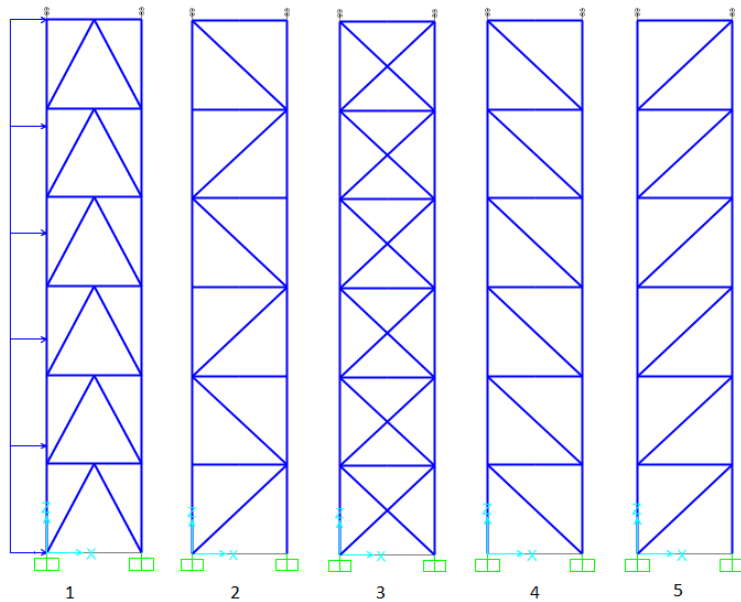


Figure 4.11: Bracing-systems

A uniform distributed load was applied along the z-axis in the positive x-axis direction. The deflections were compared in Table 4-3.

Table 4-3: Maximum deformation caused by uniform distributed load on bracing systems

	Deformation					
		x-axis	y-axis	z-axis	x-axis	z-axis
		[m]	[m]	[m]	[relative] [m]	[relative] [m]
Concrete	System 1	0,16037	0	-0,01129	1,0000	1,0009
	System 2	0,182524	0	-0,01554	1,1381	1,3777
	System 3	0,167614	0	-0,01471	1,0452	1,3041
	System 4	0,197136	0	-0,01128	1,2293	1,0000
Steel	System 1	0,379628	0	-0,01136	1,3404	1,0009
	System 2	0,375293	0	-0,0154	1,3251	1,3568
	System 3	0,283212	0	-0,01471	1,0000	1,2960
	System 4	0,44145	0	-0,01135	1,5587	1,0000
	System 5	0,469229	0	-0,01855	1,6568	1,6344

It was not possible to compare the concrete and steel deflections against each other since different volumes had been used for concrete and steel. However, the different systems were

compared for concrete and steel separately. For the concrete bracings, the best performing system was system 1 followed by system 3 in deflection in x-direction. The deflection in z-direction was smallest for system 4, but since this system had 23 % higher deflection in x-direction and that the deflection in z-direction was less than 1/10 of the deflection in the x-direction, system 1 and 3 had better performance. This was the same when using steel. However, when using steel system 3 was performing much better than the other systems. With respect to this pre-study, system 3 was chosen as the bracing system for the desired models.

4.2 Structural systems

Two different shapes were to be analyzed. The 450 m high, 7° inclined building and the 270 m high, 15° inclined building. For these buildings, the two types of TMF according to Jenny Svård and Arezo Partovis (2016) result were tested. Bracing system 3 according to the pre-study regarding braces was also applied on the buildings instead of the shear walls. And also a moment frame with and without belt walls and mega columns with six mega columns instead of three was tested. In total, five different structural system was tested for each building.

450 m, 7°

- Perimeter frame, one-story belt walls
- Perimeter frame, without belt wall
- Three mega columns, one-story belt walls
- Six mega columns, one-story belt walls
- Three mega columns, bracing system 3

270 m, 15°

- Perimeter frame, one-story belt walls
- Perimeter frame, without belt wall
- Three mega columns, one-story belt walls
- Six mega columns, one-story belt walls
- Three mega columns, bracing system 3

5 ETABS analysis

The amount of material volume used in all structural systems were approximately the same, which was to ease the comparison between them. The models were analyzed with and without P-delta effect to see the differences. The columns were run as stick model while the belt walls were meshed by automatic rectangular mesh of 1.25m element size. The floor slab was a 250 mm thick concrete slab. Cracking of concrete and limitation regarding serviceability was not considered.

5.1 Loads acting on the building

5.1.1 Dead load

The dead load was gravitational load of the building which included all the self-weight from frames, beams, braces, walls and floor slabs. Those members were made of reinforced concrete with a density of 25 kN/m³.

5.1.2 Live load

The load of 2,5 KN/m² was put on the floors as a live load for offices based on Eurocode 1, EN 1991-1-1.

5.1.3 Wind load

In order to apply wind loads on the building, diaphragms had been created on the all three legs and above the legs separately see Figure 5.1 and Figure 5.2. The input values for the analysis was taken from the previous master thesis by Han Zhang (2014), see Figure 5.3.

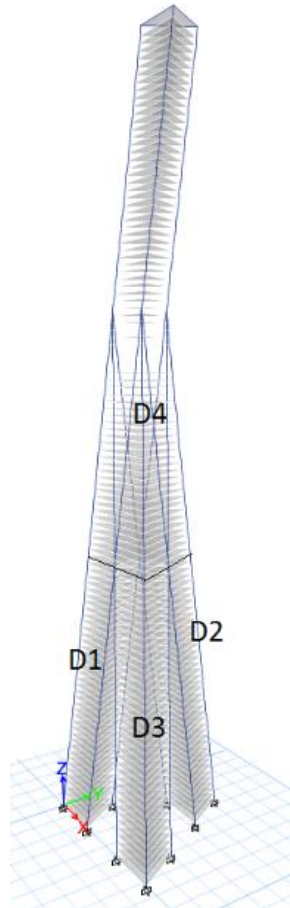


Figure 5.1: Diaphragms for different part of the building, 450 m

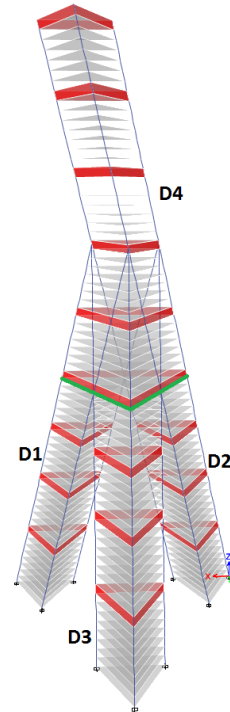


Figure 5.2: Diaphragms for different part of the building, 270 m

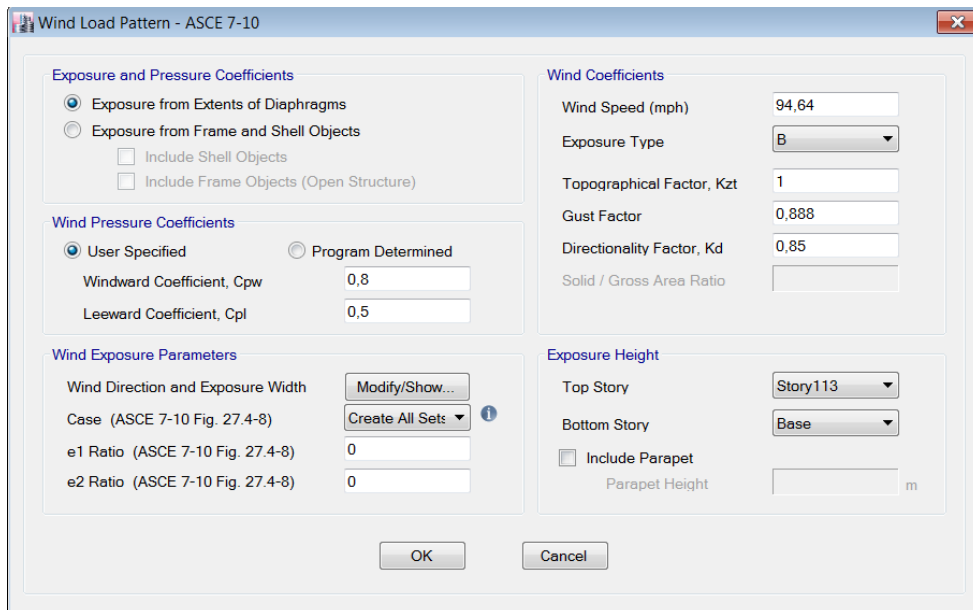


Figure 5.3: Input data for wind load

ETABS generated wind load for 12 different sets and four cases. The different cases are shown in Figure 5.4.

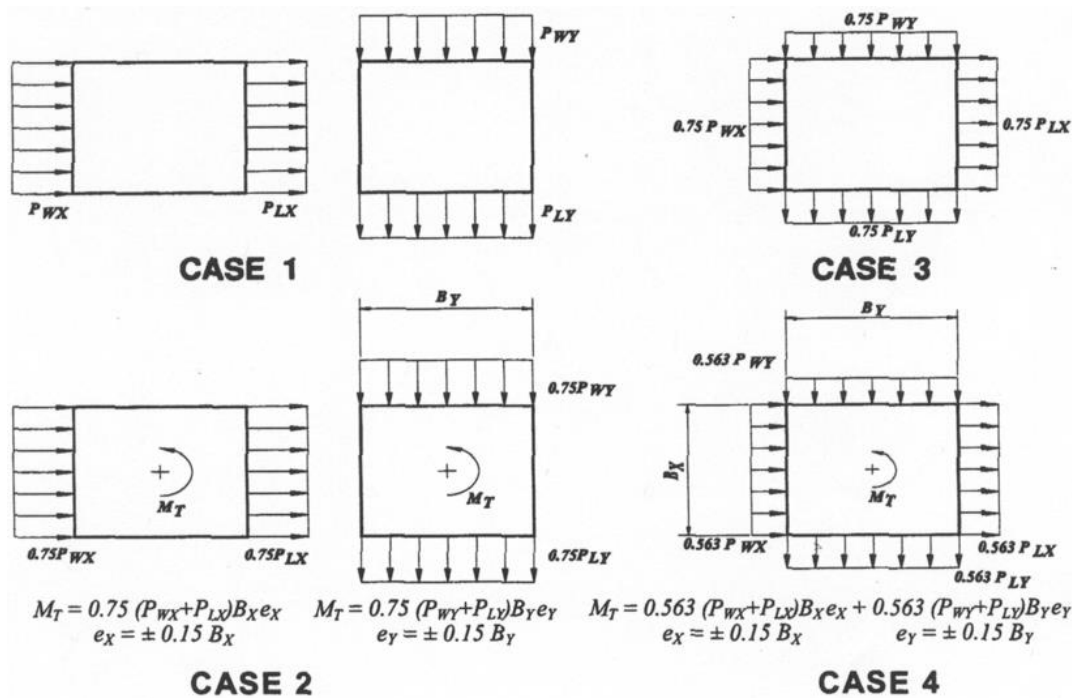


Figure 5.4: Wind cases acting on the building (American Society of Civil Engineers, 2013)

Explanation for the cases are from ASCE 7-10 (American Society of Civil Engineers, 2013).

- Case 1.** Full design wind pressure acting on the projected area perpendicular to each principal axis of the structure, considered separately along each principal axis.
- Case 2.** Three quarters of the design wind pressure acting on the projected area perpendicular to each principal axis of the structure in conjunction with a torsional moments as shown, considered separately for each axis.
- Case 3.** Wind loading as defined in case 1, but considered to act simultaneously at 75% of the specified value.
- Case 4.** Wind loading as defined in case 2, but considered to act simultaneously at 75% of the specified value.

Table 5-1 shows how ETABS used the different cases for the sets.

Table 5-1: Wind cases for both buildings

	270 m		450 m	
Set	Angle	Case	Angle	Case
1	0	1	90	1
2	90	1	180	1
3	0	2	90	2
4	0	2	90	2
5	90	2	180	2
6	90	2	180	2

7	0	3	90	3
8	90	3	180	3
9	0	4	90	4
10	0	4	90	4
11	90	4	180	4
12	90	4	180	4

5.1.4 Seismic load

ETABS automatically generated 6 different cases from different direction around the building for the seismic load. The input data for the seismic load were taken from thesis work done by Han Zhang (2014), see Figure 5.5.

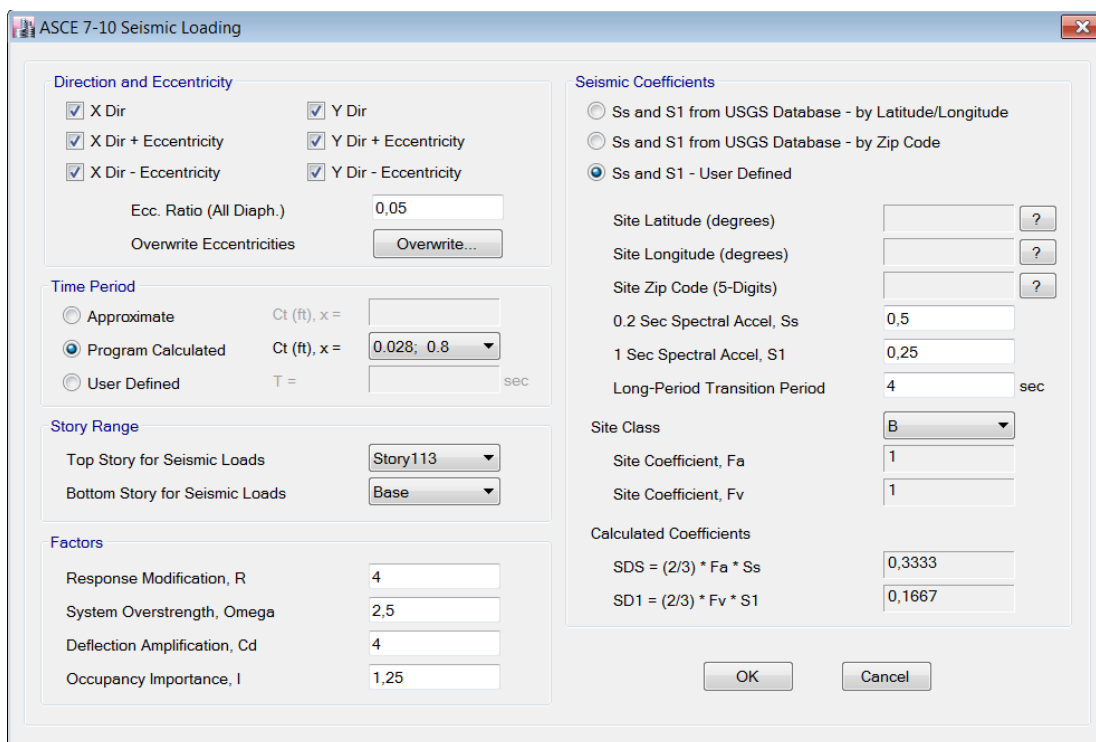


Figure 5.5: Input data for seismic load

5.2 Structural systems

The tube mega frame structures were already introduced in the previous studies and proved to have better performance than the core system. Different types of tube mega frames were applied for this slanted tripod building with two different heights. There were five models built with those systems for each height. The lateral displacement due to wind load and seismic load in the ultimate limit state according to ASCE and also natural periods were evaluated.

5.2.1 Properties

The buildings were tripod shaped with equilateral triangular cross sections. The dimension of the triangular cross sections in each leg were 30 m. The buildings were 270 m and 450 m high with 70 and 113 stories respectively. Each floor had the height, h according to equation (4-5).

$$h = 4 \cdot \sin(\alpha) \quad (4-5)$$

Where α is the angle of the building to the horizontal plane. For the 270 m and the 450 m high building the floor height was 3.86 m and building 3.97 m respectively. Each building was modelled with a 250 mm thick concrete slab of class 90/105. The belt walls had the thickness of 750 mm and had the same strength class as the concrete slab. The mega columns were hollow and made of reinforced concrete with strength class 90/105.

5.2.2 Mega columns with belt wall

This system had a perimeter frame of three mega columns enclosed by belt walls. For the 450 m building, the belt walls were placed at every seventh floor except for the joint area where belt wall was placed at sixth floor. Beams of dimension $1.5 \times 1.1 \text{ m}^2$ as shown in Figure 5.6 connected the top floor. For the 270 m building, the belt wall was at every eight floor, except at the third and fourth belt wall with a spacing of seven floors, see Figure 5.7. The belt wall had a thickness of 750mm. The mega columns were hollow rectangular reinforced concrete of strength class 90/105 as shown in

Figure 5.8. The orientations of the columns were the same as the inclination of the building for all the mega column buildings, see Figure 5.9.

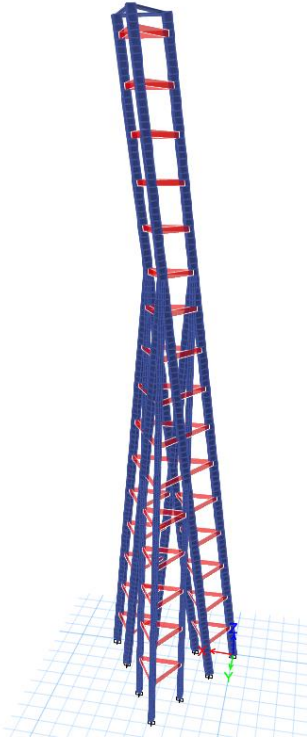


Figure 5.6: 3 Mega columns with belt wall, 450 m high

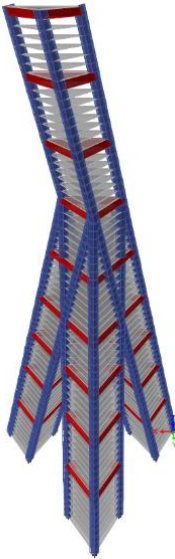


Figure 5.7: 3 Mega columns with belt wall, 270 m high

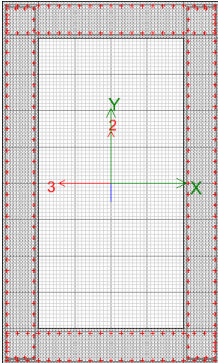


Figure 5.8: Cross-section, 5x3x0.5 m³

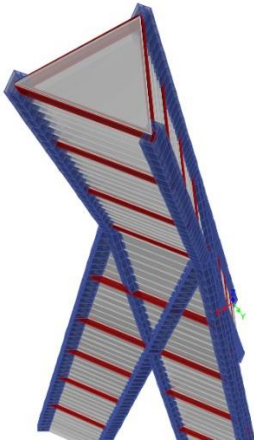


Figure 5.9: Direction of the cross section

5.2.3 Six mega columns with belt wall

This system had a perimeter frame of six concrete columns enclosed by belt walls. The belt walls were at every floor according to the 3 mega columns for the 450 m and the 270 high building, see Figure 5.10 and Figure 5.11. The belt wall had a thickness of 750mm. The mega columns were hollow rectangular reinforced concrete of strength class 90/105 as shown in Figure 5.8.

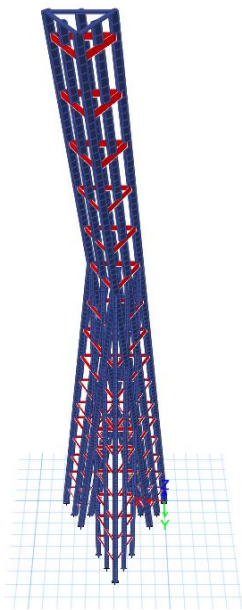


Figure 5.10: 6 mega columns with belt wall, 450 m high



Figure 5.11: 6 mega columns with belt wall, 270 m high

5.2.4 Mega columns with bracings

This system had perimeter frame of mega columns and X-bracings. For the 450 m high building, X-bracings were placed at every seventh floor as shown in Figure 5.12. For the 270 m building, the distance of the bracings were eight floors for the two lowest, seven floors for the third and fourth bracings, eight floors for the fifth and sixth and the upper four are six floors, see Figure 5.13. Horizontal beams tied up the braces across the floor plan. The force from the mega hollow column were transferred to the X- bracings as a compressional and tensional stress. The mega columns were the same size as used in mega column with belt walls.



Figure 5.12: 3 mega columns with bracings,
450 m high



Figure 5.13: 3 mega columns with bracings,
270 m high

5.2.5 Perimeter frame with belt wall

This system had a perimeter frame of concrete columns and beams encircled by belt walls. The belt walls were at every floor according to the 3 mega columns for the 450 m and the 270 m high building, see Figure 5.14 and Figure 5.15. The belt wall had a thickness of 750mm. The concrete had the highest strength capacity of C90/105 and reinforcement bar of size of 25mm. The columns were quadratic and were placed in the central distance of 3.75 m from each other. There were nine columns in each side of the leg which were rigidly drawn to ground. Quadratic beams were placed in every floor as shown in Figure 5.16.

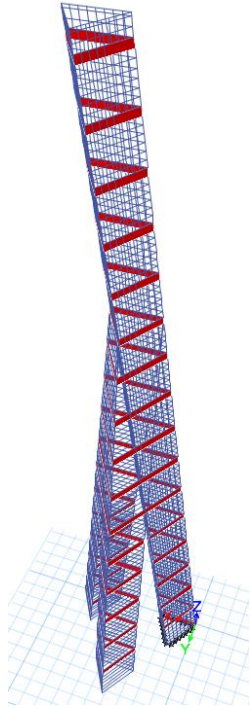


Figure 5.14: Perimeter frame with belt walls, 450 m high

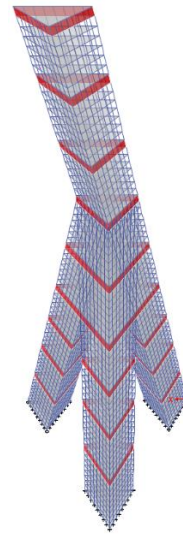


Figure 5.15: Perimeter frame with belt walls, 270 m high

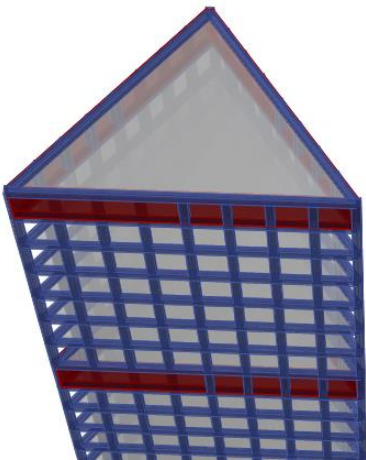


Figure 5.16: 3D view of perimeter frame with belt walls

5.2.6 Perimeter frame

This system was similar to the perimeter frame with belt wall but it lacked belt walls as shown in Figure 5.17 and Figure 5.18.

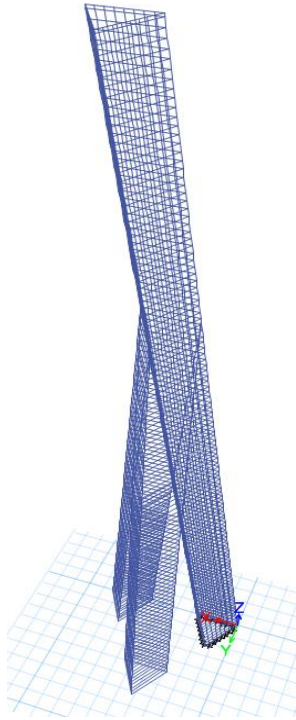


Figure 5.17: Perimeter frame, 450 m high

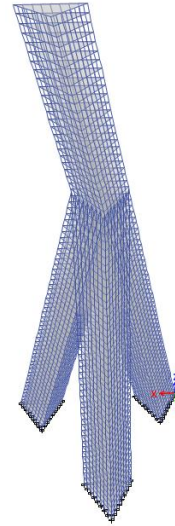


Figure 5.18: Perimeter frame, 270 m high

5.3 Comparison

To achieve constancy of one factor, i.e. total volume of the building, the dimension of the building was estimated in consideration of equal total volume for all the models. To begin with, dimensions for the three mega columns with belt wall i.e. $5 \times 3 \times 0.5 \text{ m}^3$ as shown in

Figure 5.8, were chosen as the basis for calculation of dimensions for rest of the models. The volume of belt walls used in mega columns were equivalent to the total volume of bracings used in system for mega column with bracings. The volume of three mega columns were equivalent to the volume of six mega column system. In addition, the volume of belt walls was equivalent to the beams that were used in perimeter frame system without belt walls. For the perimeter frame with belt wall the, volume of both columns and beams were equivalent to the volume of three mega columns. The dimensions for all the systems are shown in Table 5-2. For more detail, see Appendix C – Hand calculations.

Table 5-2: Dimensions for all the systems

System, 450 m		Dimension
Three Mega columns	Columns	$5 \times 3 \times 0.5 \text{ m}^3$
	Belt walls	0.75 m
Six Mega columns	Columns	$3.5 \times 2.1 \times 0.35 \text{ m}^3$
	Belt wall	0.75m
Three Mega columns with bracings	Columns	$5 \times 3 \times 0.5 \text{ m}^3$
	Bracings	$0.907 \times 0.907 \text{ m}^2$
Perimeter frame with belt walls	Columns	$0.755 \times 0.755 \text{ m}^2$
	Beams	$0.629 \times 0.629 \text{ m}^2$
	Belt walls	0.75 m^2
Perimeter frame without belt walls	Columns	$0.930 \times 0.930 \text{ m}^2$
	Beams	$0.629 \times 0.629 \text{ m}^2$
System, 270 m		
Three Mega columns	Columns	$5 \times 3 \times 0.5 \text{ m}^3$
	Belt walls	0.75 m
Six Mega columns	Columns	$3.5 \times 2.1 \times 0.35 \text{ m}^3$
	Belt wall	0.75m
Three Mega columns with bracings	Columns	$5 \times 3 \times 0.5 \text{ m}^3$
	Bracings	$0.827 \times 0.827 \text{ m}^2$
Perimeter frame with belt walls	Columns	$0.774 \times 0.774 \text{ m}^2$
	Beams	$0.587 \times 0.587 \text{ m}^2$
	Belt walls	0.75 m
Perimeter frame without belt walls	Columns	$0.936 \times 0.936 \text{ m}^2$
	Beams	$0.587 \times 0.587 \text{ m}^2$

5.3.1 Deformations and periods for the 450 m high building

The building was asymmetric and slanted. Because of that displacement in both x and y directions were evaluated. As it can be seen in Table 5-3, the least displacement where P-delta effect is excluded, was achieved by the bracings system for both wind and seismic load which was 327 mm in x-axis, 377 mm in y-axis and 423 mm in x-axis 432 in y-axis respectively. The highest displacement was achieved by perimeter frame with belt walls, which was 808 mm in y-axis due to wind load and 1040 mm in y-axis due to seismic load. The 3D view of displacement was presented in Appendix A – Deformations.

Table 5-3: Displacement due to wind load and seismic load without p-delta effect

450 m (P-delta effects excluded)	Wind disp. UX [mm]	Wind disp. UY [mm]	Seismic disp. UX [mm]	Seismic disp. UY [mm]
TMF: 3 mega columns with belt walls	352.3	415.1	465.4	495.5
TMF: 6 mega columns with belt walls	426.12	509.0	575.3	624.3
TMF: 3 mega columns with bracings	327.4	376.6	423.0	431.9
TMF: Perimeter frame with belt walls	707.5	808.3	1002.8	1040.0
Perimeter frame	585.6	669.1	815.6	852.7

When the P-delta effect was introduced in the model, for the perimeter frame, the displacement due to wind load increased from 808 mm to 873 mm (7.9%) in y-axis and the displacement due to seismic load increased from 1040 mm to 1137 mm (9.3%) in y-direction. Table 5-4 shows the increase of displacement when P-delta is included in the analysis.

Table 5-4: Displacement due to wind load and seismic load with p-delta effect

450 m (P-delta effects included)	Wind disp. UX [mm]	Wind disp. UY [mm]	Seismic disp. UX [mm]	Seismic disp. UY [mm]
TMF: 3 mega columns with belt walls	363.7	429.2	481.4	513.9
TMF: 6 mega columns with belt walls	443.2	531.2	600.6	655.3
TMF: 3 mega columns with bracings	337.5	388.3	436.1	445.6
TMF: Perimeter frame with belt walls	763.8	872.7	1087.1	1136.6
Perimeter frame	704.7	799.9	1036.4	1097.0

Because of the tripod shape, the building was stiff on the base. Therefore, the modal periods were rather small for a building of these heights as shown in Table 5-5 and Table 5-6. The first and second period showed lateral movement in the x-direction and third period showed the torsional movement. The second period was smaller than the first one since the vibration of the building was absorbed by its three legs. The highest period was obtained in the perimeter frame for both including p-delta effects and excluding p-delta effects. And the lowest period was obtained in the mega columns with bracings for both including and excluding P-delta effects.

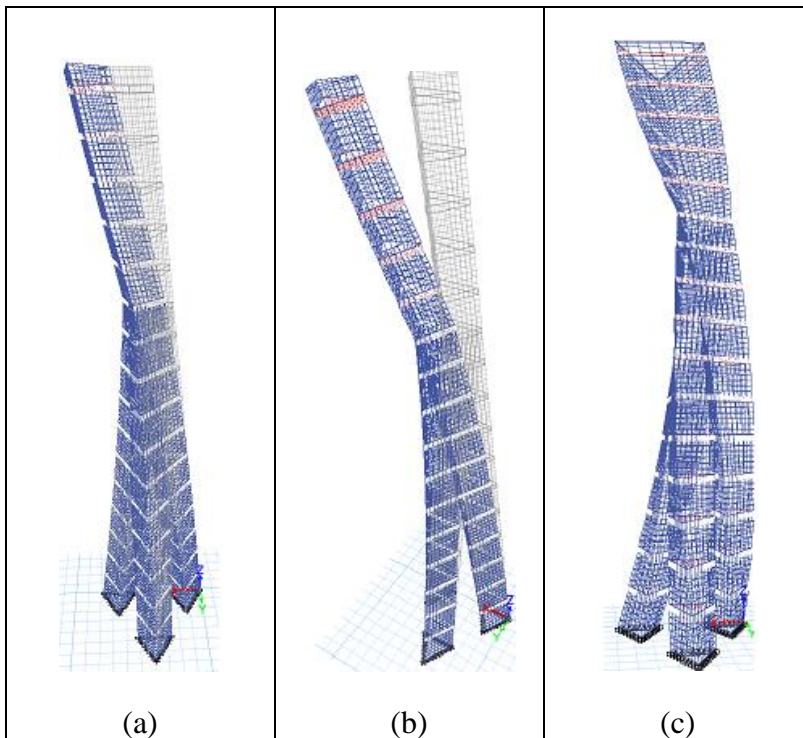


Figure 5.19: Example of modal deformation (a) mode 1, (b) mode 2 and (c) mode 3

Table 5-5: Periods without P-delta effects

450 m (P-delta effects excluded)	Period Mode 1 [s]	Period Mode 2 [s]	Period Mode 3 [s]
TMF: 3 mega columns with belt walls	5.039	4.841	2.894
TMF: 6 mega columns with belt walls	5.543	5.202	3.212
TMF: 3 mega columns with bracings	4.693	4.632	2.174
TMF: Perimeter frame with belt walls	7.049	6.791	4.328
Perimeter frame	6.398	6.088	4.272

Table 5-6: Periods with P-delta effects

450 m (P-delta effects included)	Period Mode 1 [s]	Period Mode 2 [s]	Period Mode 3 [s]
TMF: 3 mega columns with belt walls	5.13	4.916	2.955
TMF: 6 mega columns with belt walls	5.679	5.299	3.302
TMF: 3 mega columns with bracings	4.765	4.700	2.207
TMF: Perimeter frame with belt walls	7.388	7.032	4.586
Perimeter frame	6.673	6.277	4.25

The percentage increase of displacement with P-delta effect and without P-delta effect are presented in Table 5-7.

Table 5-7: Percentage increase of displacement when p-delta effect is included

450 m	Wind disp. UX [%]	Wind disp. UY [%]	Seismic disp. UX [%]	Seismic disp. UY [%]
TMF: 3 mega columns with belt walls	3.2	3.4	3.4	3.7
TMF: 6 mega columns with belt walls	4.0	4.4	4.4	4.96
TMF: 3 mega columns with bracings	3.0	3.1	3.1	3.2
TMF: Perimeter frame with belt walls	7.9	7.9	8.4	9.3
Perimeter frame	20.3	19.5	27.0	28.7

Figure 5.20 shows the diaphragm center of mass displacement for two diaphragms. Not all three displacement of the legs were included, because the main purpose was to show different performance of all five systems that were used in the buildings. The diaphragm D1 started from base to story 40. From story 40 to 113 was a prolongation of D1 which is named Diaphragm D4. The displacement for each diaphragm representing each leg are shown in Appendix B – Displacements. The figures show the maximum value of displacement in y-direction only, for all cases. The MF in the legend of the all the displacement figures is the Perimeter frame which acts as a moment frame and the MC are the mega columns. The number after MC indicates the number of mega columns.

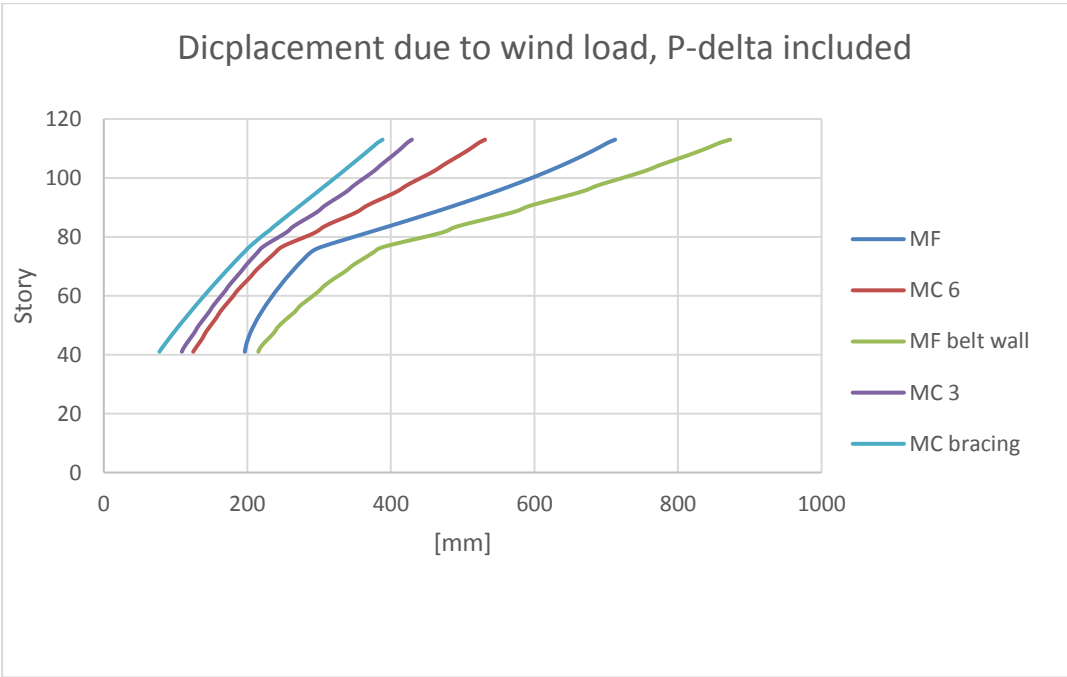


Figure 5.20: Diaphragm D1 and D4 displacement due to wind load, P-delta included in 450 m building

The bracing system showed rather continuous and constant increase of displacement in comparison to moment frame, which showed a rough movement of building on wind load with high and low curvature as shown in Figure 5.20. As for the displacement, due to seismic load, the lower part of the building was not at risk. However, the top part was inclined and was only connected at one point, therefore the bigger deflection. The building with bracings followed the

same pattern as the wind load deflection but the worst case seemed to be in the moment frame, where top story deflection was much larger as shown in Figure 5.21.

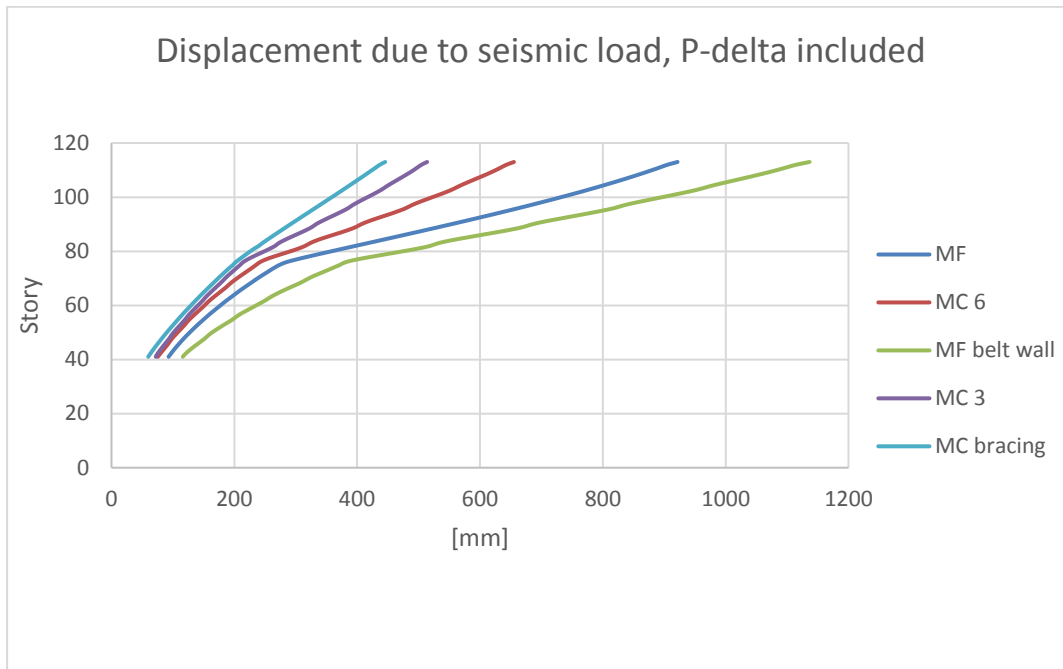


Figure 5.21: Diaphragm D1 and D4 displacement due to seismic load, P-delta included

Figure 5.22 and Figure 5.23 shows the displacement due to wind load and seismic without P-delta effect. The curvature seemed to follow the same pattern as with p-delta effect but shows less magnitude of deflection.

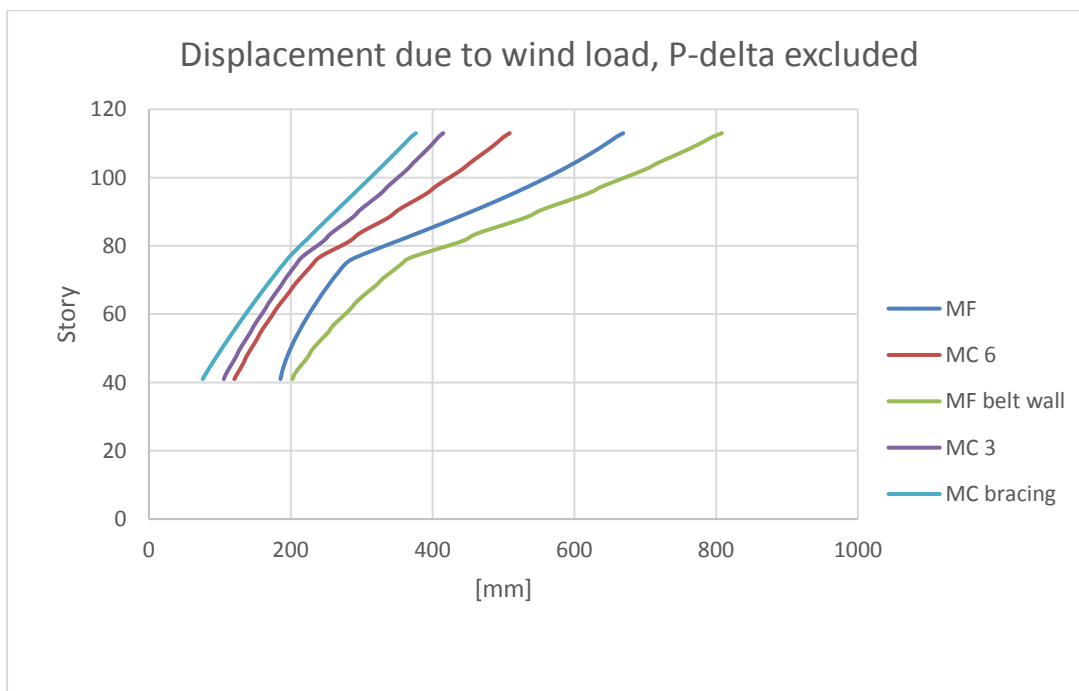


Figure 5.22: Diaphragm D1 and D4 displacement due to wind load, p-delta excluded

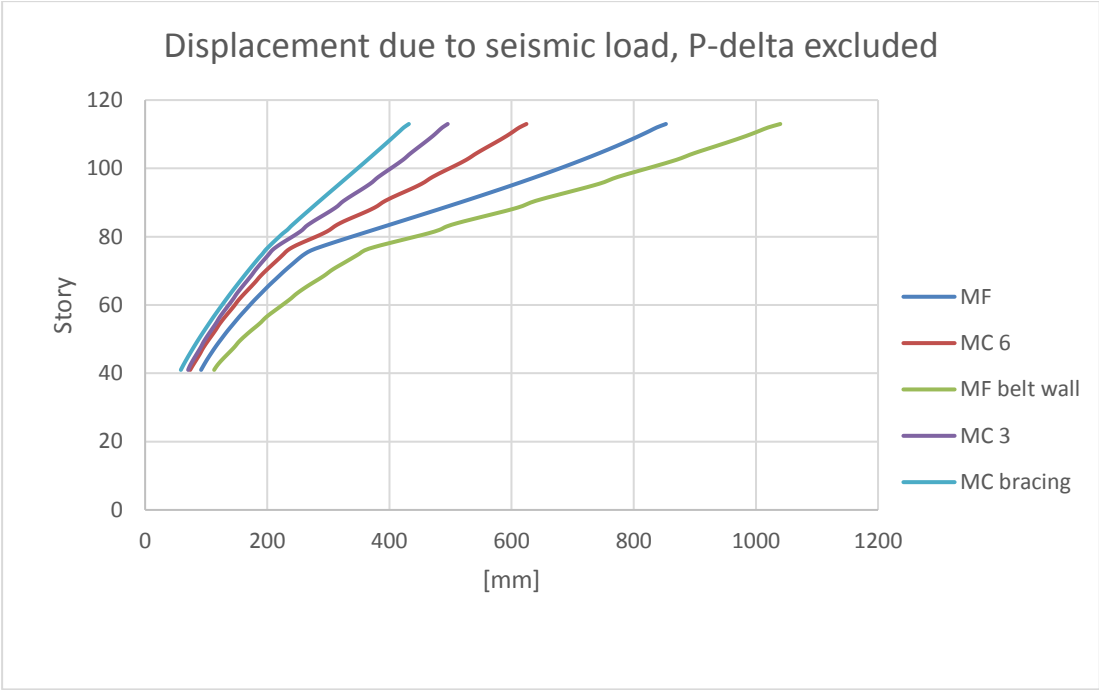


Figure 5.23: Diaphragm D1 and D4 displacement due to seismic load, p-delta excluded

5.3.2 Deformations and periods for the 270 m high building

As it can be seen in Table 5-8: Displacement due to wind load and seismic load without p-delta effect, similar to the 450 m building, the smallest displacement was achieved by the bracings system for both wind and seismic load which was 34 mm in x-axis, 39 mm in y-axis and 82 mm in x-axis 83 in y-axis respectively. The highest displacement was achieved by perimeter frame with belt walls, which was 103 mm in y-axis due to wind load and 229 mm in y-axis due to seismic load. The 3D view of displacement is presented in Appendix B.

Table 5-8: Displacement due to wind load and seismic load without p-delta effect

270 m (P-delta effects excluded)	Wind disp. UX [mm]	Wind disp. UY [mm]	Seismic disp. UX [mm]	Seismic disp. UY [mm]
TMF: 3 mega columns with belt walls	40.9	52.5	97.9	138.8
TMF: 6 mega columns with belt walls	50.2	66.8	138.4	166.9
TMF: 3 mega columns with bracings	33.9	39.3	81.7	83.2
TMF: Perimeter frame with belt walls	90.0	102.7	214.3	229.0
Perimeter frame	87.4	100.5	203.6	215.9

When the P-delta effect was introduced in the model similarly to the 450 m building, for the perimeter frame with belt walls, the displacement due to wind load was increased from 103 mm to 105 mm (2.5%) in y-axis and the displacement due to seismic load was increased from 214 mm to 234 mm (2.1%) in y-direction. Table 5-9 showed the increase of displacement when P-delta effects was included in the analysis. Compared to the 450 m high building it was possible to see that P-delta effects have a higher impact on higher buildings.

Table 5-9: Displacement due to wind load and seismic load with p-delta effect

270 m (P-delta effects included)	Wind disp. UX [m]	Wind disp. UY [m]	Seismic disp. UX [mm]	Seismic disp. UY [mm]
TMF: 3 mega columns with belt walls	41.2	53.0	98.6	139.7
TMF: 6 mega columns with belt walls	50.8	67.9	138.9	168.7
TMF: 3 mega columns with bracings	34.1	39.6	82.0	83.6
TMF: Perimeter frame with belt walls	92.6	105.3	218.2	233.7
Perimeter frame	89.8	103.1	207.2	220.2

The lower shape and the wide base made the 270 m high building very stiff and therefore gave low periods as showed in Table 5-10 and Table 5-11. The highest period was obtained in the perimeter frame with belt walls for both including p-delta and excluding p-delta. The lowest periods were obtained in the mega columns with bracings for both including and excluding p-delta effect.

Table 5-10: Periods without P-delta effects

270 m (P-delta effects excluded)	Period Mode 1 [s]	Period Mode 2 [s]	Period Mode 3 [s]
TMF: 3 mega columns with belt walls	2.06	1.76	1.35
TMF: 6 mega columns with belt walls	2.44	1.95	1.49
TMF: 3 mega columns with bracings	1.68	1.60	1.05
TMF: Perimeter frame with belt walls	3.06	2.79	2.16
Perimeter frame	2.91	2.69	2.11

Table 5-11: Periods with P-delta effect

270 m (P-delta effects included)	Period Mode 1 [s]	Period Mode 2 [s]	Period Mode 3 [s]
TMF: 3 mega columns with belt walls	2.08	1.77	1.36
TMF: 6 mega columns with belt walls	2.47	1.97	1.62
TMF: 3 mega columns with bracings	1.69	1.60	1.05
TMF: Perimeter frame with belt walls	3.15	2.85	2.20
Perimeter frame	2.98	2.74	2.14

The percentage increase of displacement with p-delta effect and without p-delta effect are presented in Table 5-12.

Table 5-12: Percentage increase of displacement when p-delta effect is included

270 m	Wind disp. UX [%]	Wind disp. UY [%]	Seismic disp. UX [%]	Seismic disp. UY [%]
TMF: 3 mega columns with belt walls	0.7	1.0	0.7	0.6
TMF: 6 mega columns with belt walls	1.2	1.6	0.4	1.1
TMF: 3 mega columns with bracings	0.6	0.8	0.4	0.5
TMF: Perimeter frame with belt walls	2.9	2.5	1.8	2.1
Perimeter frame	2.7	2.6	1.8	2.0

The displacement diagram for each diaphragm representing each leg are shown Appendix B – Displacements. Figure 5.24 shows the maximum value of displacement due to wind load including P-delta, in y-direction only, for all systems. Similar to the 450 m building, the bracing system showed rather continuous and constant increase of displacement in comparison to perimeter frame, which showed a rough movement of building on wind load with high and low curvature as shown in Figure 5.24.

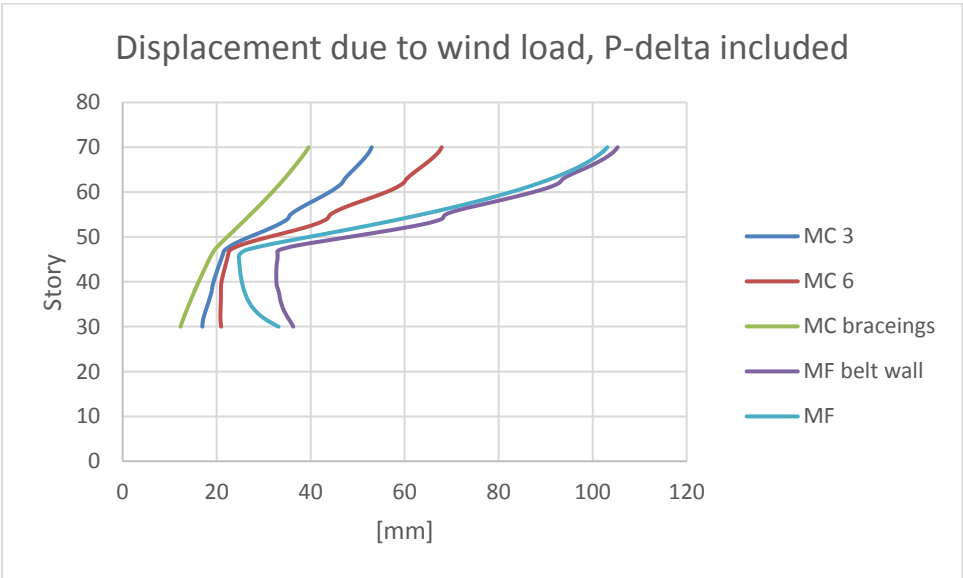


Figure 5.24, Diaphragm displacement due to wind load, P-delta included

Similar to the 450 m building, the lower part of the building was not at risk due to seismic load. However, the top part was inclined and was only connected at one point, therefore gave the bigger deflection. The building with bracings showed the same pattern as wind load deflection but the worst case seemed to be in moment frame, where top story deflection was much larger as shown in Figure 5.25.

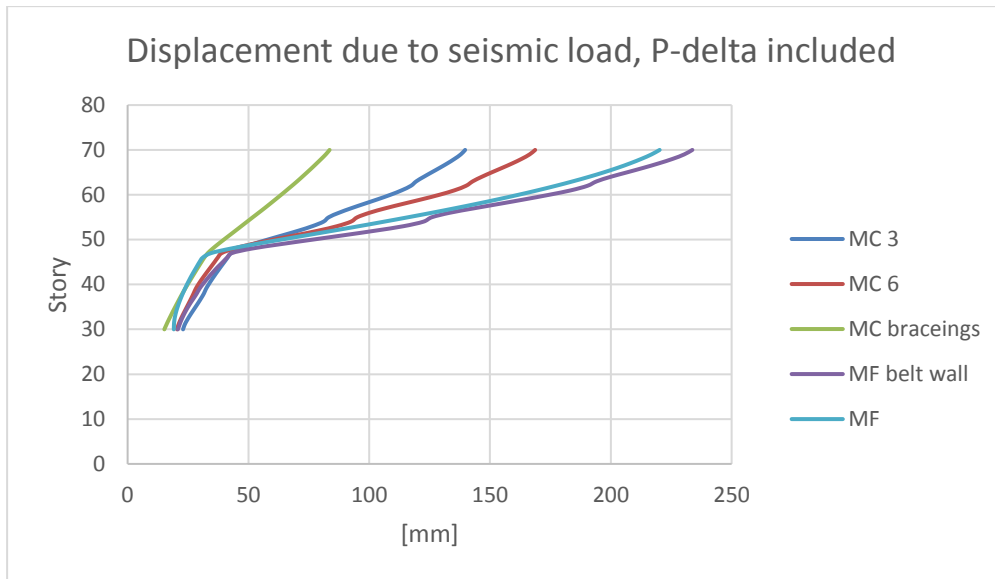


Figure 5.25, Diaphragm D3 and D4 displacement due to seismic load, P-delta included

Figure 5.26 and Figure 5.27 shows the displacement due to wind load and seismic without p-delta effect. The curvature seemed to follow the same pattern as with P-delta effect but showed less magnitude of deflection.

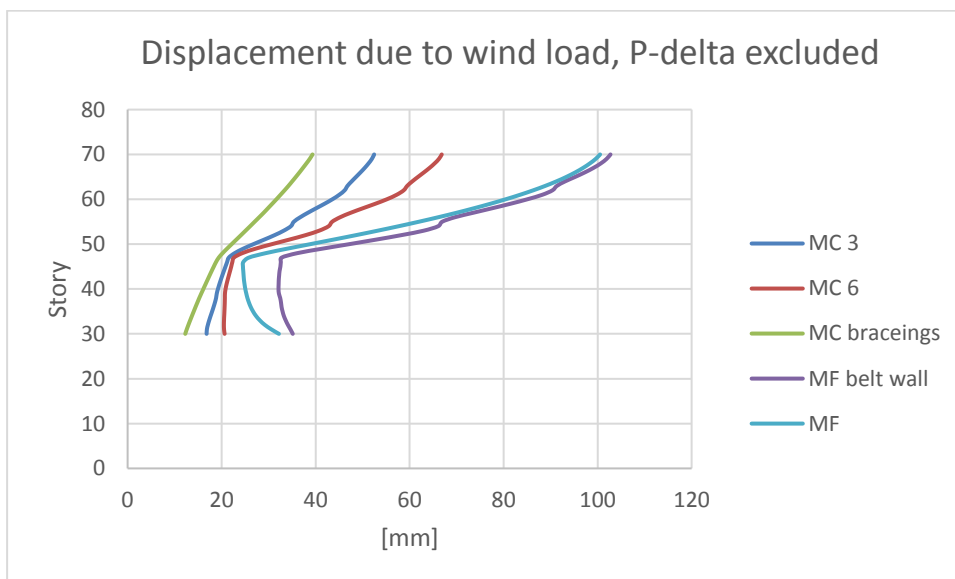


Figure 5.26, Diaphragm D3 and D4 displacement due to wind load, P-delta excluded

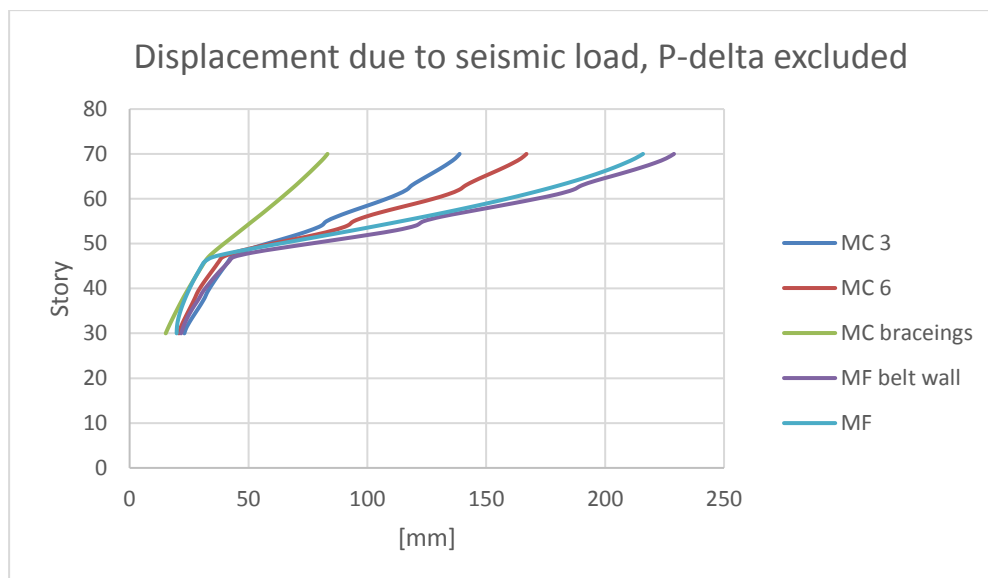


Figure 5.27: Diaphragm D3 and D4 displacement due to seismic load, P-delta excluded

5.4 Verification

The weights of the models were checked for and compared to hand calculations, see Appendix C for hand calculations. ETABS generated base reactions were close to the hand calculated weight for all the models. See difference.

Table 5-13 and Table 5-14 for calculated difference.

Table 5-13: Base reaction verifications, 270 m building

Systems for 270 m	Base reactions Fz [kN]	Hand calculated Fz [kN]	Difference %
Six mega columns with belt walls	826347	823876	0.3
Three mega columns with belt walls	826351	823876	0.3
Three mega columns with bracings	826390	824000	0.3
Perimeter frame with belt walls	804889	823876	2.4
Perimeter frame without belt walls	804896	823876	2.4

Table 5-14: Base reaction verifications, 450 m building

Systems for 450 m	Base reactions Fz [kN]	Hand calculated Fz [kN]	Difference %
Six mega columns with belt walls	1341751	1349239	2
Three mega columns with belt walls	1341871	1346340	1.6
Three mega columns with bracings	1338389	1346340	1.36
Perimeter frame with belt walls	1336204	1320454	1.19
Perimeter frame without belt walls	1322472	1384671	2.6

6 Discussion and conclusion

The results showed that the TMF mega column system with X-bracings performed significantly better than the other systems. This regarding both wind and seismic load, but also with and without P-delta effects. The reason for this could be that the bracing systems only take compression and tension forces compared to the other systems where the stiffness comes from the bending resistance of the members. It is possible to see that the P-delta effects affected the higher building more and this is possibly because the deflections were bigger for taller buildings and because the dead load increased with the height.

It is reasonable to think that the 270 m high building had a shorter period. The inclination of 15° made the buildings perimeter base of whole building a bit wider in comparison to the 450m high building with inclination of 7° . Three legs spreading out in three different directions equally, made it rather stiff and stable, because the forces could be taken as compression due to the inclination of the legs. Even for the taller building the periods seemed smaller than for the conventional buildings. The worst case appears when buildings reaches the same periods as the earthquakes has and it's around 2 to 2.5. The TMF mega columns with bracings is stiffer than other system and has periods around 4.

The displacement curves due to wind load showed how different the systems performed under wind load. The bracings system seemed to have functioned as it should do where all the horizontal forces had spread through the building smoothly. It could be observed that displacement curve for the bracings was more smooth and parabolic in comparison to the perimeter frame. The perimeter frame divided the forces among the columns by the bending stiffness of the frame. This made it weaker than the bracings system. The use of mega columns itself made the system better than the moment frame because mega column was hollow and wide which made it stiffer and lighter. Most of the lateral forces tended to be taken by the mega column's bending stiffness and the belt walls made it even easier for the forces to spread to the other columns equally. The traces of belt walls could also be seen in the displacement curves as it seemed to be holding the columns together.

Placing more columns on the perimeter did not seem to increase stiffness of the building. The deflection was increasing while comparing the three mega columns, six mega columns and perimeter frame respectively. Bigger, stiffer and lighter columns (compared to its size) seemed to be the better choice for the tall building, especially for slanted ones.

From the result, it could be noticed that the deflection for the perimeter frame with belt walls was a bit higher than without belt walls. The reason lays on the modeling of the buildings. Initially the building should have an equivalent total volume which made the perimeter frame without belt walls to have bigger dimension than the one with belt walls. The addition of belt walls in the system led to decreased volume of the columns. The smaller columns led to bigger deflections on the TMF perimeter frame with belt walls. What could have been done better is that the columns would have stayed constants and a reduction of the beams and belt walls instead. There were other options one can consider and that were to make moment frame or perimeter frame stiffer, such as placing a bigger column in the corners while making the others smaller. The position of the columns in the corners, had influence on the total stiffness of the building. For example, the mega columns were rectangular and the second area moment of

inertia along the longer side of section was much higher than along shorter side. The columns were placed in such way that the direction where the building was inclined, was the same direction where the columns had higher second area moment of inertia.

The construction of the foundation was not the part of the study but the curiosity rises, concerning how the three legs should be put together in the place. The model in the ETABS had a fixed base on the ground which is not accurately true in real life situation. The possible way of approaching similar condition would be to tie up these three legs together under the ground by some cables or concrete piles. Nevertheless, taking care of base forces was not a main concern here because the vertical forces were much bigger than the forces on horizontal directions.

In ETABS, all the columns were modeled as stick elements for simplification. The mega columns were big enough to act as walls and the possible correct way of modeling might be meshing columns as rectangular, shell models. The shear deformations can lead to bigger total deformation in comparison to the deformation presented in the result. However, it is just a matter of choice and what deformations that are acceptable. Tall buildings can have very high deflections as long as they do not collapse and reach the limit where person living inside the building can sense the movement and feel inconvenience. When designing a high rise building, the main concern is a maximum story drift ratio, not the maximum top deflection of the building.

In the analysis, material non-linearity such as cracking of concrete was not taken into consideration while calculating deflections. The concrete may crack due to tension and lose its stiffness, something which should be further investigated. Tension forces are taken only by reinforcement, cracking of concrete and yielding of reinforcement cause additional deformations.

P-delta effect did not seem to influence much on the deflections since the building was already slanted and the dead load caused secondary moment effect.

7 Further research

Further research could be to design all the different systems in detail for some building and compare them. In this design, it would be good to also consider other materials than concrete, steel for example, because of the high tensile strength of steel. Or even combining steel and concrete. It would be a good idea to add other systems, such as the diagrid system and other types of bracing systems. Another further research could be to pay closer attention to the part of the building where all three legs meet, since this is a very complex area and the bending moments are high. This part of the building is so complex that it would take another thesis to dive in to it. Furthermore, an investigation on how the foundation would act to the inclined building would be of interest.

Bibliography

American Society of Civil Engineers, 2013. *Minimum Design Loads for Buildings and other Structures*. 3 ed. Reston: American Society of Civil Engineers.

Choi, H. S., Ho, G., Joseph, L. & Mathias, N., 2012. *Outrigger Design for High-Rise Buildings: An output of the CTBUH Outrigger Working Group*, Chicago: Council on Tall Buildings and Urban Habitat.

Civilsimplified, 2017. *What are Shear Walls?*. [Online]
Available at: <http://www.civilsimplified.com/resources/what-are-shear-walls>
[Accessed 15 May 2017].

CSI ETABS, 2017. *ETABS 2016*. [Online]
Available at: <https://www.csiamerica.com/products/etabs>
[Accessed 15 May 2017].

CSI knowledge base, 2013. *P-Delta effect*. [Online]
Available at: <https://wiki.csiamerica.com/display/kb/P-Delta+effect>
[Accessed 21 February 2017].

CSI knowledge base, 2014. *Buckling*. [Online]
Available at: <https://wiki.csiamerica.com/display/kb/Buckling>
[Accessed 13 April 2017].

CSI SAP2000, 2017. *SAP2000 v19*. [Online]
Available at: <https://www.csiamerica.com/products/sap2000>
[Accessed 15 May 2017].

CTBUH, 2016. *About the CTBUH*. [Online]
Available at: <http://www.ctbuh.org/AboutCTBUH/tabid/483/language/en-US/Default.aspx>
[Accessed 11 December 2016].

CTBUH, 2017. *Tall, Supertall & Megatall Buildings*. [Online]
Available at:
<http://www.ctbuh.org/TallBuildings/HeightStatistics/Criteria/tabid/446/language/en-US/Default.aspx>
[Accessed 4 March 2017].

Dhatt, G., Touzot, G. & Lefrancois, E., 2012. *Finite Element Method*. 1st ed. London: ISTE Ltd.

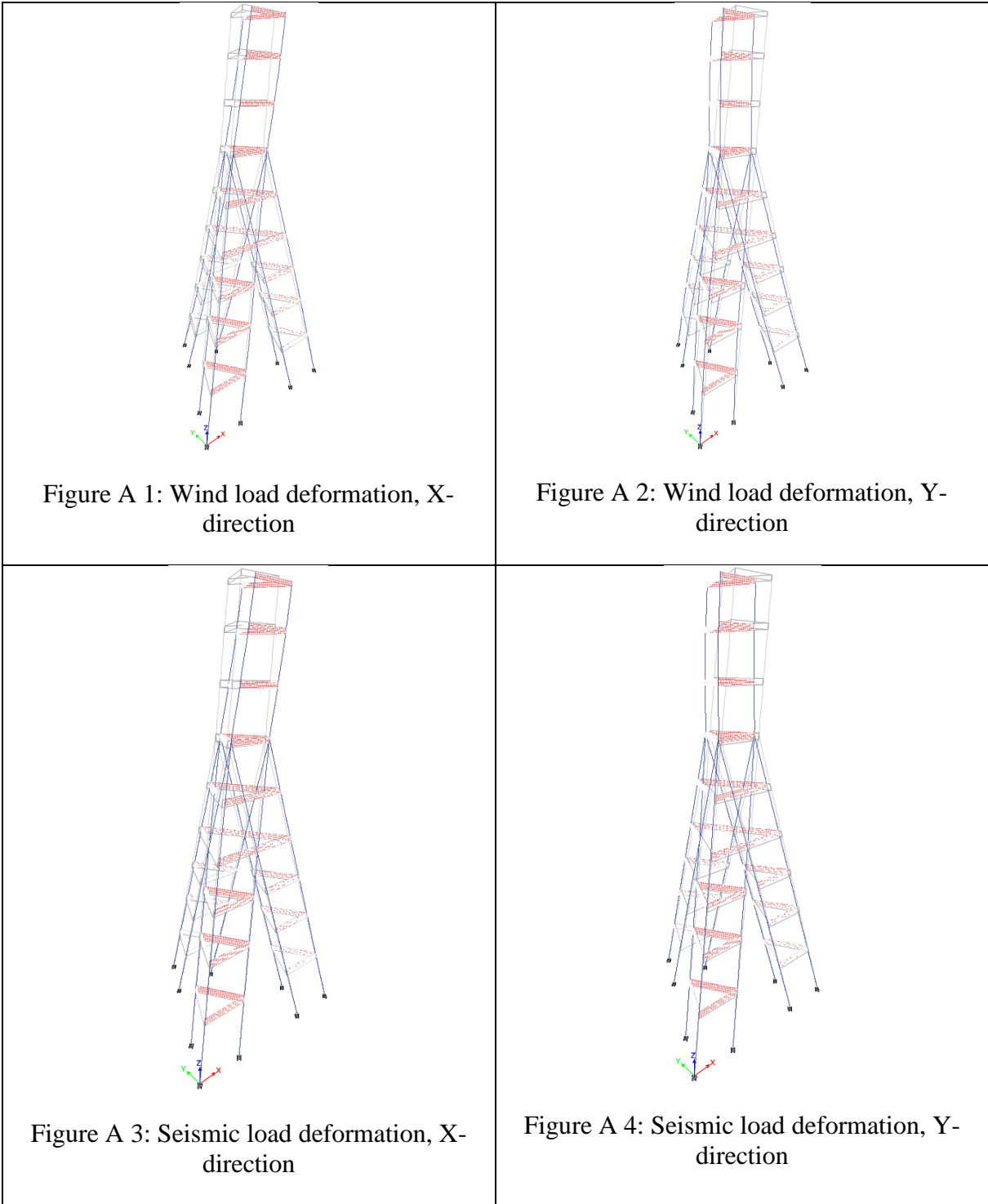
Dr. Bhandari, N. M., Dr. Krishna, P., Dr. Kumar, K. & Dr. Gupta, A., n.d. *An Explanatory Handbook on Proposed IS 875 (Part3), Wind load on Buildings and structures*, Kanpur: Indian Institute of Technology Kanpur.

- King, F., Hallgren, M., Svärd, J. & Partovi, A., 2016. *Tubed Mega Frame Structural Systems for Tall Buildings*, Stockholm: IABSE Congress.
- Klemencic, R., n.d. *Why are Tall Buildings Often Considered Safer Than Low-Rise Buildings During Earthquakes?*, Chicago: Council on Tall Buildings and Urban Habitat.
- Leander, J., 2015. *Statically indeterminate structures*. Stockholm: Royal Institute of Technologies.
- Schofield, J., 2012. Capital Gate, Abu Dhabi. *CTBUH Journal 2012*, Issue II, pp. 12-17.
- Scott, D., Farnsworth, D., Jackson, M. & Clark, M., 2007. The Effects of Complex Geometry on Tall Buildings. In: G. C. Hart, ed. *The Structural Design of Tall and Special Buildings*. New Jersey: John Wiley & Sons, Ltd, pp. 441-455.
- SMStsunamiwarning, 2017. *Earthquakes: tectonic plates*. [Online]
Available at: <http://www.sms-tsunami-warning.com/pages/tectonic-plates#.WRl4x2nyi0l>
[Accessed 24 April 2017].
- Svärd, J. & Partovi, A., 2016. *Global Analysis of Tall Buildings with Tubed Mega Frame Structures*, Stockholm: Royal Institute of Technology.
- ThyssenKrupp, 2016. *MULTI, A new era of mobility in buildings*. [Online]
Available at: <https://multi.thyssenkrupp-elevator.com/en/>
[Accessed 4 December 2016].
- UCAR, 2017. *What is wind?*. [Online]
Available at: https://eo.ucar.edu/basics/wx_2_c.html
[Accessed 21 February 2017].
- Winstanley, T., 2011. *AD Classics: Puerta De Europa*. [Online]
Available at: <http://www.archdaily.com/157275/ad-classics-puerta-de-europa-philip-johnson-john-burgee>
[Accessed 23 February 2017].
- Zhang, H., 2014. *Global Analysis and Structural Performance of the Tubed Mega Frame*, Stockholm: Royal Institute of Technology.

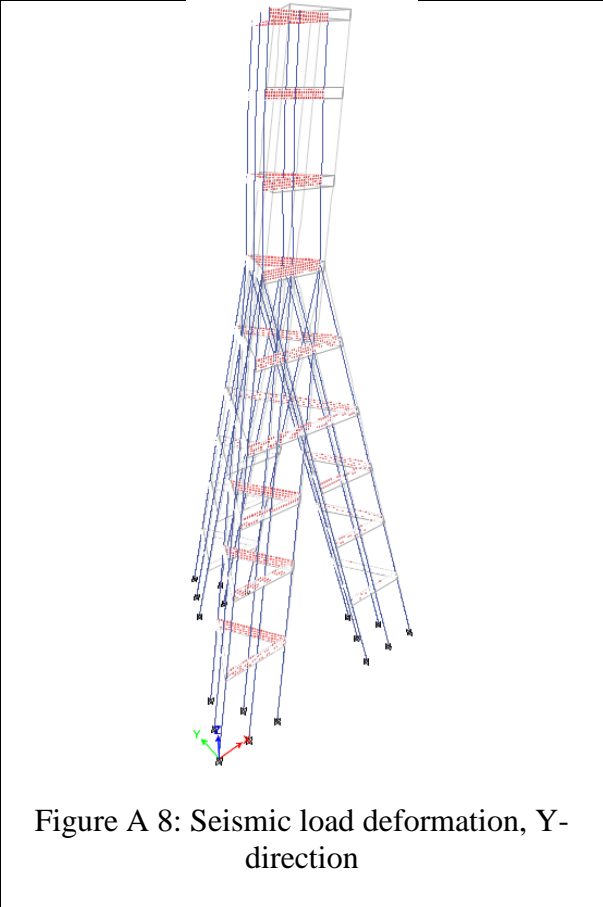
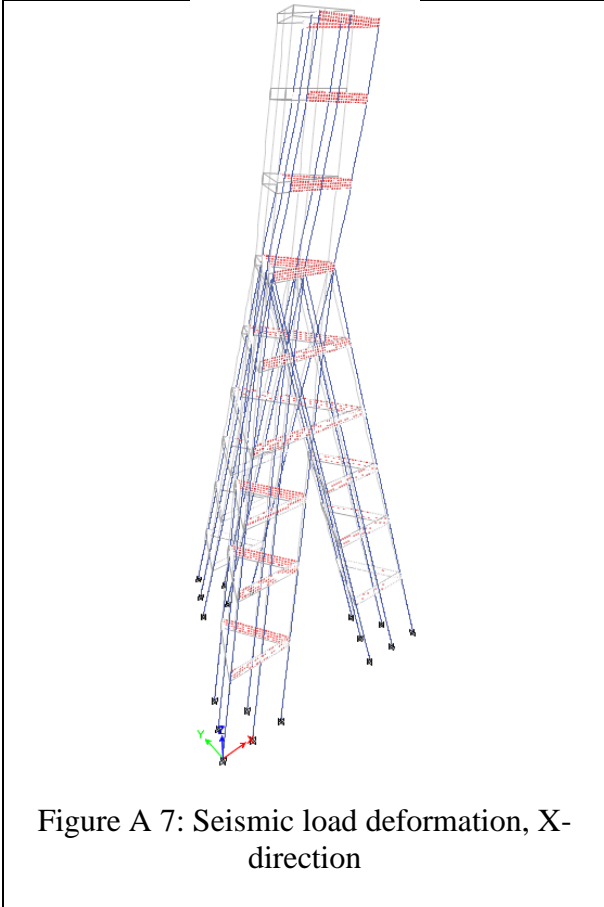
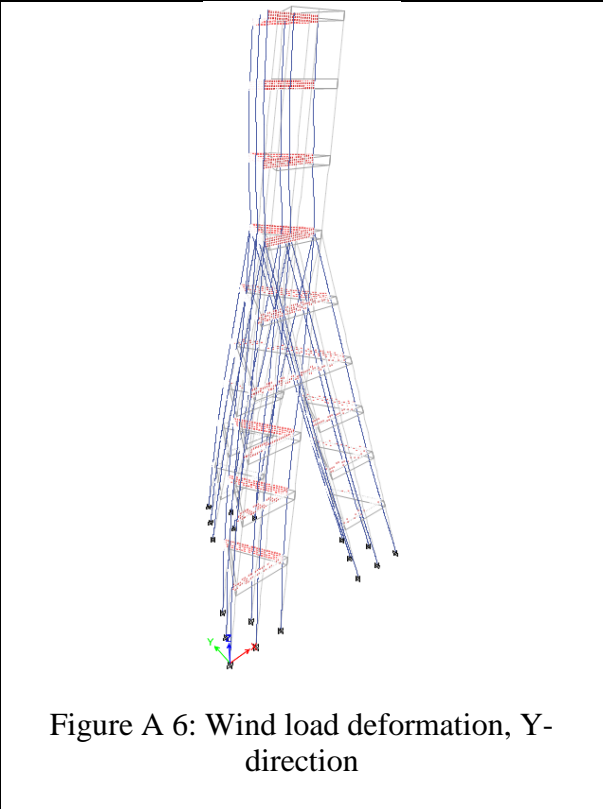
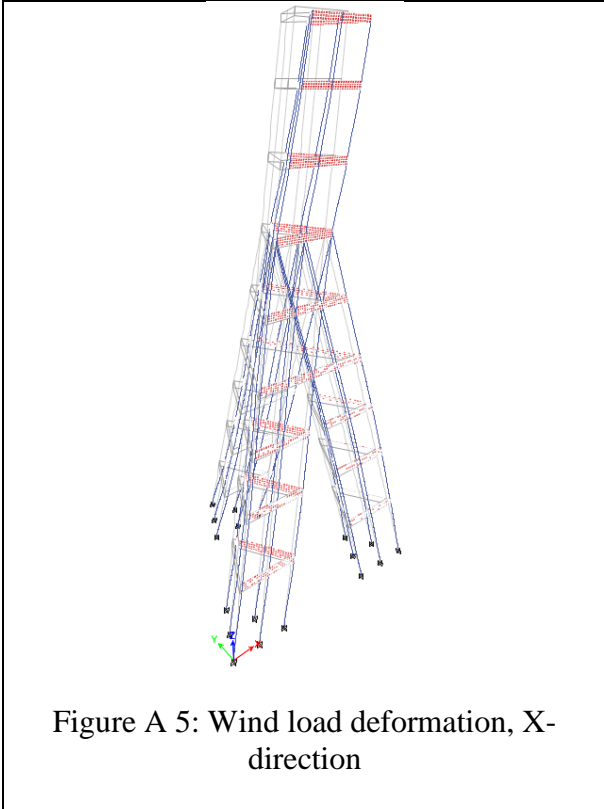
Appendix A – Deformations

270 m high building

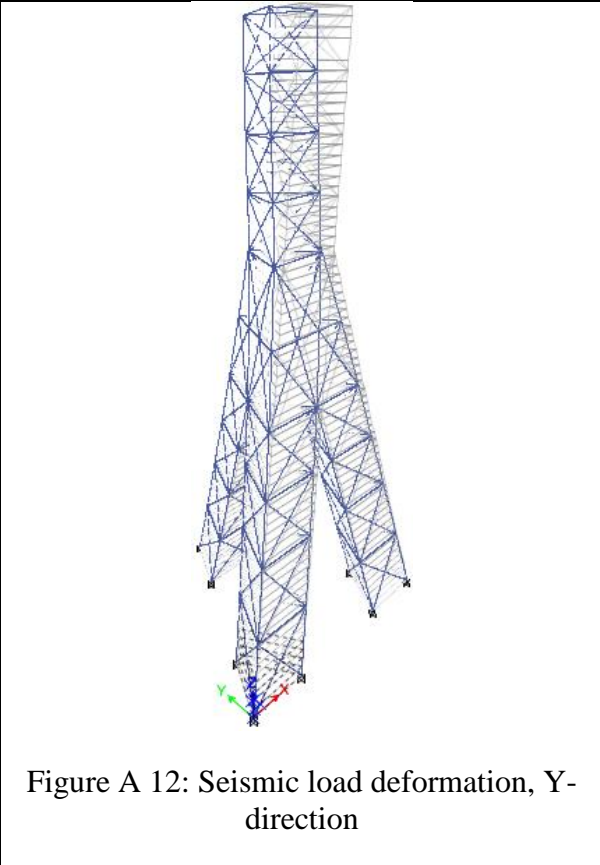
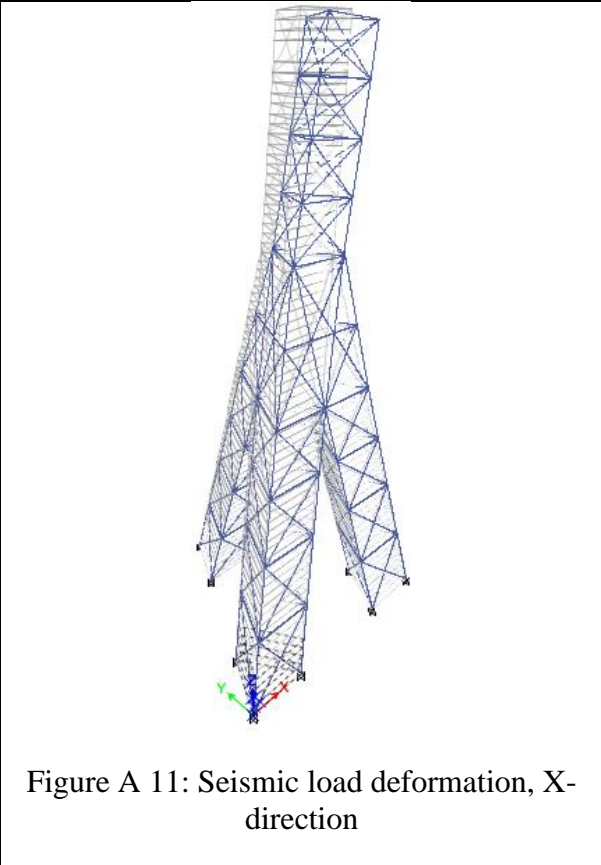
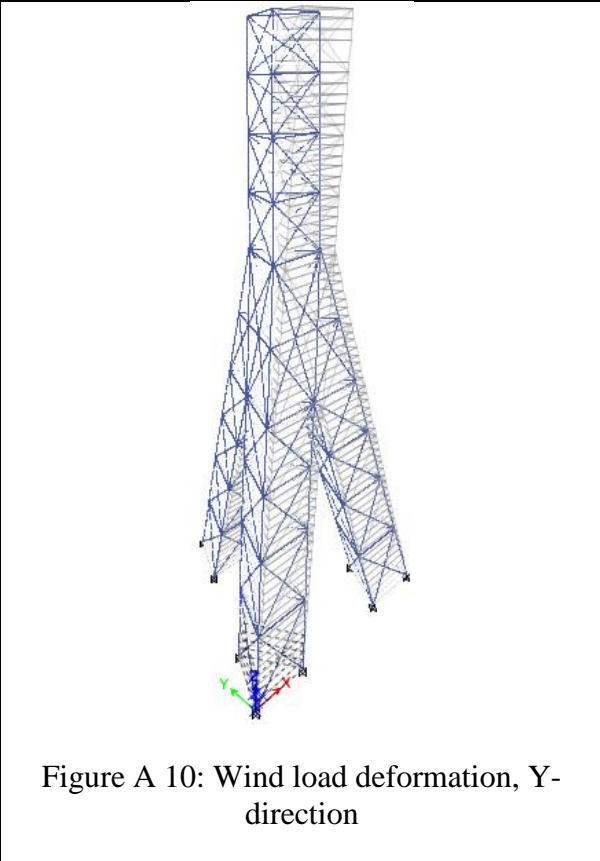
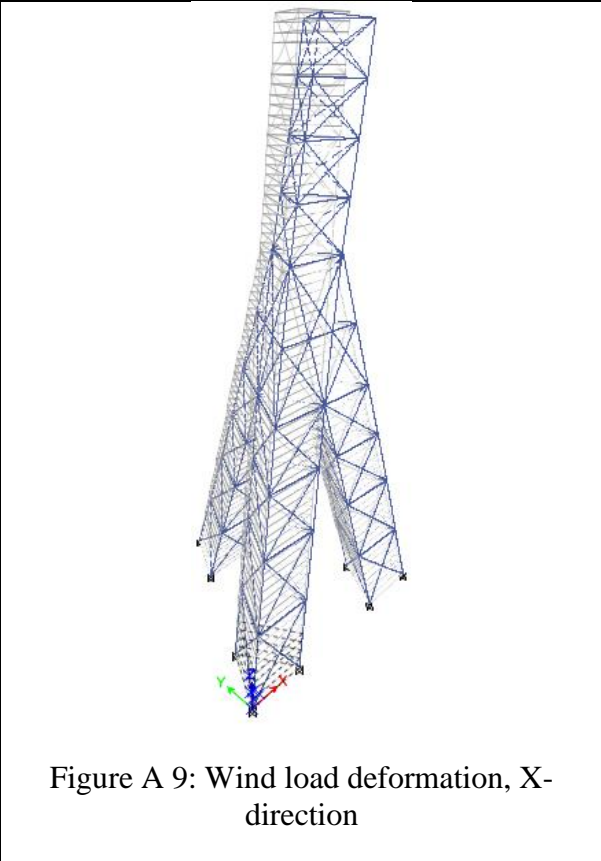
Three mega columns with belt walls



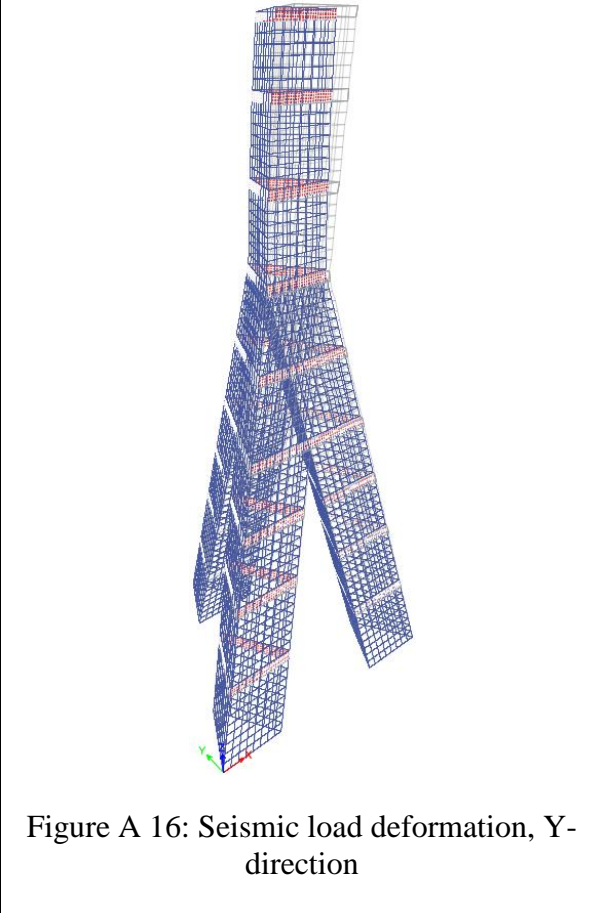
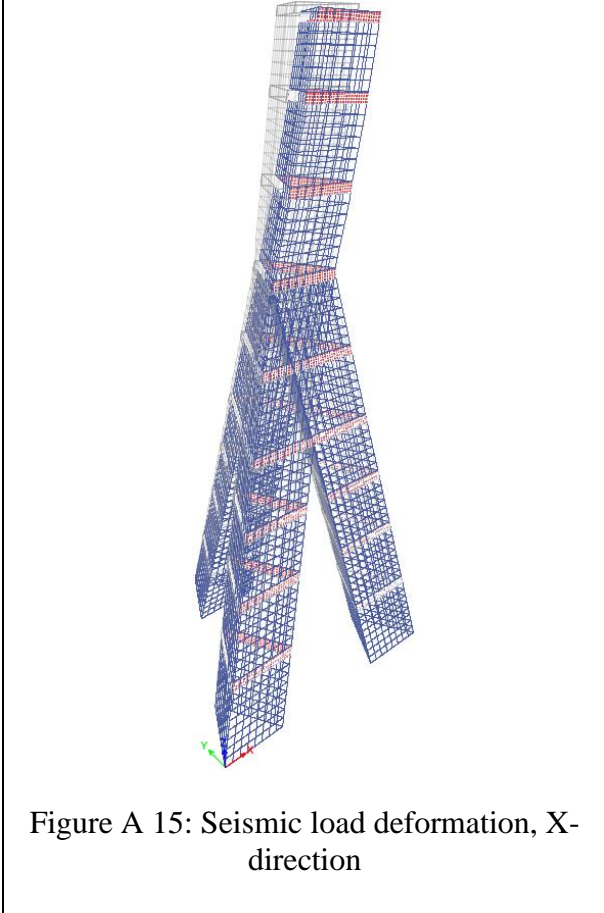
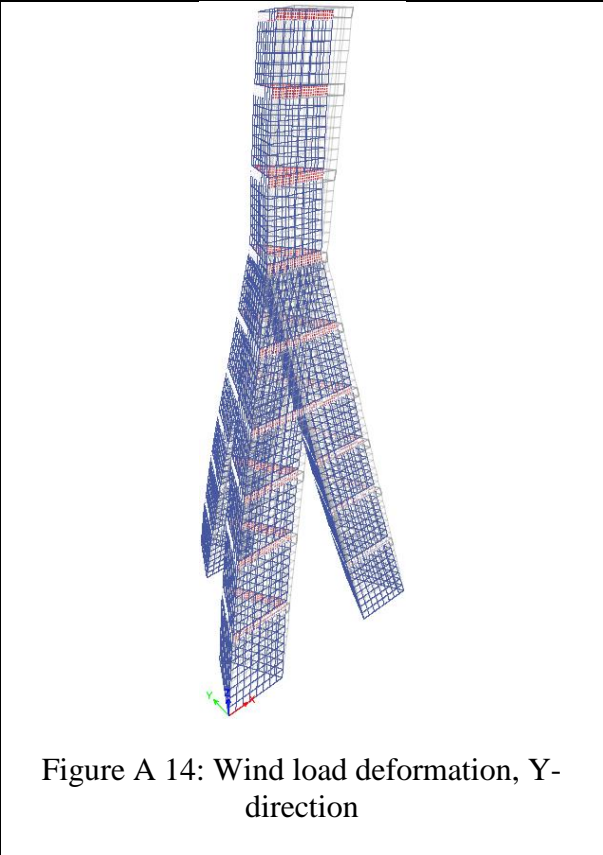
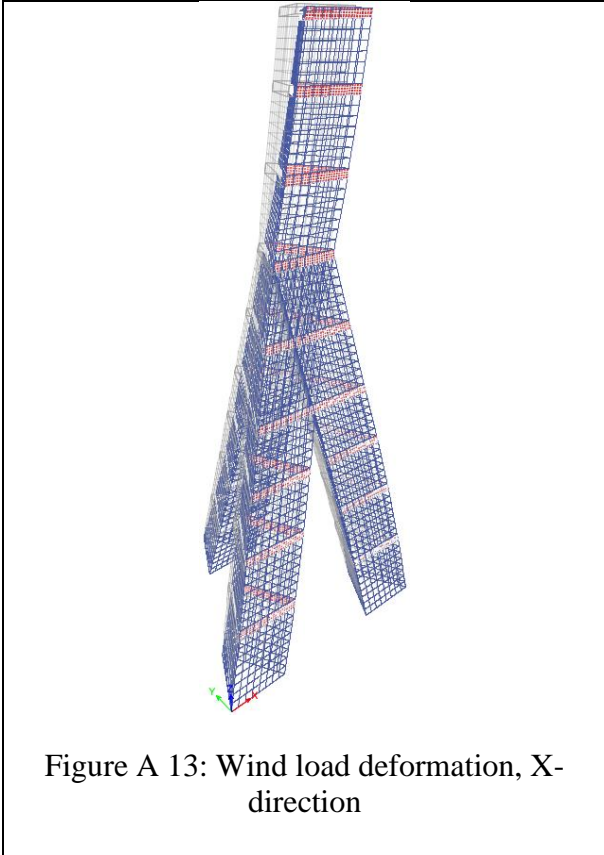
Six mega columns with belt walls



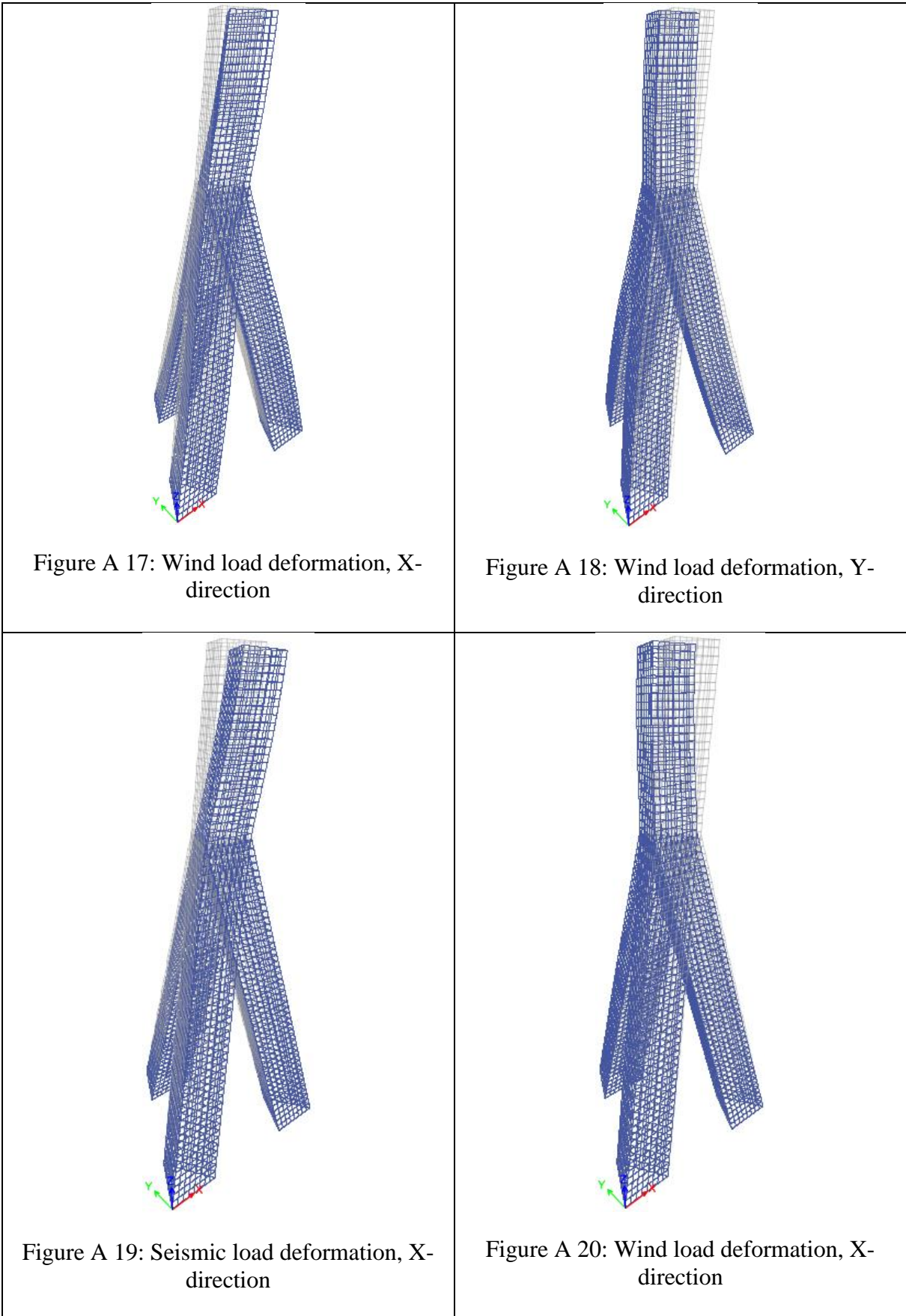
Mega columns with bracings



Moment frame with belt walls



Moment frame



450 m high building

Three mega columns with belt walls

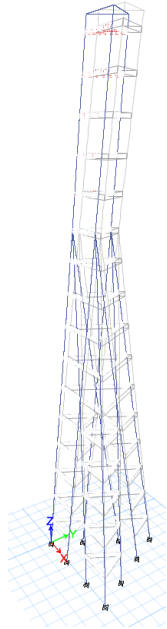


Figure A 21: Wind load deformation, X-direction

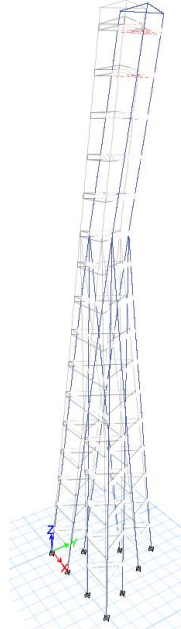


Figure A 22: Wind load deformation, Y-direction

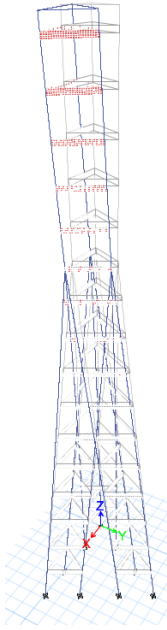


Figure A 23: Seismic load deformation, X-direction

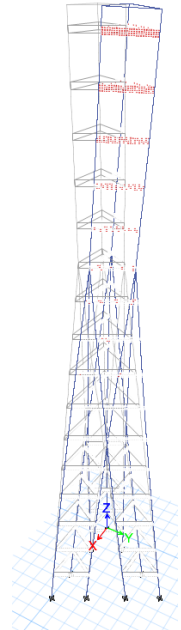
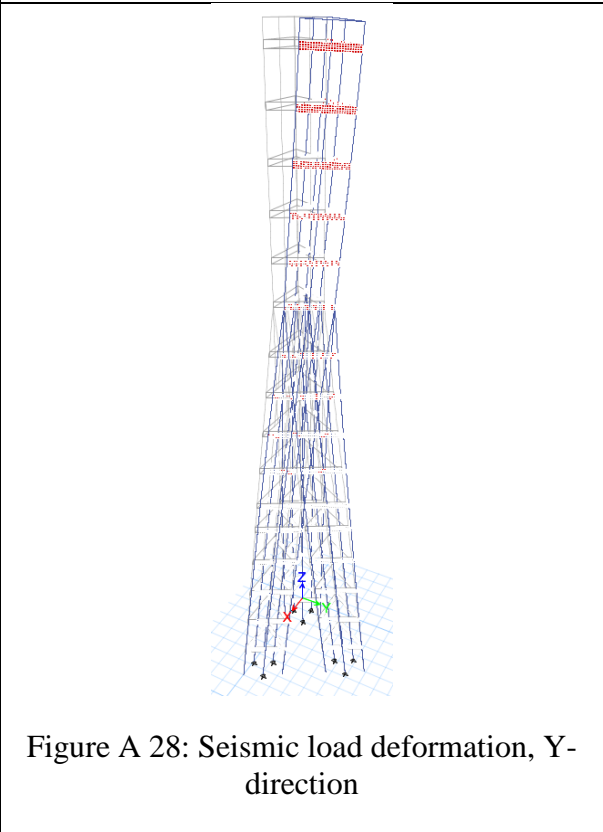
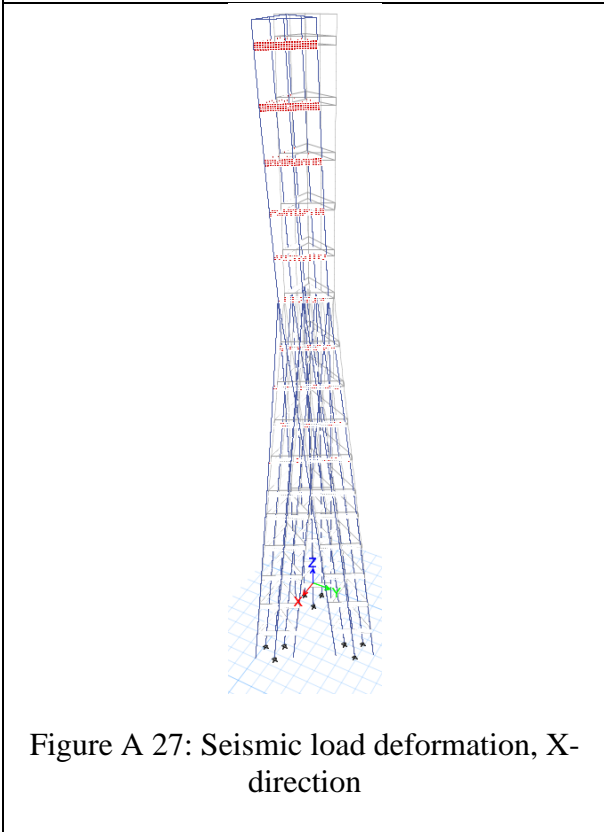
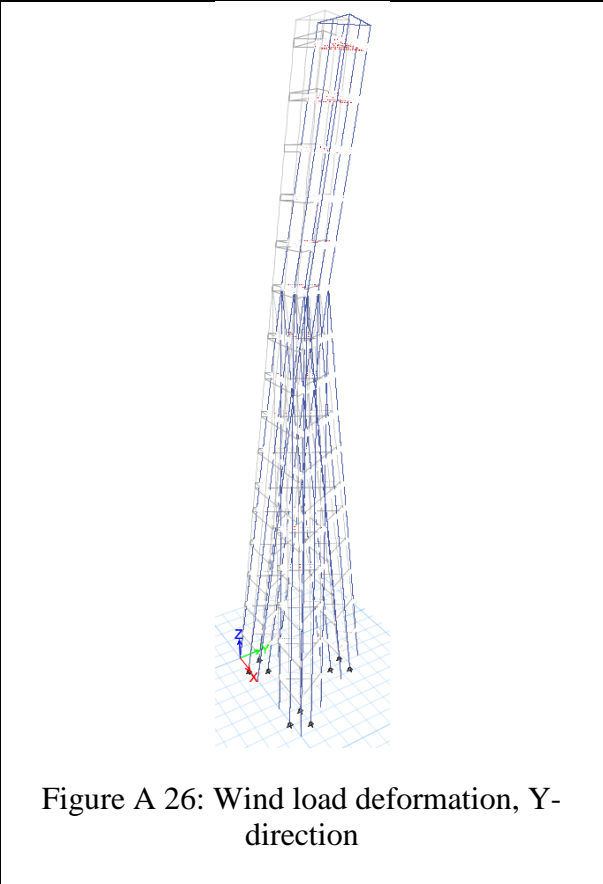
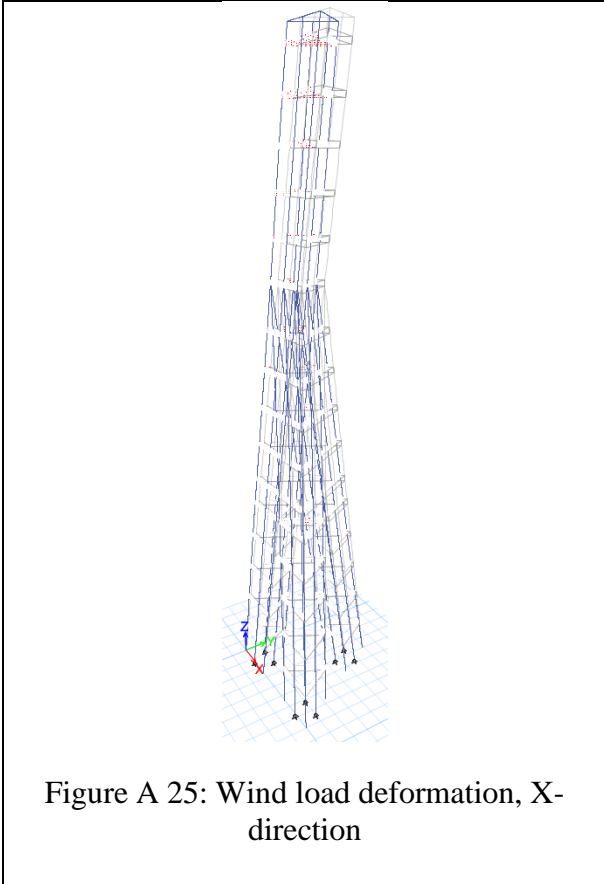


Figure A 24: Seismic load deformation, Y-direction

Six mega columns with belt walls



Mega columns with bracings

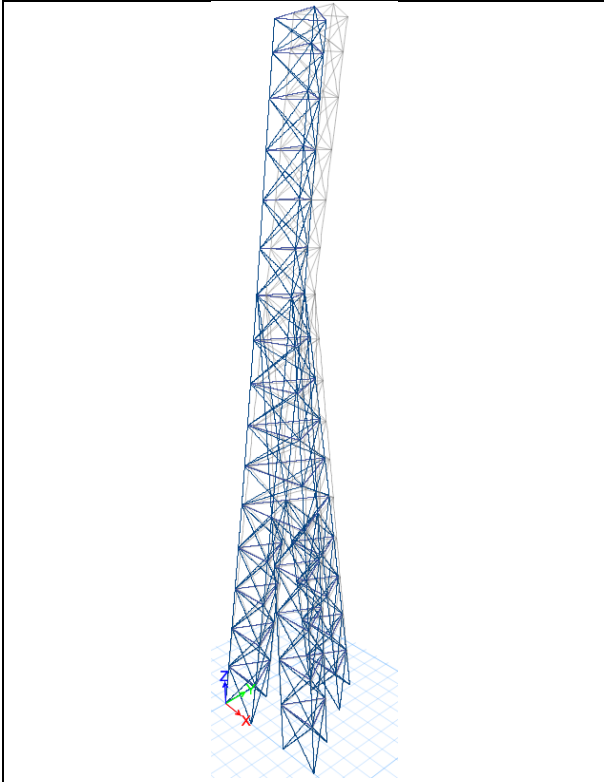


Figure A 29: Wind load deformation, X-direction

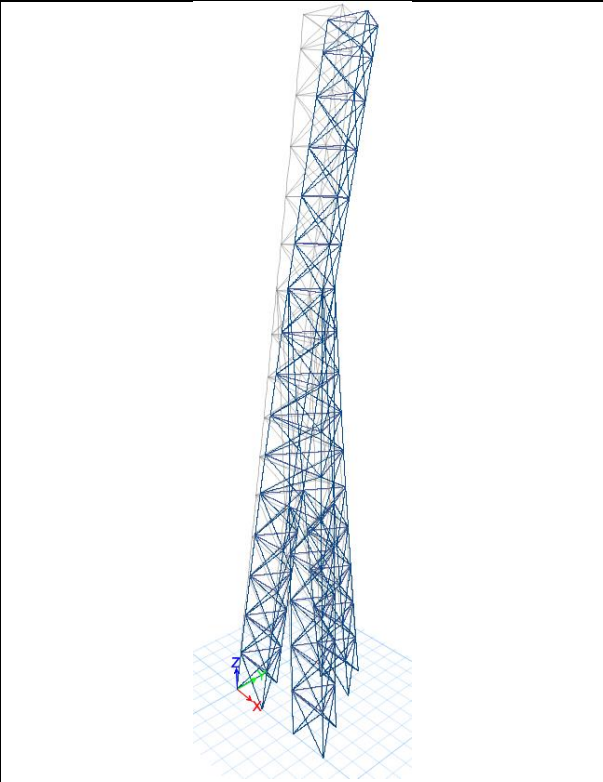


Figure A 30: Wind load deformation, Y-direction

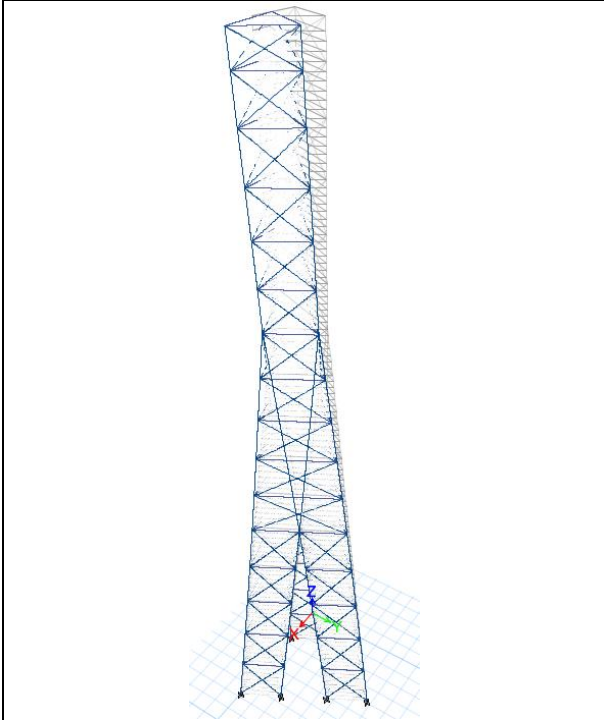


Figure A 31: Seismic load deformation, X-direction

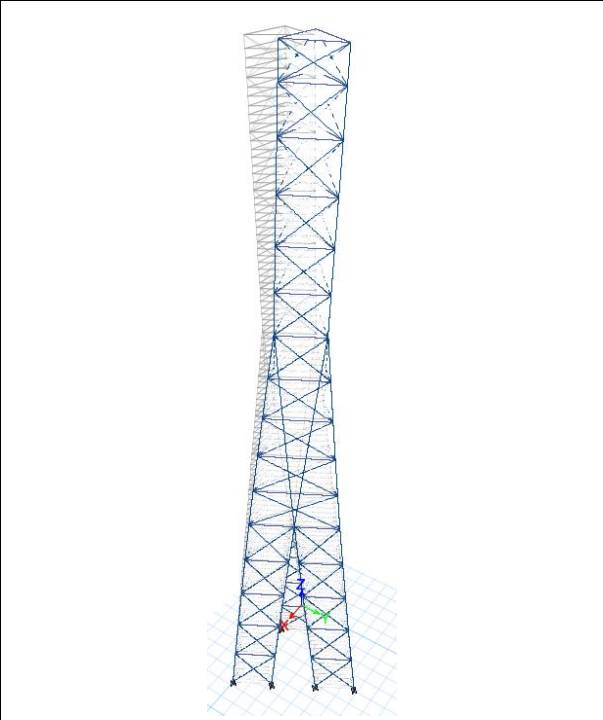


Figure A 32: Seismic load deformation, Y-direction

Moment frame with belt walls



Figure A 33: Wind load deformation, X-direction

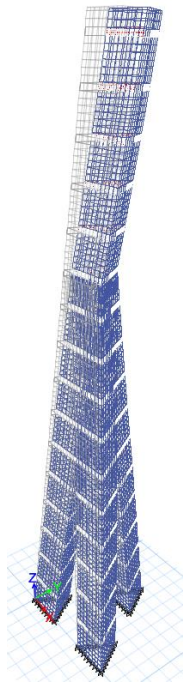


Figure A 34: Wind load deformation, Y-direction

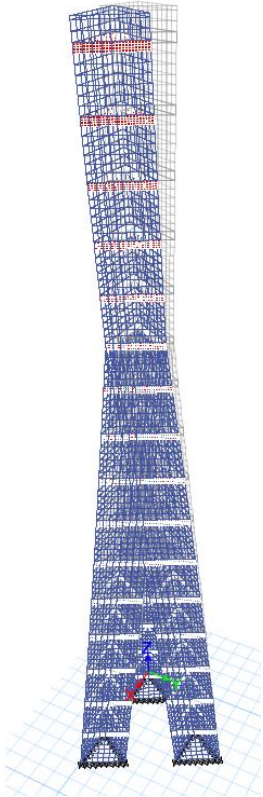


Figure A 35: Seismic load deformation, X-direction

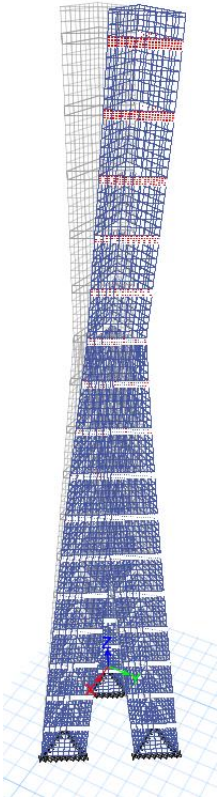
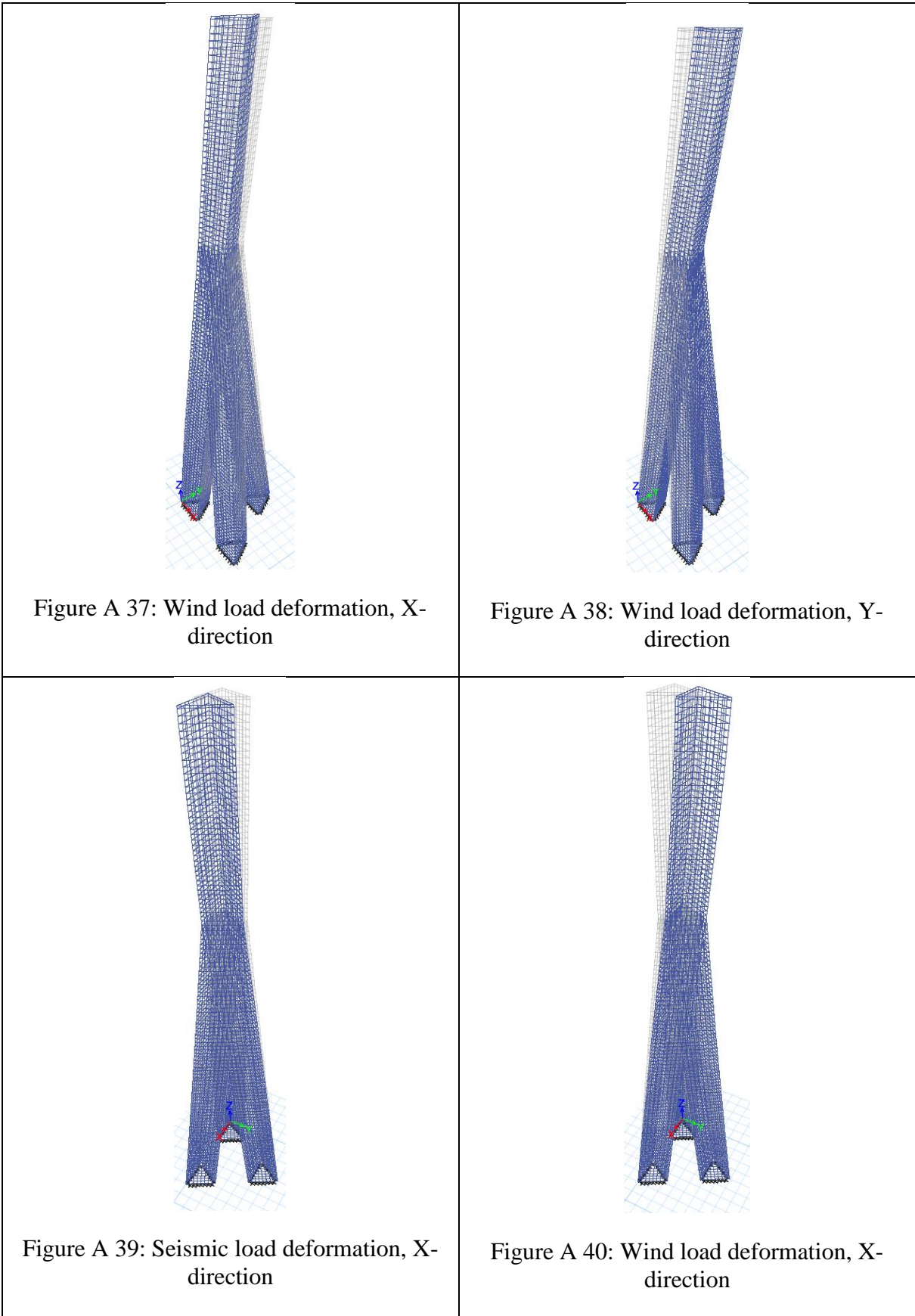


Figure A 36: Seismic load deformation, Y-direction

Moment frame without belt walls



Appendix B – Displacements

270 m high building

Displacement due to wind load, P-delta included

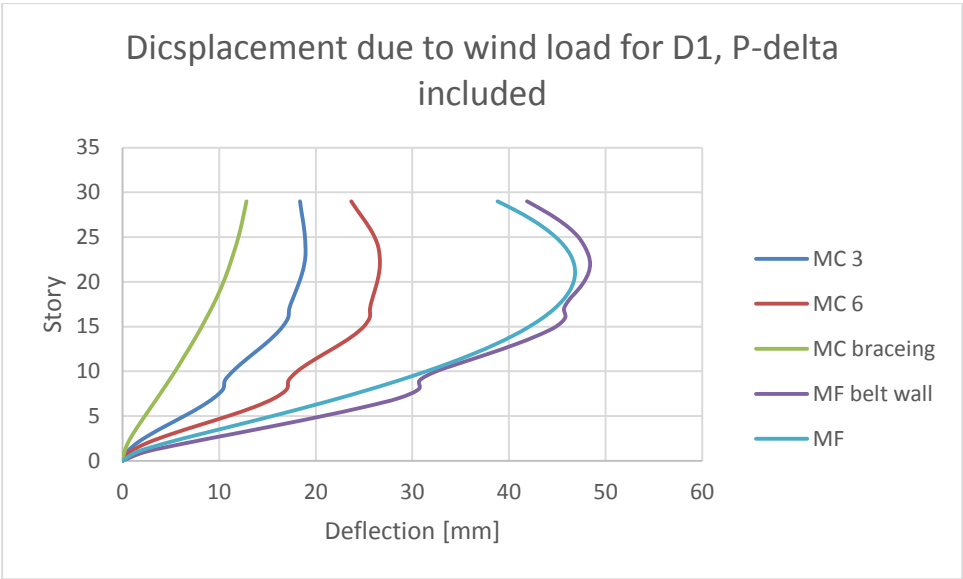


Figure B 1: Displacement due to wind load in y-direction for diaphragm D1, P-delta included

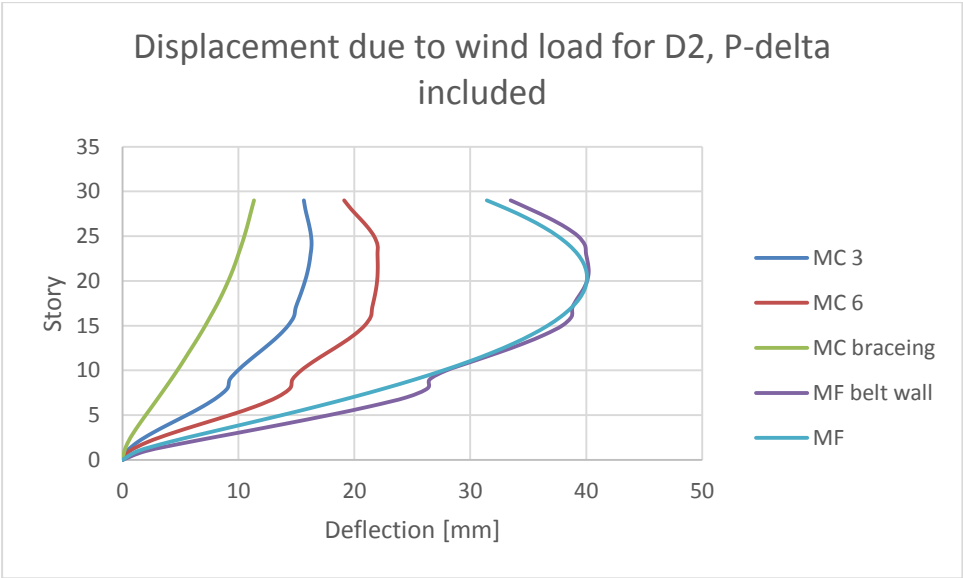


Figure B 2: Displacement due to wind load in y-direction for diaphragm D2, P-delta included

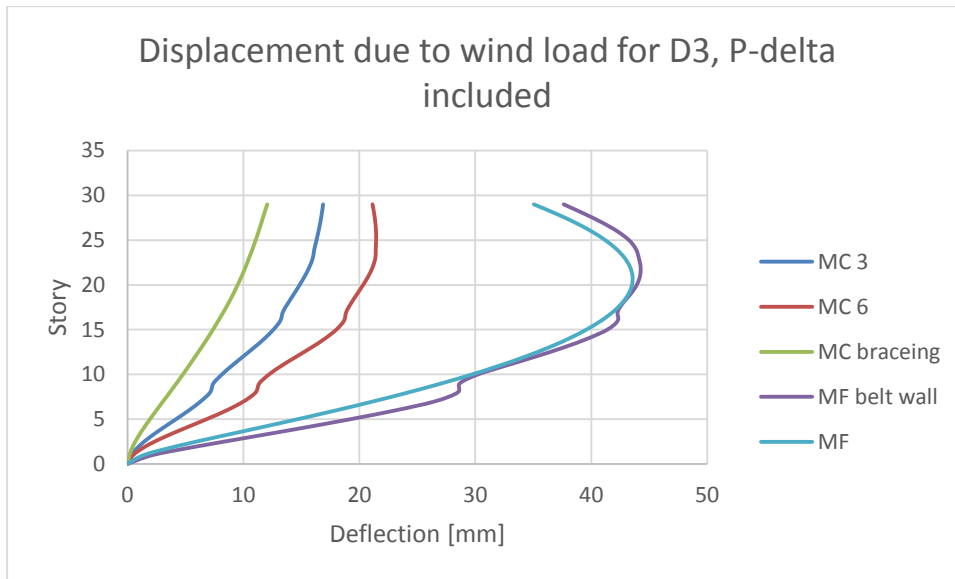


Figure B 3: Displacement due to wind load in y-direction for diaphragm D3, P-delta included

Displacement due to wind load, P-delta excluded

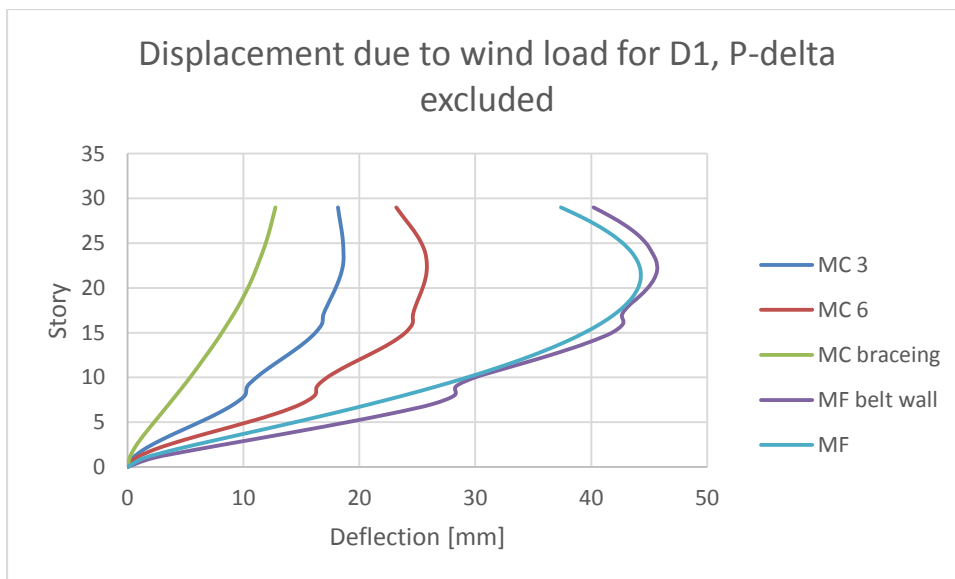


Figure B 4: Displacement due to wind load in y-direction for diaphragm D1, P-delta excluded

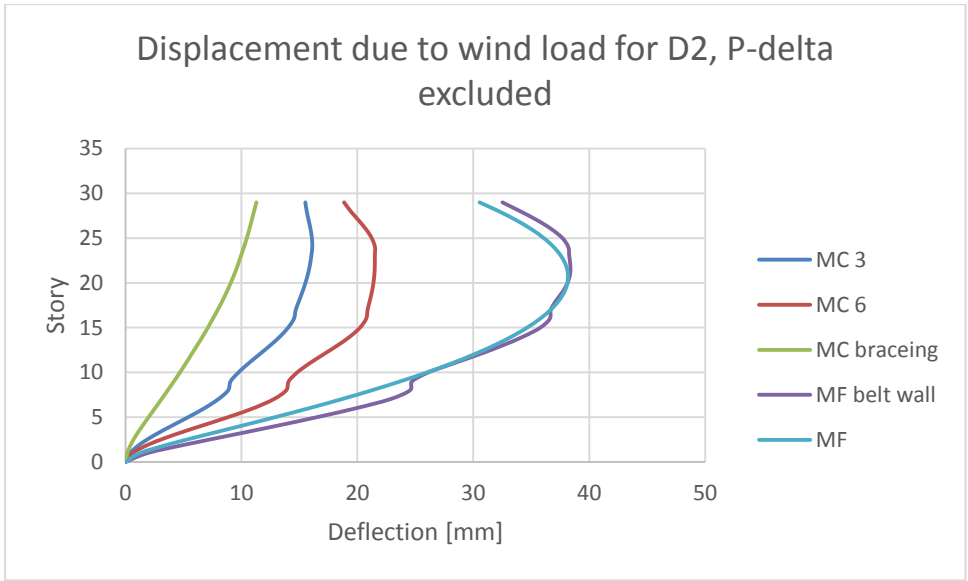


Figure B 5: Displacement due to wind load in y-direction for diaphragm D2, P-delta excluded

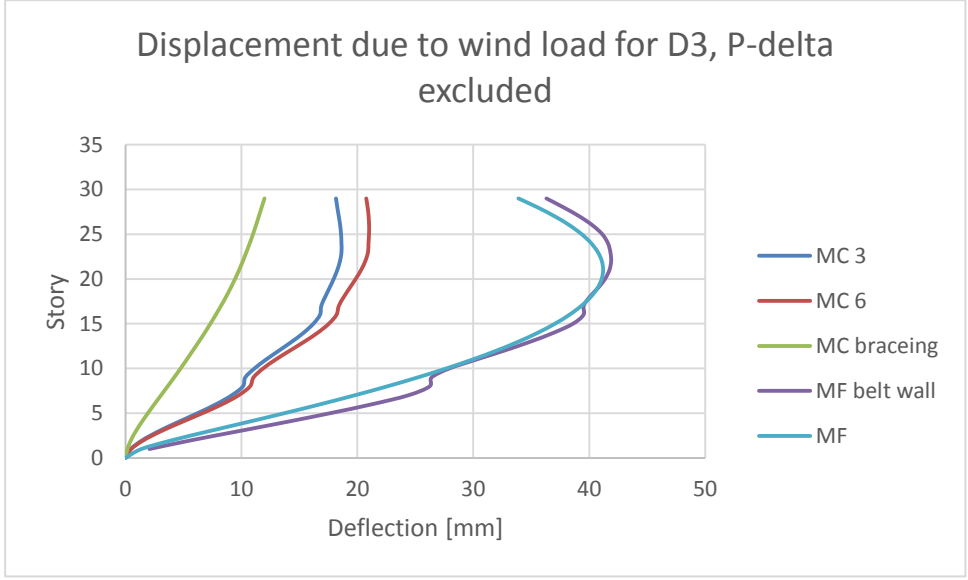


Figure B 6: Displacement due to wind load in y-direction for diaphragm D3, P-delta excluded

Displacement due to seismic load, P-delta included

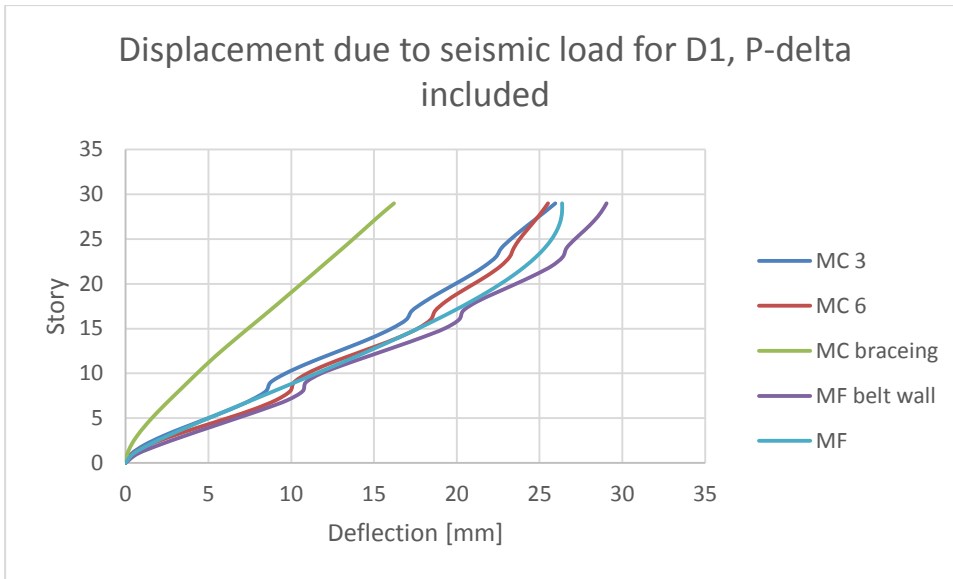


Figure B 7: Displacement due to seismic load in y-direction for diaphragm D1, P-delta included

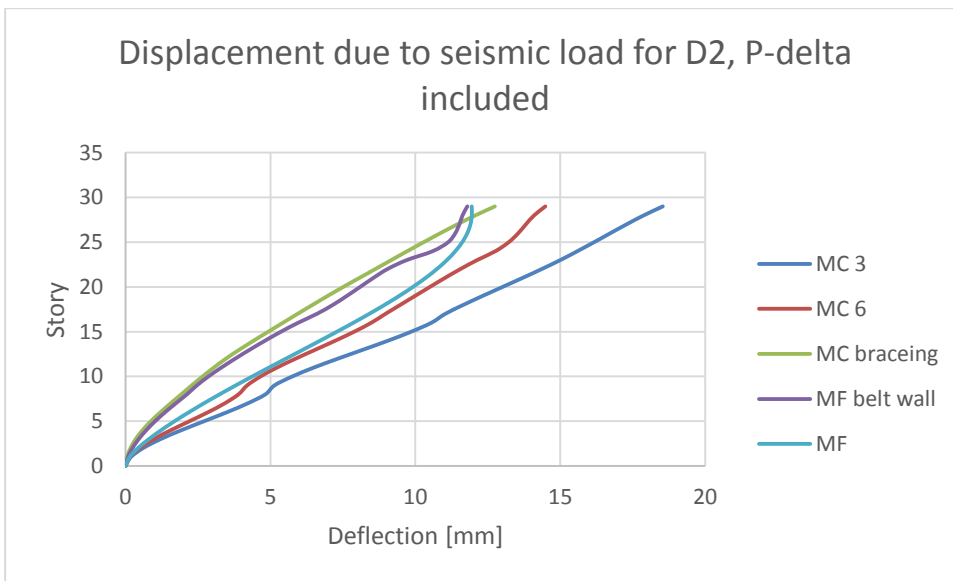


Figure B 8: Displacement due to seismic load in y-direction for diaphragm D2, P-delta included

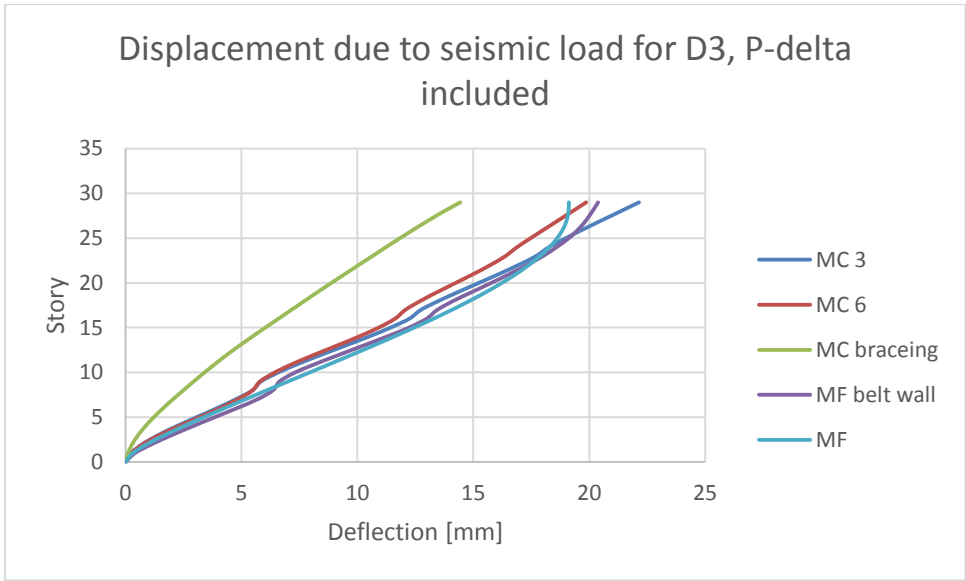


Figure B 9: Displacement due to seismic load in y-direction for diaphragm D3, P-delta included

Displacement due to seismic load, P-delta excluded

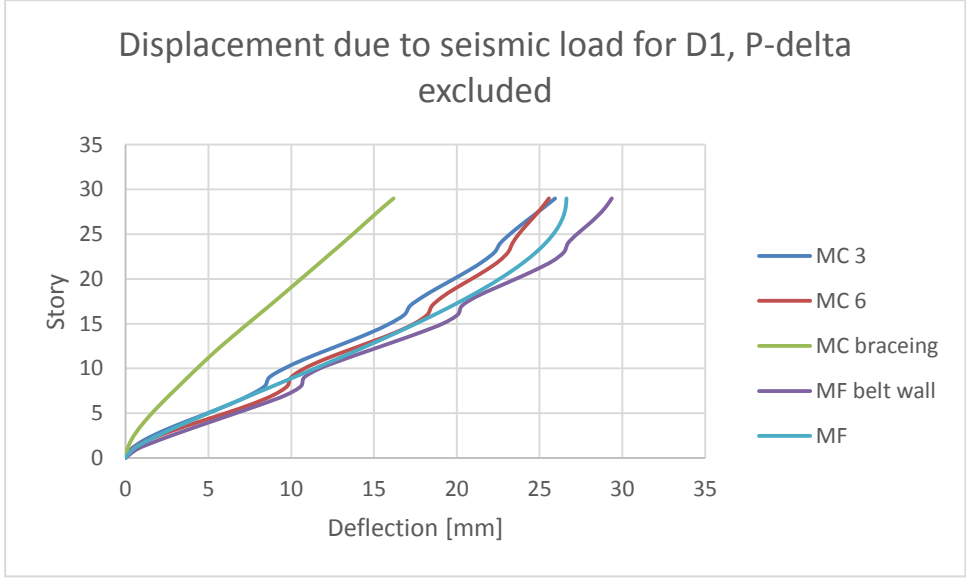


Figure B 10: Displacement due to seismic load in y-direction for diaphragm D1, P-delta excluded

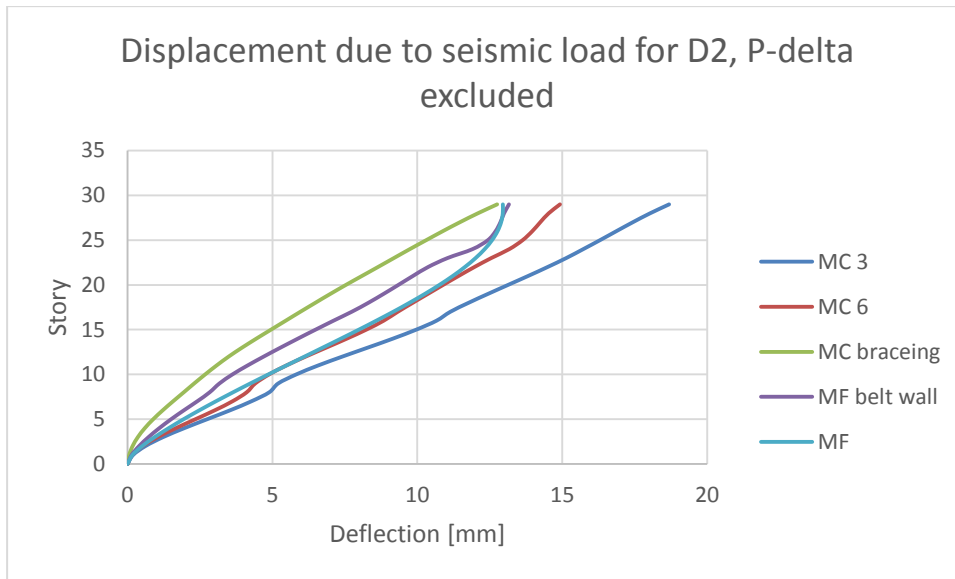


Figure B 11: Displacement due to seismic load in y-direction for diaphragm D2, P-delta excluded

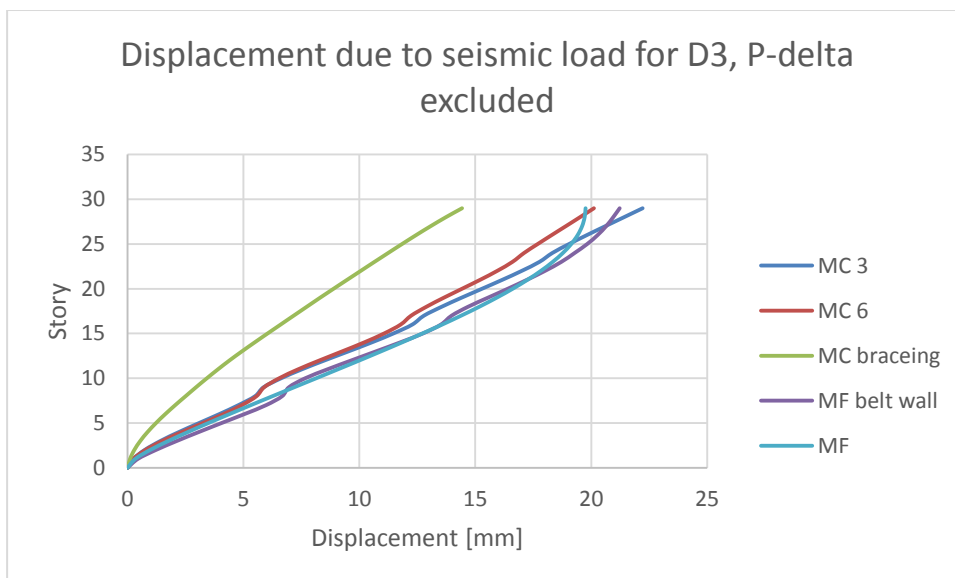


Figure B 12: Displacement due to seismic load in y-direction for diaphragm D3, P-delta excluded

450 m high building

Displacement due to wind load, P-delta included

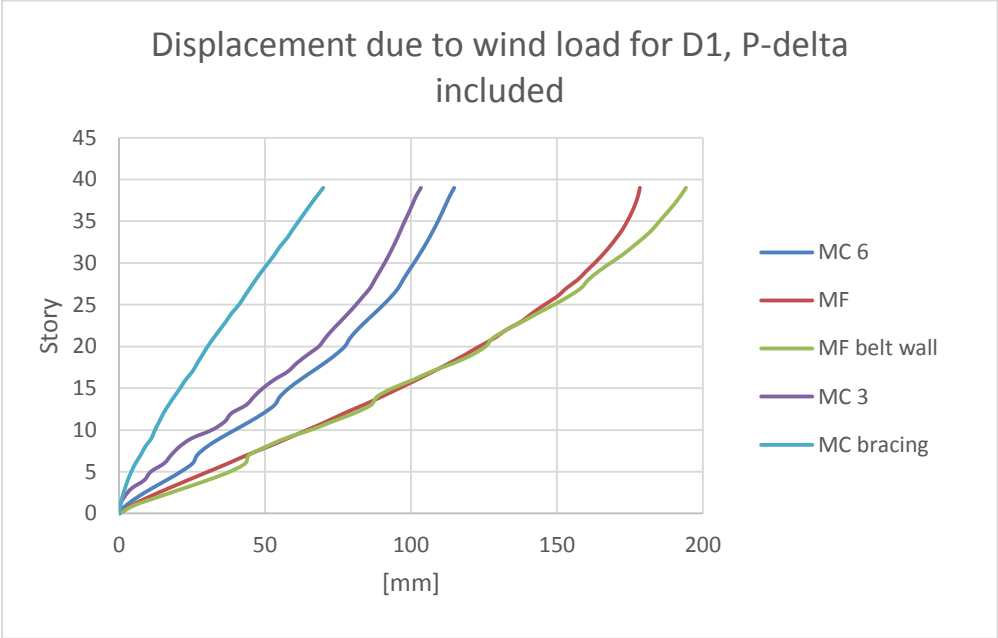


Figure B 13: Displacement due to wind load in y-direction for diaphragm D1, P-delta included

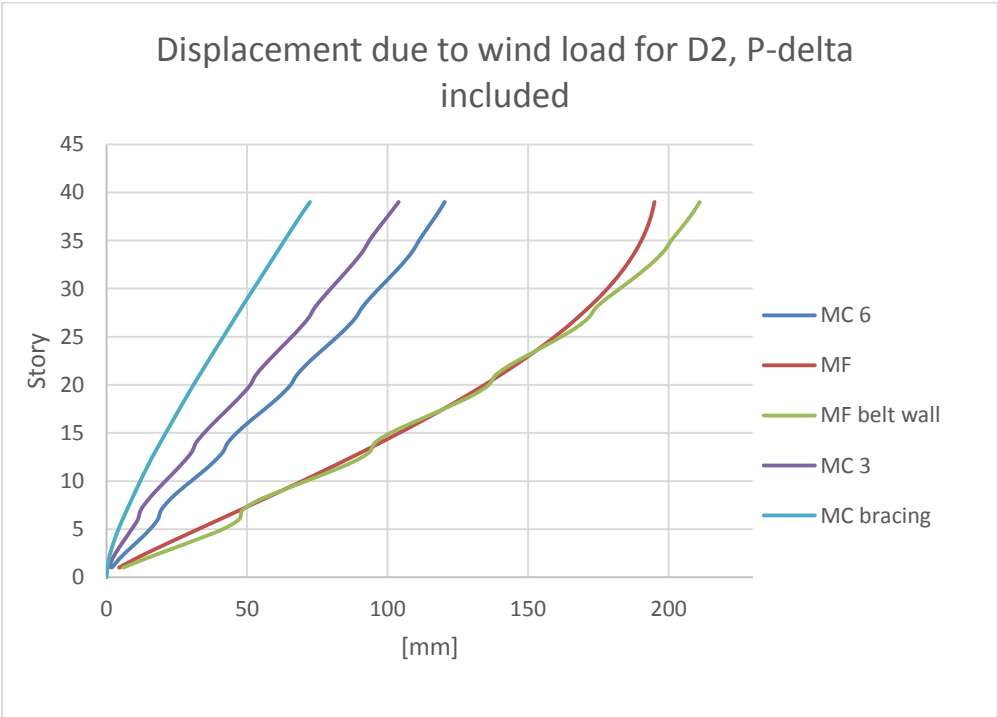


Figure B 14: Displacement due to wind load in y-direction for diaphragm D2, P-delta included

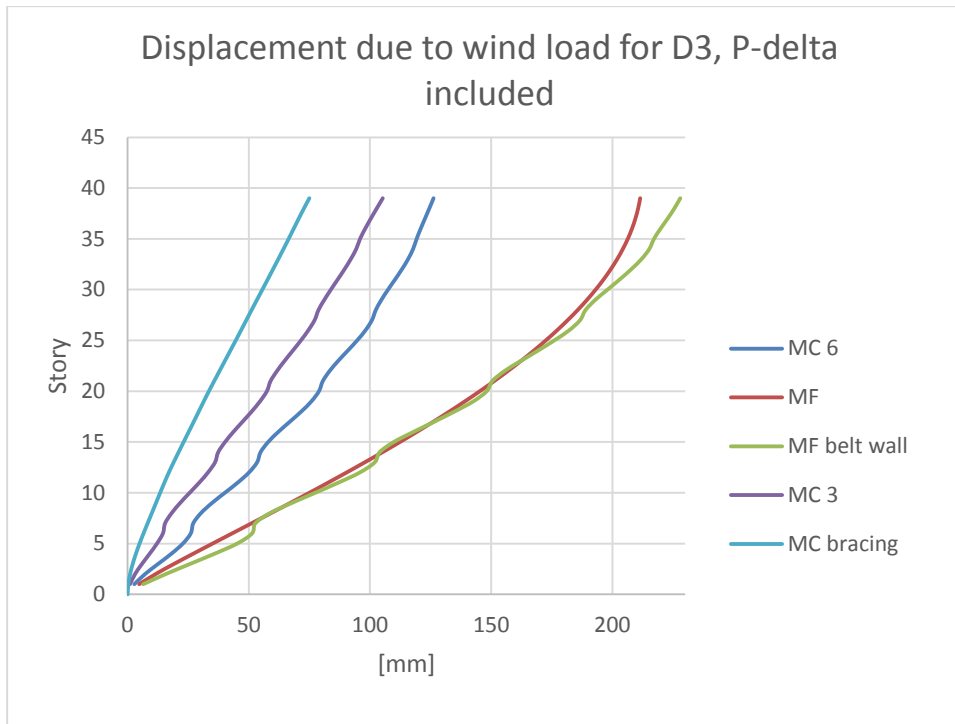


Figure B 15: Displacement due to wind load in y-direction for diaphragm D3, P-delta included

Displacement due to wind load, P-delta excluded

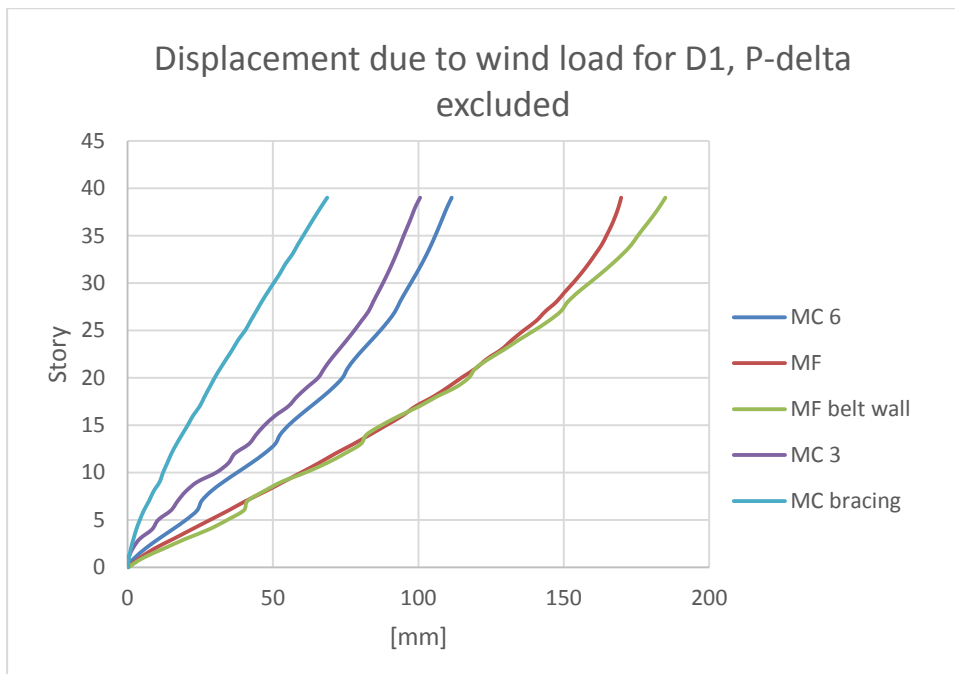


Figure B 16: Displacement due to wind load in y-direction for diaphragm D1, P-delta excluded

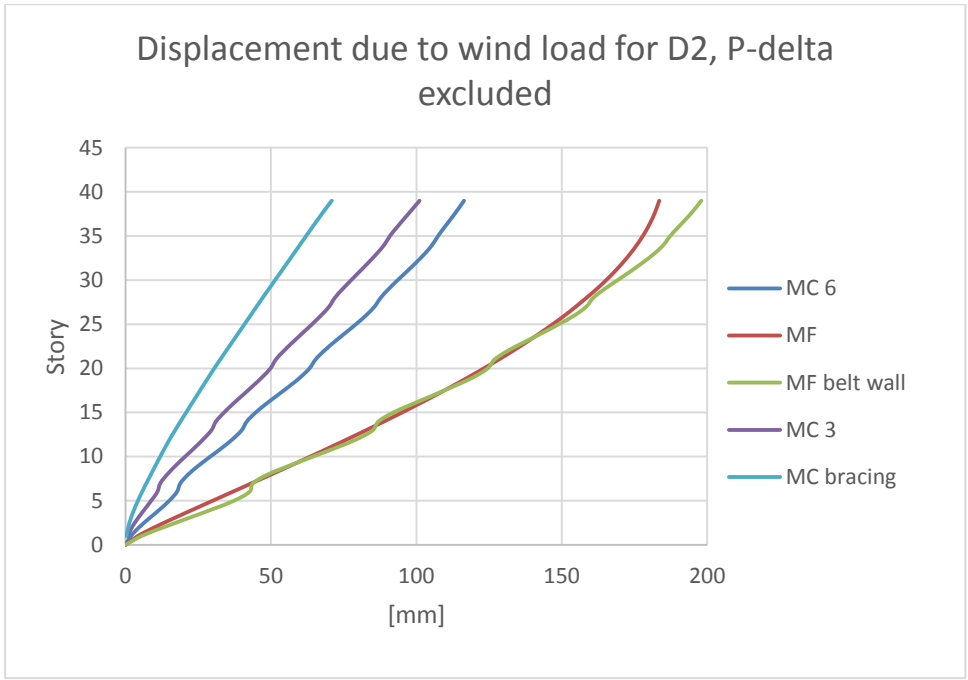


Figure B 17: Displacement due to wind load in y-direction for diaphragm D2, P-delta excluded

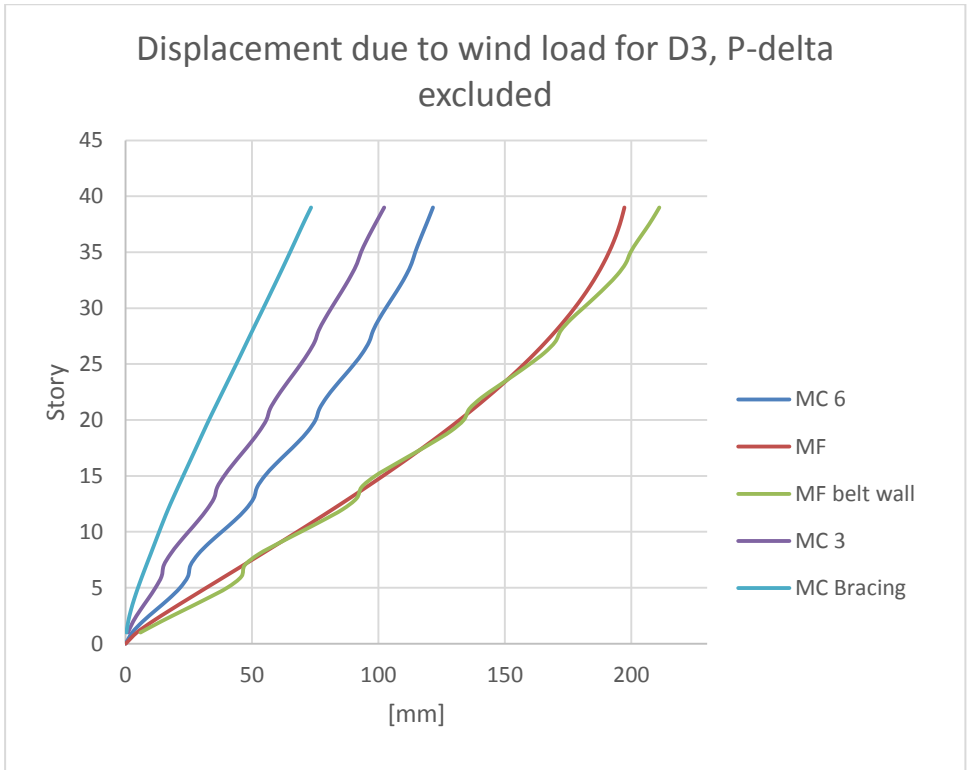


Figure B 18: Displacement due to wind load in y-direction for diaphragm D3, P-delta excluded

Displacement due to seismic load, P-delta included

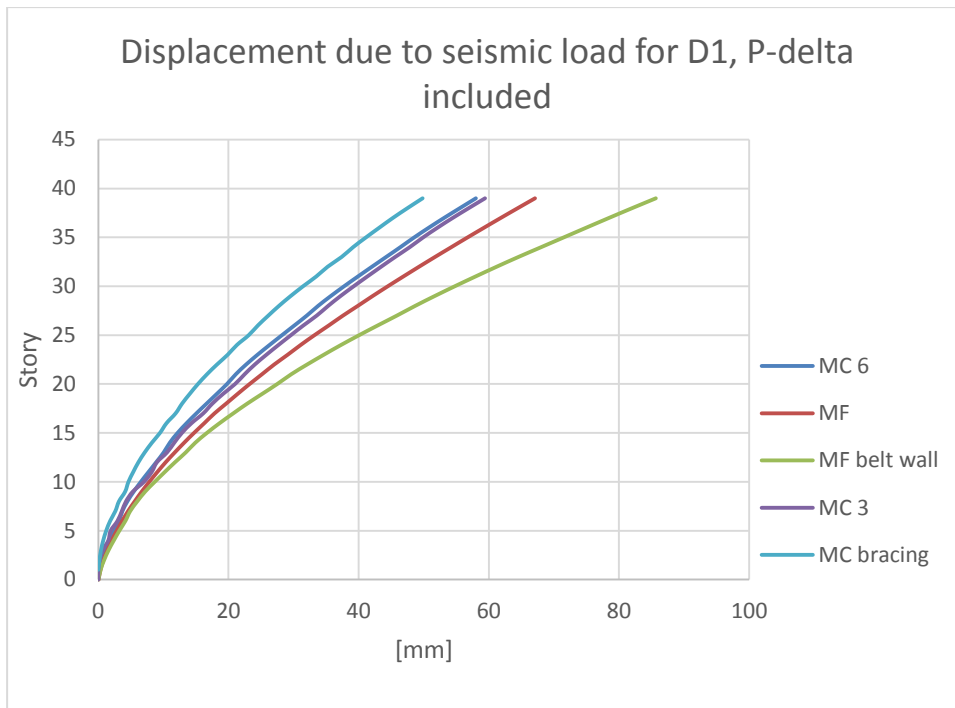


Figure B 19: Displacement due to seismic load in y-direction for diaphragm D1, P-delta included

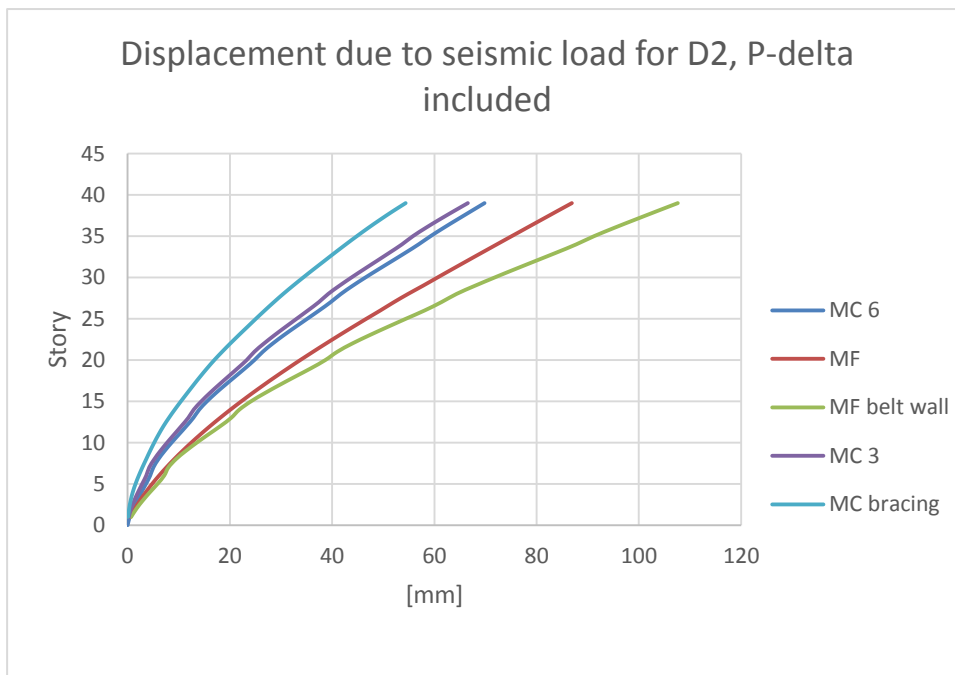


Figure B 20: Displacement due to seismic load in y-direction for diaphragm D2, P-delta included



Figure B 21: Displacement due to seismic load in y-direction for diaphragm D3, P-delta included

Displacement due to seismic load, P-delta excluded



Figure B 22: Displacement due to seismic load in y-direction for diaphragm D1, P-delta excluded

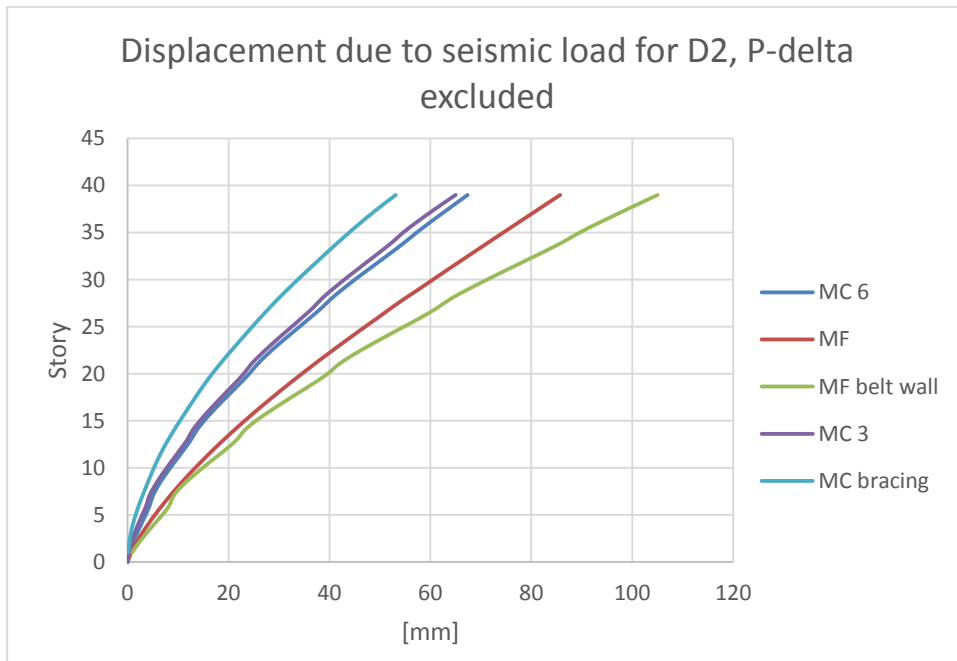


Figure B 23: Displacement due to seismic load in y-direction for diaphragm D2, P-delta excluded

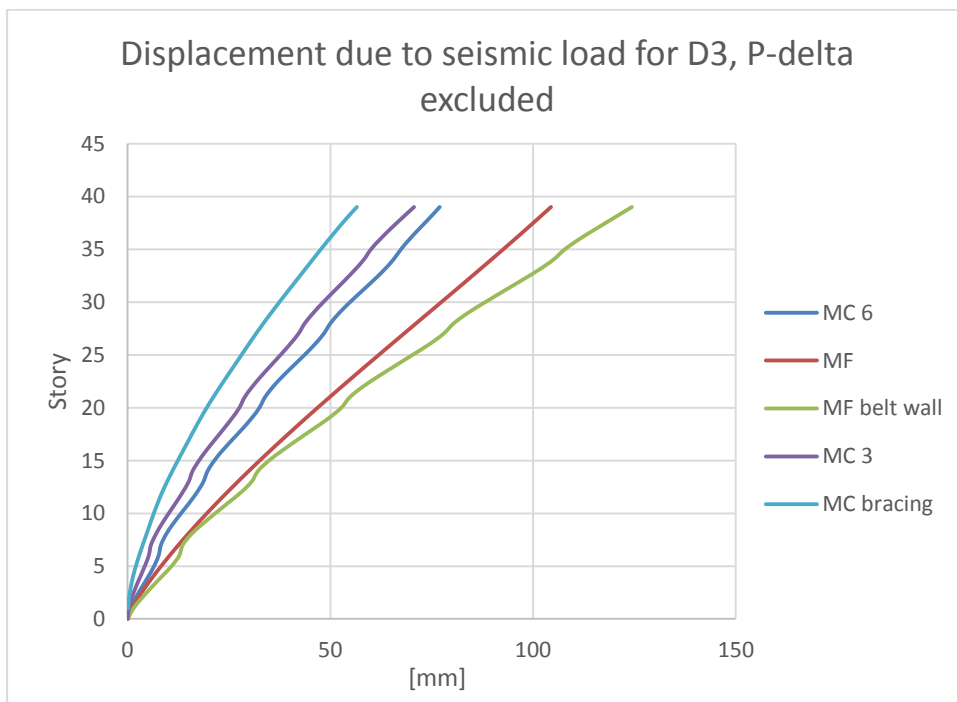


Figure B 24: Displacement due to seismic load in y-direction for diaphragm D3, P-delta excluded

Appendix C – Hand calculations

Cross-section calculation, 270 m

The total volume of all model is estimated to be the same. Mega columns with belt wall has a certain dimension and from that dimension, rest of the models dimension are calculated.

Chosen cross section:

Height, $H = 5 \text{ m}$

Width, $B = 3 \text{ m}$

Flange thickness, $t = 0.5 \text{ m}$

Cross-sections area, $A = 7 \text{ m}^2$

Three mega columns with belt wall

Values from AutoCAD and ETABS:

Total column length, $L_{c,tot} = 1956.772 \text{ m}$

Total mega column volume, $V_{MC,tot} = 13696.7 \text{ m}^3$

Total belt wall volume, $V_{bw,tot} = 4327.268 \text{ m}^3$

Six mega columns with belt walls

To keep the volume constant the area should be half of the area of the mega column that is chosen as the fixed column. The area, A of the cross section is:

$$A = B \cdot H - (B - 2t)(H - 2t)$$

If the dimensions is kept linear, that is:

$$\text{Thickness} = \frac{H}{10}$$

$$\text{Widht} = \frac{3H}{5}$$

The area is a function of the height only, and with a fix area, the height can be written as:

$$H = \sqrt{25 \frac{A}{7}}$$

Since the area for the six mega columns should be half as for the three mega columns the height is:

$$H = \sqrt{25 \frac{\frac{A}{2}}{7}} = \sqrt{25 \frac{3.5}{7}} = 3.535 \text{ m}$$

$$t = \frac{H}{10} = 0.3535 \text{ m}$$

$$B = \frac{3H}{5} = 2.121 \text{ m}$$

Three mega columns with bracings

The mega columns will remain the same size, the volume of the belt walls will be replaced with bracings.

Total bracing length, $L_{br,tot} = 6323.606 \text{ m}$

$$\text{Cross-sectional area of bracings, } A_{br} = \frac{V_{bw,tot}}{L_{br,tot}} = \frac{4327.268}{6323.606} = 0.6843 \text{ m}^2$$

$$\text{Quadratic cross-sectional height, } h_q = \sqrt{0.6843} = 0.827 \text{ m}$$

Moment frame with belt walls

The total volume of belt walls is equivalent to beams total volume

Total beam length, $L_{b,tot} = 12575.33 \text{ m}$

$$\text{Cross-sectional area of beams, } A_b = \frac{V_{bw,tot}}{L_{b,tot}} = \frac{4327.268}{12575.33} = 0.3441 \text{ m}^2$$

$$\text{Quadratic cross-sectional height, } h_q = \sqrt{0.3441} = 0.587 \text{ m}$$

The belt wall should be installed in the building so the volume of belt wall is subtracted from total volume of mega columns and resulted volume is then transformed into moment frames volume.

Total moment frame length (beams excluded), $L_{MF,tot} = 15653.38 \text{ m}$

Total moment frame volume, $V_{MF,tot} = V_{MC,tot} - V_{bw,tot} = 9369.436 \text{ m}^3$

$$\text{Cross sectional area of moment frame, } A_{MF} = \frac{V_{MF,tot}}{L_{MF,tot}} = 0.5986 \text{ m}^2$$

Quadratic cross-sectional height, $h_q = \sqrt{0.5986} = 0.774 \text{ m}$

Moment frame without belt walls

There is eight columns on a mega columns, therefore the area is

$$A_{MF} = \frac{7}{8} = 0.875 \text{ m}^2$$

$$h_q = \sqrt{0.875} = 0.935 \text{ m}$$

Base reaction calculation, 270 m

Three mega columns with belt walls

$$V_{bw,tot} = 4327.268 \text{ m}^3$$

$$V_{MC,tot} = 13696.7 \text{ m}^3$$

$$\text{Total floor area, } A_{f,tot} = 59776.95 \text{ m}^2$$

$$\text{Total floor volume, } V_{f,tot} = 14949.24 \text{ m}^3$$

$$\text{Total volume, } V_{tot} = 32968.21 \text{ m}^3$$

$$\text{Weight concrete, } \gamma_c = 24.99 \frac{\text{kN}}{\text{m}^3}$$

$$\text{Total weight, } \gamma_{tot} = \gamma_c \cdot V_{tot} = 24.99 \cdot 32968.21 = 823875.5 \text{ kN}$$

Six mega columns with belt walls

$$V_{bw,tot} = 4327.268 \text{ m}^3$$

$$V_{c,tot} = 13696.7 \text{ m}^3$$

$$A_{f,tot} = 59776.95 \text{ m}^2$$

$$V_{f,tot} = 14949.24 \text{ m}^3$$

$$V_{tot} = 32968.21 \text{ m}^3$$

$$\gamma_{tot} = \gamma_c \cdot V_{tot} = 24.99 \cdot 32968.21 = 823875.5 \text{ kN}$$

Three mega columns with bracings

$$L_{br,tot} = 6323.606 \text{ m}$$

$$A_{br} = 0.6843 \text{ m}^2$$

$$V_{br,tot} = 4327,24 \text{ m}^3$$

$$V_{MC,tot} = 13696.7 \text{ m}^3$$

$$V_{f,tot} = 14949.24 \text{ m}^3$$

$$V_{tot} = 32973.18 \text{ m}^3$$

$$\gamma_{tot} = \gamma_c \cdot V_{tot} = 24.99 \cdot 32968.18 = 823999.8 \text{ kN}$$

Moment frame with belt walls

$$V_{b,tot} = 4327.268 \text{ m}^3$$

$$V_{bw,tot} = 4327,27 \text{ m}^3$$

$$V_{c,tot} = 9369,436 \text{ m}^3$$

$$V_{f,tot} = 14949.24 \text{ m}^3$$

$$V_{tot} = 32973.21 \text{ m}^3$$

$$\gamma_{tot} = \gamma_c \cdot V_{tot} = 24.99 \cdot 32968.21 = 823875.5 \text{ kN}$$

Moment frame without belt walls

$$V_{bw,tot} = 4327,27 \text{ m}^3$$

$$V_{c,tot} = 13696.7 \text{ m}^3$$

$$V_{f,tot} = 14949.24 \text{ m}^3$$

$$V_{tot} = 32973.21 \text{ m}^3$$

$$\gamma_{tot} = \gamma_c \cdot V_{tot} = 24.99 \cdot 32968.21 = 823875.5 \text{ kN}$$

Cross-section calculations, 450 m

Three mega columns with belt wall

$$L_{c,tot} = 3173.656 \text{ m}$$

Columns cross-section

$$H = 5 \text{ m}$$

$$B = 3 \text{ m}$$

$$t = 0.5 \text{ m}$$

$$A = 7 \text{ m}^2$$

$$V_{MC,tot} = 22215.596 \text{ m}^3$$

$$V_{bw,tot} = 7739.6175 \text{ m}^3$$

Six mega columns with belt walls

$$H = \sqrt{25 \frac{A}{7}} = \sqrt{25 \frac{3.5}{7}} = 3.535 \text{ m}$$

$$t = \frac{H}{10} = 0.3535$$

$$B = \frac{3H}{5} = 2.121 \text{ m}$$

Three mega columns with bracings

The mega columns will remain the same size as with belt walls but belt walls volume will transform into volume of bracings.

$$L_{br,tot} = 9401.187 \text{ m}$$

$$A_{br} = \frac{V_{bw,tot}}{L_{br,tot}} = \frac{7739.6175}{9401.187} = 0.823259 \text{ m}^2$$

$$h_q = \sqrt{0.823259} = 0.9073 \text{ m}$$

Moment frame with belt walls

The total volume of belt walls is equivalent to beams total volume

$$L_{b,tot} = 19549.035 \text{ m}$$

$$A_b = \frac{V_{bw,tot}}{L_{b,tot}} = \frac{7739.6175}{19549.035} = 0.3959 \text{ m}^2$$

$$h_{q,b} = \sqrt{0.3959} = 0.62921 \text{ m}$$

The belt wall should be installed in the building so the volume of belt wall is subtracted from total volume of mega columns and resulted volume is then transformed into moment frames volume.

$$L_{MF,tot} = 25389.248 \text{ m}$$

$$V_{MF,tot} = V_{MC,tot} - V_{bw,tot} = 22215.592 - 7739.6175 = 14475.9745 \text{ m}^3$$

$$A_{MF} = \frac{14475.9745}{L_{MF,tot}} = \frac{14475.9745}{25389.248} = 0.57016 \text{ m}^2$$

$$h_{q,MF} = \sqrt{0.57016} = 0.7551 \text{ m}$$

Moment frame without belt walls

$$A_b = \frac{V_{bw,tot}}{L_{b,tot}} = \frac{7739.6175}{19549.035} = 0.3959 \text{ m}^2$$

$$h_{q,b} = \sqrt{0.3959} = 0.62921 \text{ m}$$

$$A_{MF} = \frac{3173.656 \cdot 7}{L_{mf}} = 0.875 \text{ m}^2$$

$$h_{q,MF} = \sqrt{0.875} = 0.9354 \text{ m}$$

Base reaction calculations, 450 m

Three mega columns with belt walls

$$L_{c,tot} = 3173.656 \text{ m}$$

$$A = 7 \text{ m}^2$$

$$A_{f,tot} = 95610.68 \text{ m}^2$$

$$V_{f,tot} = 0.25 \cdot A_f = 0.25 \cdot 95610.68 = 23902.62 \text{ m}^3$$

$$\rho_c = 2549 \frac{\text{kg}}{\text{m}^3}$$

$$g = 9.807 \frac{\text{m}}{\text{s}^2}$$

$$V_{c,tot} = 3173.656 \cdot 7 = 22215.592 \text{ m}^3$$

$$V_{bw,tot} = 7739.6175 \text{ m}^3$$

$$V_{tot} = 53857.83 \text{ m}^3$$

$$\gamma_{tot} = \rho \cdot g \cdot V_{tot} = 2.5 \cdot 9.807 \cdot 53857.83 = 1346340.34 \text{ kN}$$

Six mega columns with belt walls

$$L_{c,tot} = 6380.438 \text{ m}$$

$$A = 3.5 \text{ m}^2$$

$$V_{c,tot} = 6380.438 \cdot 3.5 = 22331.533 \text{ m}^3$$

$$A_{f,tot} = 95610.68 \text{ m}^2$$

$$V_{f,tot} = 0.25 \cdot A_f = 0.25 \cdot 95610.68 = 23902.62 \text{ m}^3$$

$$V_{bw,tot} = 7739.6175 \text{ m}^3$$

$$V_{f,tot} = 0.25 \cdot A_f = 0.25 \cdot 95610.68 = 23902.62 \text{ m}^3$$

$$V_{tot} = 53973.77 \text{ m}^3$$

$$\gamma_{tot} = \rho \cdot g \cdot V = 2.5 \cdot 9.807 \cdot 53973.77 = 1349238.636 \text{ kN}$$

Three mega columns with bracings

$$V_{tot} = 22215.592 + 23902.62 + 9401.187 \cdot 0.823259 = 53857.8238 \text{ m}^3$$

$$\gamma_{tot} = \rho \cdot V \cdot g = 2.549 \cdot 53857.8238 \cdot 9.807 = 1346340.195 \text{ kN}$$

Moment frame with belt walls

$$\begin{aligned} V_{tot} &= 23902.62 + 7739.6175 + 0.3959 \cdot 19549.035 + 0.57016 \cdot 25389.24 \\ &= 53857.629 \text{ m}^3 \end{aligned}$$

$$\gamma_{tot} = \rho \cdot V \cdot g = 2.549 \cdot 53857.629 \cdot 9.807 = 1346335.326 \text{ kN}$$

Moment frame without belt walls

$$V_{tot} = 23902.62 + 0.3959 \cdot 19549.035 + 0.9354 \cdot 25389.2 = 55391.178 \text{ m}^3$$

$$\gamma_{tot} = \rho \cdot V \cdot g = 2.549 \cdot 55391.178 \cdot 9.807 = 1384671.049 \text{ kN}$$